N. T. K. KHALID

COMPARATIVE STUDY OF WIND AND EARTHQUAKE LOADS ON REINFORCED CONCRETE BUILDINGS WITH DIFFERENT FLOOR CONFIGURATIONS

THE GRADUATE SCHOOL OF NATURAL AND APPLIED SCIENCES
OF
ATILIM UNIVERSITY

NOORULDEEN TAREQ KHALID KHALID

A MASTER OF SCIENCE
THESIS
IN
THE DEPARTMENT OF CIVIL ENGINEERING

July, 2020

ATILIM UNIVERSITY 2020

COMPARATIVE STUDY OF WIND AND EARTHQUAKE LOADS ON REINFORCED CONCRETE BUILDINGS WITH DIFFERENT FLOOR CONFIGURATIONS

A THESIS SUBMITTED TO

THE GRADUATE SCHOOL OF NATURAL AND APPLIED SCIENCES

OF

ATILIM UNIVERSITY

BY

NOORULDEEN TAREQ KHALID KHALID

IN PARTIAL FULFILLMENT OF THE REQUIREMENTS

FOR

THE DEGREE OF MASTER OF SCIENCE

IN

THE DEPARTMENT OF CIVIL ENGINEERING

July, 2020

Approval of the Graduate School of Natural and Applied Sciences, Atilim University.

_____

Prof. Dr. Ali Kara
Director

I certify that this thesis satisfies all the requirements as a thesis for the degree of **Master of Science in Civil Engineering, Atilim University**.

_____

Prof. Dr. Hasan Umur AKAY
Head of Department

This is to certify that we have read the thesis COMPARATIVE STUDY OF WIND AND EARTHQUAKE LOADS ON REINFORCED CONCRETE BUILDINGS WITH DIFFERENT FLOOR CONFIGURATIONS submitted by NOORULDEEN TAREQ KHALID KHALID and that in our opinion it is fully adequate, in scope and quality, as a thesis for the degree of Master of Science.

_____	_____
Assist. Prof. Dr. Gökhan Tunç Co-Supervisor	Assoc. Prof. Dr. Filiz Bal Koçyiğit Supervisor

Examining Committee Members:

Assoc. Prof. Dr. Ali Ateş _____
Civil Eng. Department, Bolu Abant İzzet Baysal Univ.

Assoc. Prof. Dr. Filiz Bal Koçyiğit _____
Department of Architecture, Atilim University

Assist. Prof. Dr. Gökhan Tunç _____
Civil Eng. Department, Atilim University

Assist. Prof. Dr. Riyad Şihab _____
Dept. of Building Inspection, Afyon Kocatepe Univ.

Assist. Prof. Dr. Ertan Sönmez _____
Civil Eng. Department, Atilim University

Date: *July 28, 2020*

I hereby declare that all information in this document has been obtained and presented in accordance with academic rules and ethical conduct. I also declare that, as required by these rules and conduct, I have fully cited and referenced all material and results that are not original to this work.

Name, Last Name : Nooruldeen Tareq Khalid Khalid

Signature :

ABSTRACT

COMPARATIVE STUDY OF WIND AND EARTHQUAKE LOADS ON REINFORCED CONCRETE BUILDINGS WITH DIFFERENT FLOOR CONFIGURATIONS

Nooruldeen Tareq Khalid Khalid
M.S., Civil Engineering Department

Supervisor : Assoc. Prof. Dr. Filiz Bal Koçyiğit
Co-Supervisor: Assist. Prof. Dr. Gökhan Tunç
July 2020, 99 pages

Multi-story buildings exist in every country on the planet. Therefore, it is necessary to study and analyze the impact of lateral loads, resulting from wind and earthquakes, on these buildings. In this study, comparisons were made between the wind and earthquake generated loads on select multi-story buildings with different heights, shapes, and layouts. The presence of shear walls, and the significance of their geometric (square and rectangular) shapes on the overall behavior of buildings, was also examined. For this purpose, a total of 26 building models, assumed to be located on a shoreline in the city of Sinop, Turkey, with variable heights of 10, 20, 30, and 40 floors, were designed in ETABS. The structural calculations and analyses of the wind loads were performed according to the rules and regulations of Turkish Standard 498 (TS 498, Design Loads for Buildings) and American Society of Civil Engineers, 7-16 (ASCE 7-16, Minimum Design Loads for Buildings and Other Structures). For the earthquake loads, the current Turkish Earthquake Code (TEC 19) was used by applying a response spectrum method. Two types of earthquake loads were applied to the buildings: DD2 (earthquake with a return period of 475 years) and DD4 (earthquake with a return period of 43 years). DD2 was applied to all, whereas DD4 was applied only to the 40 story building, since it was the sole tall building. The results of the wind and earthquake loads were investigated by studying variations in the following parameters: (a) base shear forces, (b) rooftop displacements, (c) fundamental periods, and (d) drifts. Based on the results, it was concluded that DD2 type of earthquake loads have a stronger impact on buildings

than wind loads. When the results of the TS 498 and ASCE 7-16 wind loads were compared to each other, it was observed that the results of TS 498 were more pronounced than those of ASCE 7-16 for the 10 and 40 story buildings. However, for the 20 and 30 story buildings, the results of ASCE 7-16 were more significant compared to TS 498. Overall, buildings with layouts featuring shear walls at their center were most effective in resisting lateral loads.

Keywords: Wind Loads, Earthquake Loads, Reinforced Concrete Buildings, Floor Layout

ÖZ

FARKLI KAT PLANLARINA SAHİP BETONARME BİNALAR ÜZERİNDE RÜZGAR VE DEPREM YÜKLERİNİN MUKAYESELİ ÇALIŞMASI

Nooruldeen Tareq Khalid Khalid

Yüksek lisans (M.S)., İnşaat Mühendisliği Bölümü

Tez Yöneticisi : Doç.Dr. Filiz Bal Koçyiğit

Ortak Tez Yöneticisi : Dr.Öğr.Üyesi.Gökhan Tunç

Temmuz 2020, 99 sayfa

Çok katlı binalar pek çok ülkede yaygın bir şekilde kullanılmaktadır. Bu yüzden, bu tür binalar üzerinde hem deprem hem de rüzgâr yüklerinden dolayı oluşan yatay yüklerin etkisinin araştırılması ve çalışılması zorunludur. Bu çalışmada, farklı yükseklik, geometrik şekil ve kat planlarına sahip seçili yüksek katlı binalar üzerinde deprem ve rüzgâr yüklemesinin sonuçları karşılaştırılmıştır. Herhangi bir perde duvarın kat planında yer alması ile sahip farklı kesit özelliklerinin (kare veya dikdörtgen olması) binalar üzerindeki davranışa olan etkisi çalışmanın bir kapsamını oluşturmuştur. Bu kapsamda farklı yüksekliklere sahip 10, 20, 30 ve 40 katlı toplamda 26 adet bina ETABS programı kullanılarak modellenmiştir. Binaların tamamının Sinop şehir merkezi içerisinde ve deniz kıyısında yer aldığı varsayılmıştır. Rüzgâr yükleri, Türk Standartları 498 (TS 498) ve Amerikan yönetmeliği, ASCE 7-16'ya uygun olarak hesaplanmıştır. Deprem yükleri için güncel Türkiye Bina Deprem Yönetmeliği'ndeki (TBDY 2019) Mod Birleştirme Yöntemi kullanılmıştır. Bu kapsamda binalara 2 farklı deprem yer hareketi uygulanmıştır; tekrar periyodu 475 yıl olan DD2 ve tekrar periyodu 43 yıl olan DD4. DD2 deprem yer hareketi bütün binalara uygulanmış, DD4 ise DD2 ile birlikte sadece 40 katlı binaya yüksek bina kategorisine girdiği için uygulanmıştır. Rüzgâr ve deprem yüklerine bağlı olarak ortaya çıkan analiz sonuçları maddeler halinde verilen şu parametreler esas alınarak incelenmiş ve karşılaştırılmıştır: (a) taban kesme kuvvetleri, (b) çatı katı yer değiştirmesi, (c) doğal periyod değerleri ve (d) göreceli kat ötelemeleri. Analiz sonuçlarına göre DD2 tür depremin binalar üzerindeki etkisi rüzgâr yüklemelerine

göre çok daha etkili olmuştur. TS 498 ve ASCE 7-16 yönetmeliklerine uygun olarak hesaplanan rüzgâr yükleri mukayese edildiğinde sırası ile 10 ve 40 katlı binalarda TS 498'e göre belirlenen rüzgâr yüklerinin daha etkili olduğu görülmüştür. Bununla birlikte 20 ve 30 katlı binalarda ise ASCE 7-16'ya göre hesaplanan rüzgârın daha baskın olduğu belirlenmiştir. Binaların kat planlarına bakıldığında ise geometrik şekilden bağımsız olarak çekirdek perdeli kat planınım hem deprem hem de rüzgâr yükleri etkisi altında daha etkili olduğu görülmüştür.

Anahtar Kelimeler: Rüzgâr Yükleri, Deprem Yükleri, Betonarme Binalar, Kat Planı

To

My father, Dr. Tareq Al Nuaimi

Who strived to put us on the top always

To

My mother, Shatha Fadhel

The heart that loved me and prayed for my sake always

To

My brothers,

Dr. Muhammad Tareq,

Dr. Nidaauldeen Tareq,

My sister, Eng. Maryam Tareq

Who were always far away from me, but they are always in the depths of my heart

To

Eng. Ameer Muhammed Salman

Who taught me the ABCs of Engineering, trusted my abilities and supported me in my early beginnings

To

My dear friends

Ahmed, Firas, Omar, Haitham, Mustafa, and to Atoogy

You were my second family here. You made my days better

I can't find enough expression to describe my love for all of you.

Thanks

ACKNOWLEDGMENTS

I would like to express my appreciation to my supervisor Assoc. Prof. Dr. Filiz Bal Koçyiğit and special thanks to my Co-Supervisor Assist. Prof. Dr. Gökhan Tunç, who gave me the endless guidance, limitless encouragements, advice, and support provided by them throughout the study.

I would also like to thank the members of the thesis jury for their time and efforts in this work.

I would like to also thank my family and friends for their support, patience and faith since they endlessly provided them to me.

TABLE OF CONTENTS

LIST OF TABLES

LIST OF FIGURES

CHAPTER 1

INTRODUCTİON

1.1. Introduction

One of the most important parameter in the building's design process is the fulfillment of safety requirements by taking the structural, architectural, and economic aspects into account. When performing structural design calculations of buildings, it is important to account for all the loads and stresses that a building is expected to experience, and thus to find sound and safe ways to deal with them.

The most common loads in building design are the vertical ones. Although these loads come from various sources, they can be classified into two basic groups: live and dead loads. However, there are other types of loads that should be given high importance in building analysis, and they are horizontal or sometimes called lateral loads. The most important types of these loads are wind and earthquake loads.

The effect of horizontal loads caused by wind movement or earthquakes depends on several factors; the most important of them is its architectural design or appearance, the area directly exposed to wind, the nature and quality of the materials used in the building structure, the location of the building in relation to seismic areas or coastal areas, as well as the height of the surrounding buildings, if any. All these factors must be taken into consideration when performing the structural analysis of a building.

Since wind and earthquake loads directly affect buildings in a horizontal direction, resisting these loads might require more rigorous analysis than those acting in the vertical direction. The outcome of previous studies shows that there are risks on buildings resulting from the impact of wind and earthquake loads. These loads might cause a loss in a buildings' structural stability or damage on their structural elements due to the high stresses that will generate.

1.2. Problem statement

Multi-story buildings are primarily needed for the work or residence purposes due to a shortage of area mostly in the urban areas to meet the need of increasing demand by public. The latest development in building technologies is another force behind the trend of constructing tall buildings. For these reasons, it has become more urgent to study these buildings in terms of their structural designs to evaluate their performances under wind and earthquake loads.

Horizontal loads have direct impact on the structural performance of a tall building. Although this impact varies from building to building, it also depends on several other factors, such as construction type, construction material and architectural layout. If these loads reach to a point where an associated failure of a building member or component initiates, then either a partial or full collapse can occur, which then leads to a great harm to people's lives in addition to an economic damage. Therefore, it is necessary to study the impact of these loads on buildings, and evaluate a building’s performance with respect to the guidelines and rules outlined in building codes so that an optimal design is reached to reduce the risk of failure and provide occupants with the highest safety level while maintaining an optimal cost.

The purpose of this study is to compare the effects of wind and earthquake loads on multi-story buildings with different heights, shapes, and layouts. For this purpose, a total of 26 building models with variable heights of 10, 20, 30 and 40, floors were analyzed under wind and earthquake loads. Also, in this study, the presence of shear walls and the geometric shape factor (square and rectangular shapes) were investigated. The structural calculations and analyses were performed according to the regulations specified in Turkish Standard 498 (TS 498, Design Loads for Buildings), American Society of Civil Engineers, 7-16 (ASCE 7-16, Minimum Design Loads for Buildings and Other Structures), and Turkish Earthquake Code, 2019 (TEC 19).

1.3. Conclusion

In this study, a total of 26 building models with varying layouts, number of floors, and shapes were analyzed. These buildings were divided into five groups. The first group consisted of four building models with unique layouts, all of which were 40 floors with a total height of 120 meters and contained shear walls within their structure and were subjected to the effect of earthquakes of type DD4. The buildings in the second group were the exact ones in the first group but were subjected to a type DD2 type of earthquake. The third group consisted of six 30 story building models with a total height of 90 meters -each building model had its own layout- and were subjected to a DD2 type of earthquake. The fourth group contained six building models with individual layouts. The buildings in this group had 20 floors with a height of 60 meters and were subjected to a DD2 type of earthquake. The buildings in the fifth and final group were 10 story buildings with a total height of 30 meters and were subjected to a DD2 type of earthquake. Shear walls were used in some building models of the third, fourth, and fifth groups. However, in the other building models, they were decided not to be used. A commercially available software package, ETABS, was used to perform the structural analyses of the buildings under wind and earthquake loads.

The wind loads were applied twice on these buildings; one in line with the requirements of TS 498, and the other in line with the requirements of ASCE 7-16. Earthquake loads were also considered in this study. For this purpose, TEC 19 generated loads were used. The analyses results were evaluated by considering the following parameters: the base shear, maximum displacement, drift, and fundamental periods.

This research consists of five chapters; the first chapter describes the subject of the research and its purpose. The second chapter provides details of literature review conducted in this area. The third one gives detailed explanation of all layouts used in the building models including the types of loads, and the requirements associated to the loads as described in ASCE 7-16, TS 498 and TEC 19. Chapter 4 investigates the results of the parametric study for each building model. The last chapter, Chapter 5, has the conclusions, and recommendations for future works.

CHAPTER 2

LITERATURE REVIEW

2.1 Introduction

There have been numerous researches conducted in this area studying the effect of wind and earthquake loads on buildings. In this chapter, some of these previous works will be presented according to their chronological order starting from the earliest date to the latest date.

2.2 Literature Review

2.2.1 S. Mitra, 1993 [1]

In this study, high-rise buildings that were subjected to lateral loads were investigated. The effect of air gaps on the structural design of buildings was also taken into account by reducing the amount of wind pressure. Several wind tunnel tests have been performed. Based on this study, it was concluded that the gaps had greatly reduced the pressure resulting from wind. In addition to this outcome, when performing a modified configuration test with low wind load, it was noticed that the modified configuration needed less steel quantity for a structural frame.

2.2.2 X. Qiu, 1997 [2]

A theoretical study was carried out on a possibility of reducing the acceleration of a floor in a building, which was subjected to wind. For this purpose, active control approach was used to increase the existing damping that occurred in all building components using non-structural elements. The analyses only considered wind drags. The cross-spectral density and the spectral density proposed by Simio [28] and Davenport [29] for two widely used models were also compared. Davenport's spectrum was used in the numerical calculations. The problem related to the reduction in floor acceleration was formulated by using the frequency domain approach of a transfer matrix. Analytical solutions were obtained for spectral density, mean values of ground velocities, and for the active control forces.

2.2.3 O. AlShamrani, 2007 [3]

A two-stage procedure was used in this research to choose appropriate structural materials and optimal structural framing systems. In stage one, architect's considerations were included. In stage two, the selected building materials and structural framing systems were examined to determine the best performance. As a case study, a tall building in Saudi Arabia was used to compare the results of three different structural framing systems: braced frame, shear wall, and moment frame. Also, in this study, two different materials were included: steel and concrete. These buildings were analyzed by using a software called STAAD Pro 2005 [31]. Based on the study, it was concluded that shear wall systems with concrete as a material was the best solution to decrease the lateral drift using minimum quantity of material. The results indicated that when the height of a building increased, the efficiency of reducing drift decreased, and when the building mass increased, the drift resulting from wind load decreased.

2.2.4 P. Mendis, T. Ngo, N. Haritos, A. Hira, B. Samali and J. Cheung, 2007 [4]

In this paper, the basic lines of the design levels were presented according to the wind loads within the requirements of the Australian wind load code. The benefits provided by this study were clarified in comparison with the studies related to the simplified methods followed. The wind tunnel testing and the use of Computational Fluid Dynamics on tall buildings were discussed by evaluating theri importances in achieving the optimal design under the influence of wind loads.

2.2.5 H. Mingfeng, 2008 [5]

An advanced software-based design was created using an approach of an optimized efficiency-based design for high-rise buildings in order to achieve an adequate and effective performance under various severe and hazardous wind load conditions. The result of this work provided an effective computer-automated development approach for an optimum performance-based design to provide low-risk cost-effective solutions for high-rise buildings in a city which could be vulnerable to typhoons, like Hong Kong. This study also introduced a hybrid system of dynamic analysis to predict the complex movements of buildings caused by wind. Based on

the dynamic analyses tests, the analogous static wind load approach was incorporated into the rigid layout optimization of high-rise structures subjected to dynamic serviceability design and static drift requirements for acceleration. Based on a statistical analysis process of peak responses and the statistics of the extreme uncertainty caused by the inherent variability in wind induced random vibrations were quantified and modeled. The time-varying performance of wind-induced movements in high-rise structures was studied by using the peak distribution of responses. In order to illustrate the practicality and efficiency of the proposed performance-based automated reliability optimization process, various explanations and practical applications were addressed in the study.

2.2.6 A. Estrada, 2009 [6]

Tuned mass dampers were in this study to decrease the wind-induced torsional responses of structures that were investigated based on the assumption of harmonic forces that could approximate the wind excitations even though the assumption might not be realistic. Also in this study, the effects of wind loads (translational forces and moments of torsion) were correlated. The efficiency of various nonlinear/linear tuned mass dampers were investigated to minimize the structural responses. For the formulation purpose, the structures were simplified by using the following parameters: their generalized properties, the interaction between dampers and structures, and incorporated time history of wind load effects. The results of time history analyses showed that dampers with nonlinear/linear damping mechanisms were effective in reducing the structural responses. Also, the correlation between the vasrying wind load effects influenced the selection of optimum dampers, especially in determining the ideal damping coefficients for a damper.

2.2.7 M. Montgomery, 2011 [7]

The study indicated the fact that damping was highly dependent on the dynamic responses of tall buildings. Based on the measurements of tall buildings, it was showed that the fundamental damping decreased as the building height increased. Based on the latest measurements in-situ, it was stated that the buildings with a total

height of over 250 meters had less than 1% critical damping ratios. The research showed that the slight increase in the innate damping could lead to considerable changes in a building's dynamic performance. The study proposed a new damping system called "Fork Configuration Damper" for reinforced concrete (RC) buildings with coupled walls. This new damper was experimentally validated and developed at Toronto University to eliminate the design difficulties associated to high damping.

2.2.8 B. Prajapati and D. Panchal, 2013 [8]

This study focused on the analysis and structural design of symmetrical multi-story buildings. The structural design of these buildings was tested under the influence of wind and earthquake forces by keeping their costs at minimum. Based on the study, it was concluded that the composite construction made of steel and concrete was the best material in resisting the lateral forces resulting from wind and earthquakes. By comparing the results of all building models they stated that the buildings with the composite structure were more economical from the other types of building structures.

2.2.9 G. Cheng, 2014 [9]

In this study, a model based on structural reliability was proposed to optimize the cost under wind and earthquake loads. For this purpose, two model structures were studied, on which framework was implemented, and the life-cycle cost was calculated. The methodology consisted of a first order reliability process which was performed by using MATLAB along with an integrated finite element software package called ABAQUS. The goal was to extract the reliability factors for each building under different loading intensities defined by the likelihood of lateral load excess. The estimated cost of a life cycle was calculated using the cost function of the life cycle, which contained the initial cost of construction and the estimated cost of failure. Based on the results, it was concluded that the ideal design of a building showed differences depending on the risk of earthquakes or the risk of wind or both, where the design was made for each building based on a known level of risk.

2.2.10 M. Vikram, G. Chandradhara, and K. Gowda, 2014 [10]

ETABS was used to present the effects of wind on tall buildings with different aspect ratios. All building models were idealized as a 3D structural system. Axial force and bending moment variations in columns were considered to examine the frame behavior. Based on the analysis, it was concluded that the wind effects were important compared to the gravity effects when the aspect ratio is less, however, wind effect reduces when aspect ratio increases.

2.2.11 M. Sazzad, S. Azad, 2015 [11]

The effect of the building's shape on the response of earthquake and wind was studied in this paper. A comparison was made between three building models of different shapes against the effect of lateral loads. An analysis process for each model using simulation by computer applications has been done. the results were compared and it was found that the building's shape had a major impact on reducing the building’s drift. And the model whose external shape is rectangular with an opening in the middle of it was the safest under all conditions.

2.2.12 T. Patil and B. Kadam, 2016 [12]

The design of multi-story buildings with varying length and shear wall locations were discussed in this paper. The buildings were modeled in ETABS, and the results of the base shear and displacements were used to determine the best layout based on shear wall locations. According to the results, it was concluded that the presence of shear wall positevely affected the structural behaviors of multi-story buildings subjected to wind and earthquake loads. The results indicated that the roof displacement could be reduced by placing the shear walls at the core of a layout. Base shear forces and upper displacements were also low in the case of wind analysis at low altitudes. As the height of the building increased, the wind effect intensified and became more dominant compared to the effect of an earthquake.

2.2.13 S. Muffassir and L. Kalurkar, 2016 [13]

In this study, the impact of the structural analysis wind forces on multi-story composite and reinforced concrete structures was investigated, as well as the various composite structural forms. Based on the study, it was concluded that the composite structure had a larger ductility than the structure with reinforced concrete. Since the

composite structure was less sensitive to the wind force effects than the reinforced concrete structure, it was recommended for the wind-prone areas. At higher elevations, wind force was effective on the response of multi-story buildings with varying building shapes. Based on different composite structural shapes, it was stated that the six story buildings (one ground and five upper floors) with H-shaped and U-shaped layouts generated almost the same responses. However, the responses of U-shaped buildings changed suddenly for the 16 story (G+15) and 26 story (G+25) building cases compared to the results of the buildings with other shapes. The results of various composite building shapes were compared to each other. The study showed that the building with a rectangular shape in a wind-prone area was more preferable compared to the buildings with other shapes. It was also stated that U-shaped buildings were not preferred in the wind-prone areas due to their less stiffness and large displacement capabilities.

2.2.14 A. Mohammadi, 2016 [14]

This study aims to provide a design approach (or process) for buildings based on their wind efficiencies by using high-rise buildings comprised of steel moment frames with 30, 40 and 47 stories. For this purpose, a design process was developed to evaluate the nonlinear dynamic response of a building to different wind risk levels by incorporating a three dimensional nonlinear finite element model and an IDA (wind dynamic) analysis. The 47 story building was tested for wind pressure on a rigid scaled design at the Wall of Wind (WOW) facility at Florida International University. The wind loads were collected for the other two buildings using the aerodynamic database at Tokyo Polytechnic University. Based on accessible wind quality parameters and IDA results, the wind performance evaluation methodology was developed as a feature of the fundamental wind speed reflecting the predicted performance levels. Three wind performance types were evaluated: (a) performance of structural components; (b) performance of wind-induced shear deformation cladding; and (c) performance of comfort in serviceability motion. The evaluation of the results showed noticeable lateral capacity correlated with allowing controlled structural nonlinearity, as opposed to considerations required to satisfy acceptable serviceability and non-structural (such as cladding) performances. According to the results, it was concluded that high-rise buildings with braced or moment frames

having additional dampers and vibration control systems would benefit more efficiently in enabling the nonlinearity under control while maintaining certain performance aspects. The study also recommended to implement an engineering approach to ensure the effective diagnosis of existing structures subjected wind.

2.2.15 G. Bajaj, G. Bhaskar, 2016 [15]

An 11 story (one ground floor and 10 upper floors) RC frame construction with or without a shear wall was studied to assess the impact of wall orientation on the overall behavior of the building. For this purpose, a commercially available software package, Staad Pro, was used to examine and observe the displacements in various directions, flexibility, structural stability, the behavior of each different story, and cost. Based on the results, it was stated that the shear walls were effectively lessening the torsional impacts on buildings. It was also stated that if the columns were placed away from the shear walls, the effect of torsion on buildings was high when compared to the layout with columns located near the wall.

2.2.16 F. Steffen, 2016 [16]

Acceptable levels of acceleration in tall buildings with a height over than 200 meters have been specified in various building standards and codes. In this study, new equations were proposed to predict the acceleration of a tall building at an early stage of design using a mathematical method. The acceleration values of tall buildings that were subjected to wind loads were measured using both a numerical model and a model which reduced with Ritz-vectors. The findings from these two methods were compared. The study recommended using wind tunnel testing for tall buildings.

2.2.17 S. Ebrahimi, 2016 [17]

The effect of vertical ground motion portion on the responses of high building was presented. In this study, the consideration was given to the earthquakes with reversed faults and strike-slips with shorter or longer distance to fault. Due to the inclusion of the vertical excitations in the study, the main objective was on the structural responses. The first part of this analysis dealt with the in-depth definition of techniques for structural modeling. All building components were

modeled with nonlinear materials using different effective stiffnesses in order to capture the building's behavior more accurately. The second part of this study focused on the nonlinear time history analysis of the buildings. The influence of vertical ground movement component on structural behavior was discussed by comparing the structural responses of buildings. This study had the following conclutions: (a) the axial forces on the columns increased 20 percent to 120 percent by including the effects of an earthquake's vertical component, (b) the vertical ground movement component of an earthquake had a significant impact on the vertical acceleration of a slab, (c) if an earthquake's vertical component is included, it was seen that the change in the peak inter-story drifts and story shear responses was not significant.

2.2.18 M. Rokanuzzaman, F. Khanam, A. Das, and S. R. Chowdhury, 2017 [18]

This article focused on the impact of a shear wall location in a 16-story residential building. ETABS was used to model the buildings with different floor numbers. A total of three models were analyzed under lateral loading with different shear wall locations to evaluate the following parameters: base shear force and lateral displacements. Based on the analyses results, it was concluded that a building layout with a shear wall located in the center and at the four peripheral sides showed the best performance when the base shear forces and top displacements are considered.

2.2.19 E. Azimi, 2017 [19]

This study's main goal was to assist with the analysis of the effects of high winds on New York City's existing buildings. In order to determine the risk of wind generated debris from existing New York city buildings, different variables like age, height and building code regulations, were considered. The wind-related incidents history was then evaluated on a daily base using the reports issued by the National Oceanic and Atmospheric Administration from 2010 to 2015. From a total of 44,000 accidents associated with wind, only 1,400 were linked to the existing facilities. This study analyzed the specific elements of the building that could become a source for wind generated debris. The results showed that construction elements that were most likely to produce wind-generated debris were windows, followed respectively by

balcony elements, stairs/sidewalk sheds, roof elements, and exterior fixtures. It was recommended that a special attention should be given to these components, which had higher risks of causing accidents, by employing inspectors from a Façade Inspection Safety Program (FISP). A systematic methodology was established in this research by analyzing different major wind criteria to assess the local wind speed. The study aimed at contributing a better explanation to the results of high winds on existing facilities in New York City, and to provide opportunities to explore new means and methods in this field.

2.2.20 N. Longarini, L. Cabras, M. Zucca, S. Chapain, and A. Mousaad, 2017 [20]

A slender building's behavior under the effect of wind loads was investigated in order to meet the design criteria of both serviceability (comfort) and strength. In order to evaluate the winds effects, structural analysis and wind tunnel tests were carried out by using two procedures: Pressure Integration Method with the analysis of finite element and High-Frequency Force Balance (HFFB) techniques. The results of both methods were compared to those which were obtained from the Euro code and Italian development codes, stressing the need for further understanding of the problems which were related to the wind actions on the structures with high geometrical slenderness. In a comparative study, damping and structural solutions were proposed to reduce the effects of wind-induced loads. The proposed solutions included a reduction in height, using steel belts, viscous dampers, tuning damper and switch in orientation change. Each option is examined in detail including its limitations and advantages by quantifying the reductions in structural displacements design loads and accelerations. It was stated that an improvement in building’s damping would reduce vibrations and design loads, and thus would provide an optimal balance between sustainability requirements, serviceability, and resilience.

2.2.21 S. Thilakarathna, N. Anwar, P. Norachan, and F. Naja, 2018 [21]

In this study, the performance of high-rise buildings under the impact of earthquakes was evaluated according to various levels of lateral wind forces. In the dual framing system, a combination of reinforced concrete walls and special moment-resistant frame was jointly used to resist the lateral loads. The case study building was

located in a seismic area of intermediate level and was designed separately for wind loading at three different wind speeds (high, medium and low). The Nonlinear Response History Analysis was used to assess the inelastic seismic demand and to make a comparison for the seismic behavior of the building model. The study concluded that the wind loading level could change the seismic efficiency of dual-system high-rise buildings. Consequently, it was stated that a comprehensive seismic performance was required to ensure the overall integrity of a building.

2.2.22 A. Sai, G. Devi, 2018 [22]

In this paper, tall buildings' structural behaviors were studied when they were subjected to wind and earthquake loads by investigating their impacts with and without the P-delta effects on column axial forces, story displacements and moments, and base shear forces. In order to conduct this investigation, the buildings were assumed to be located in various areas which would generate low and high lateral loads. The study concluded that the results of the analyses made by hand calculations for the base shear forces, seismic weight, and lateral forces were approximately same as the results of the software analysis. Based on the analyses, it was stated that the effects of seismic and wind loads on buildings could be decreased by adding more shear walls into the framing system.

2.2.23 M. V. Kulkarni, C. Pise, C. Deshmukh, S. Kadam, G. Lakade, and Y. P. Pawar, 2018 [23]

The effects of wind and earthquake were examined and compared in this article. As a case study, buildings with varying heights (10, 20, 30, 40 and 50 story) were selected in Pune City in India. The earthquake and wind loads were applied to the building models constructed in ETABS by following the requirements in the Indian Standard Code on construction. The case study focused on the story shear forces, and on the comparison of the wind and earthquake load results. The study stated that the construction stage must be evaluated separately for critical wind and earthquake loads. Based on the analyses results, it was concluded that for short and medium-high rise buildings, earthquake was observed to be a lot more critical while wind load was more dominant on high-rise buildings.

2.2.24 M. Kumbhar, N. Vaidkar and U. Kalwane, 2018 [24]

In this article, a summary of seismic and wind analyses of multi-story buildings with various shapes of plan was presented. The following parameters were also considered in this study: the effect of shear walls, varying seismic zones, and wind speeds. The methods proposed by the other researchers were carried out on the wind and seismic analyses of the buildings with various shapes of floor layouts. In the evaluation stage of the results, story drift, base shear, lateral displacement, story shear, moments and axial forces were used. The floor layout shape that generated the lowest internal force values was considered to be the safest one. Based on the analyses results, it was concluded that the shape of building plan played a significant role in effectively resisting the lateral loads resulting from wind and earthquakes.

CHAPTER 3

PARAMETRIC STUDIES

3.1 Introduction

In order to demonstrate the effect of wind and earthquakes on different building layouts, structural analysis of different building models are required under the influence of these loads.

ETABS is used to perform the earthquake analysis, which is in full conformity with the Turkish Earthquake Code, 2019, (TEC 19). The earthquake forces are applied horizontally and vertically using a response spectrum method. For wind loads, the Turkish Standard, TS 498, and the American Code, ASCE 7-16, are used based on the exposures of the floor diaphragm extents.

The geographical location of the residential buildings is assumed to be on the seashore of Sinop, Turkey. This location is chosen deliberately since the region is characterized by its exposure to moderate level seismic forces as shown in TEC 19, as well as its approximate to the sea, which makes the buildings directly exposed to the wind forces so that a better comparison between the impact of earthquake and wind loads can be made.

The building models selected for this study differ in their layouts as well as in their heights. For this purpose, a total of 4 different building heights (10, 20, 30 and 40 story) is selected with two distinct layouts. The first layout shape is square and the second one is rectangular. Also, two building framing systems are adopted, the first one consists of columns and beam only while the second one consists of columns, beams and shear walls. For the shear walls, two alternatives are considered. In the first alternative, the walls are assumed to be located in the center of the floor (core walls). In the second alternative, the walls are placed at the four corners and around the perimeter of the floor layout.

3.2 Models Layouts information

In this part, the details of each building model; such as layouts, shapes, number of floors, heights, structural framing, and dimensions are be provided.

3.2.1 Layout No. 1

The shape of this layout is square and it consists of columns and beams (no shear walls). The floor plan has also an opening in its center that extends from the ground floor to the top one with an area of equal to 144 square meters as shown in Figure 3.1. This layout is used for the buildings with 10, 20, and 30 stories but is not used for the buildings with 40 stories due to their low lateral strength. The floor to floor height of all the buildings in this layout is selected 3 meters. The span length in both *x* and *y* directions is selected 6 meters with a total building width of 36 meters. The total area of each story is 1,296 m^2. The columns are connected to each other by beams, and the dimensions of the columns are changed at every five floors. However, the slab and beam dimensions are kept the same for throughout the building (see Table 3.1).

3.2.2. Layout No. 2

This layout is a square shaped one and consists of columns, beams and shear walls. Similar to the layout no.1, an opening is created in the center of each floor which existed along the building height with an area equal to 144 m^2. As shown in Figure 3.2, the shear walls are distributed around this opening. This layout is used for the buildings with 10, 20, 30, and 40 stories. The floor to floor height is 3 meters, and is kept the same for all buildings. The span length in both *x* and *y* directions is 6 meters, with an overall width and length of 36 meters. The total area of each story is 1,296 m^2. The columns are connected to each other by beams, and their dimensions are changed at every five floors. The thickness of the shear walls is changed at every 10 floors. However, the dimensions of slabs and beams are kept the same for all the floors (see Table 3.1).

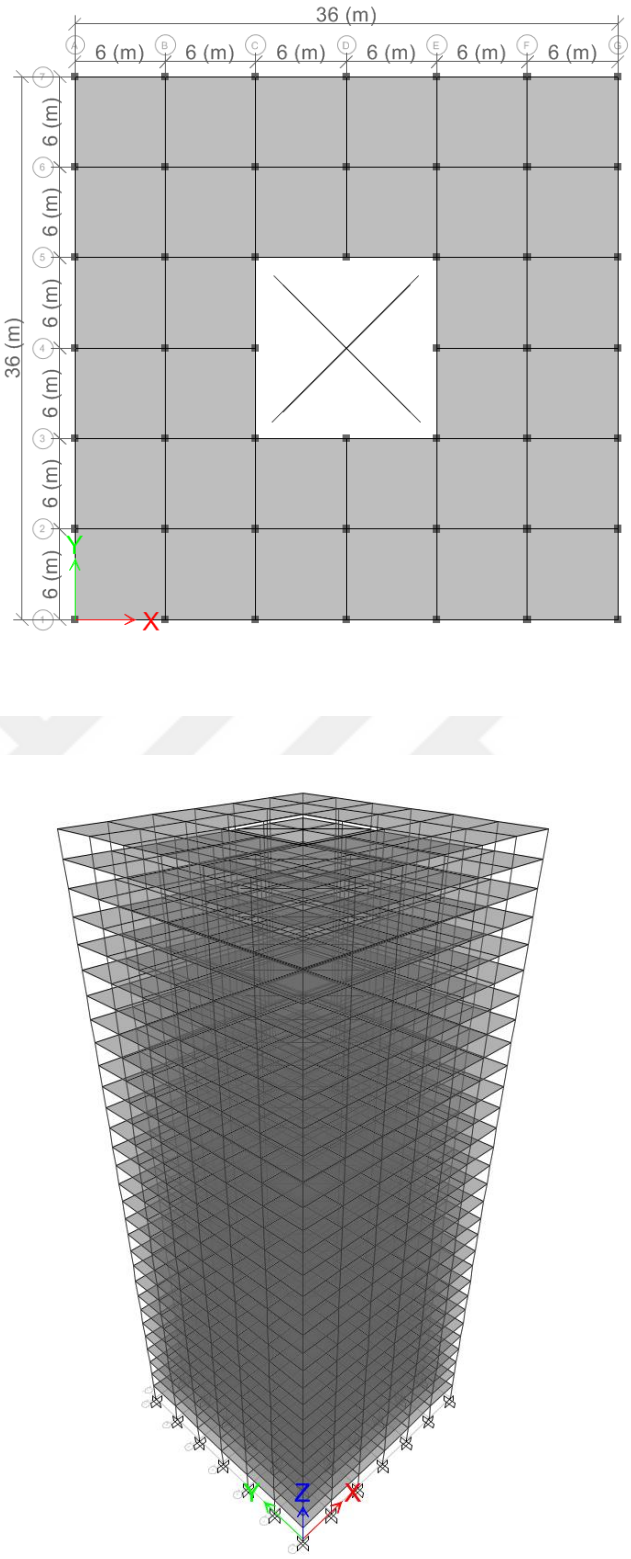

Figure 3.1 Layout No. 1

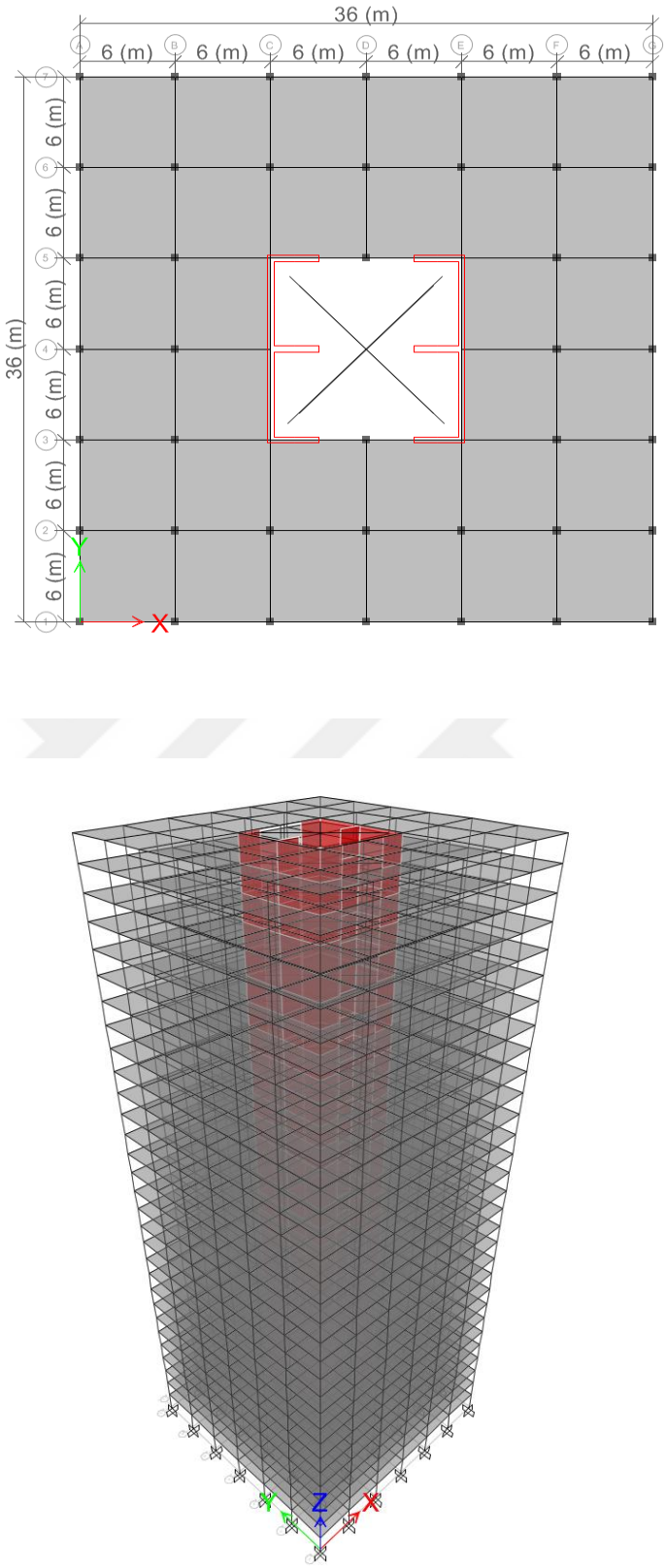

Figure 3.2 Layout No. 2

Table 3.1 Dimensions of Structural Elements

	10 Story Building		20 Story Building		30 Story Building		40 Story Building	
Story No.	**Column Dimension (cm)**	**Shear Wall Thickness (cm)**	**Column Dimension (cm)**	**Shear Wall Thickness (cm)**	**Column Dimension (cm)**	**Shear Wall Thickness (cm)**	**Column Dimension (cm)**	**Shear Wall Thickness (cm)**
1-5	70x70	40	90x90	50	110x110	60	130x130	70
6-10	50x50		80x80		100x100		120x120	
11-15	———	———	70x70	40	90x90	50	110x110	60
16-20	———		50x50		80x80		100x100	
21-25	———	———	———	———	70x70	40	90x90	50
26-30	———		———		50x50		80x80	
31-35	———	———	———	———	———	———	70x70	40
36-40	———		———		———		50x50	
Beam Dimensions for all buildings = 40x75 cm								
Slab Thickness for all buildings = 15 cm								

3.2.3 Layout No. 3

The total width of the building in this square shaped layout is 36 meters. The total area of each floor is 1,296 m^2 and the span length in each direction is 6 meters. The buildings consist of columns, beams and shear walls with an opening area of 144 m^2, which is located at the center of each floor extending along buildings' total heights. The shear walls are located around this opening as shown in Figure 3.3. This layout is used for the buildings with 10, 20, 30, and 40 stories. The floor to floor height is 3 meters for all the buildings. The columns are connected to each other by beams, and the dimensions of the columns are changed at every five floors. The thickness of the shear walls is changed at every 10 stories. The dimensions of all the slabs and beams remain the same for all floor levels, as shown in Table 3.1.

3.2.4 Layout 4

This layout is a rectangular shaped one, and it consists of columns and beams (no shear walls). The buildings with this layout have an opening with an area of 144 square meters located at the center of each floor, which extends along the height of the buildings (see Figure 3.4). This layout is used in the buildings with 10, 20, and 30 stories. The floor to floor height is 3 meters for all the buildings. The span length in both directions is 6 meters. The total width of the building is 24 meters and its length is 36 meters with a total floor area of 864 m^2. The columns are connected to each other by beams, and the dimensions of the columns are changed at every five floors. However, the dimensions of the slabs and beams are kept the same for all floors, as shown in Table 3.1.

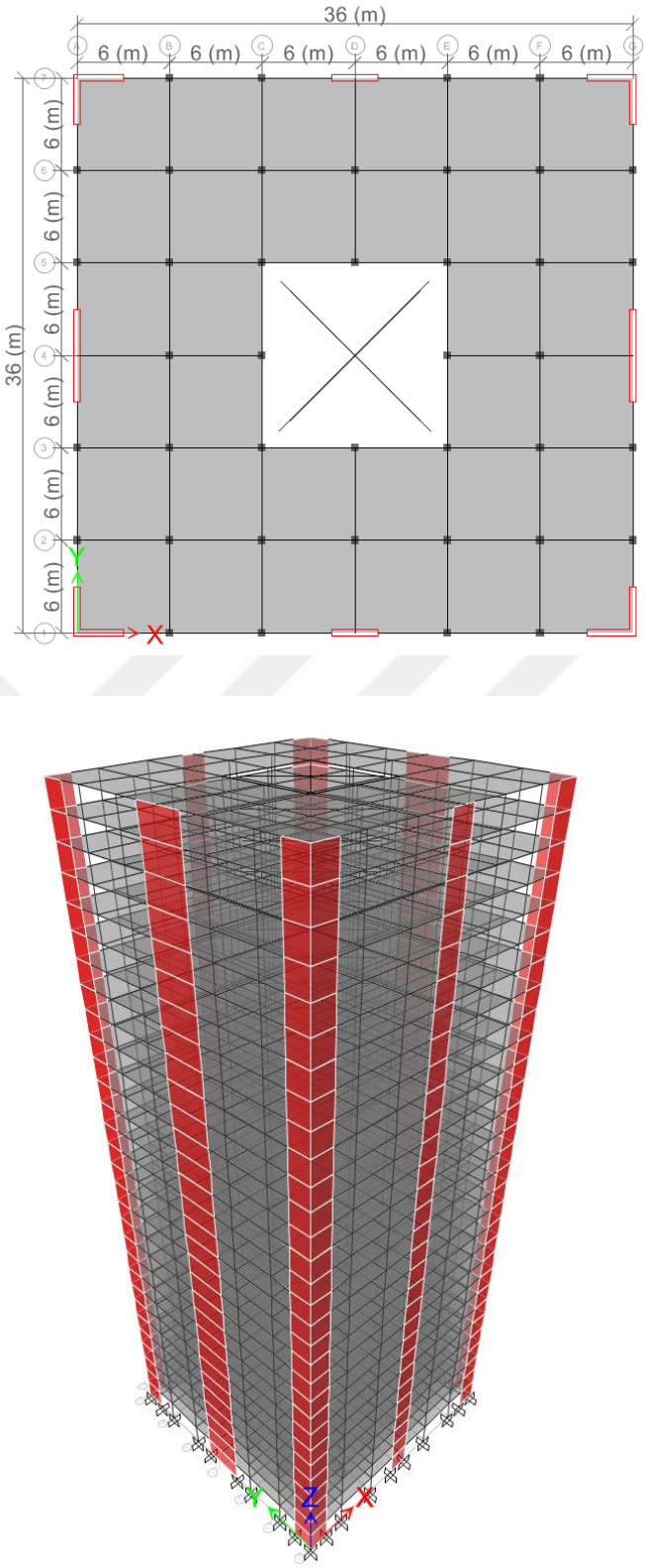

Figure 3.3 Layout No. 3

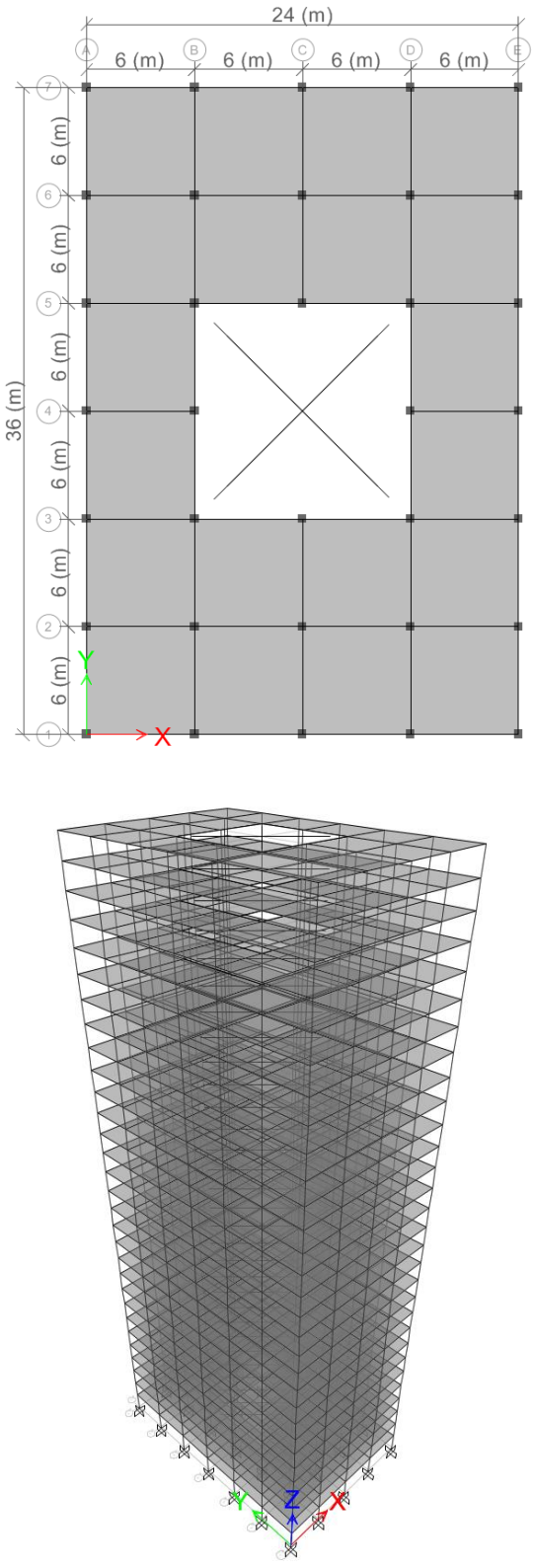

Figure 3.4 Layout No. 4

3.2.5 Layout No. 5

The total width of the building in this layout is 24 meters while its length is 36 meters, which makes it a rectangular shaped layout. The total area of each floor is 864 m^2. The span length in both directions is 6 meters. The layout consists of columns, beams and shear walls with an opening area of 144m^2 located at the center of each floor, which extends along the buildings' total heights. The shear walls are positioned around the opening as shown in Figure 3.5. This layout is used for the buildings with 10, 20, 30, and 40 stories. The story height for all the buildings is 3 meters. The columns are connected to each other by the beams. The dimensions of the columns are changed at every five floors while the thickness of the shear walls is changed at every 10 floors. The dimensions of the slabs and the beams are kept the same for all the stories as listed in Table 3.1.

3.2.6 Layout No. 6

Layout No. 6 is a rectangular one, with a length of 36 meters and a width of 24 meters occupying an area of 864 m^2 per floor. The span length in each direction is 6 meters. The structural elements that make up this layout are the columns, beams, and the shear walls, where the shear walls are positioned at the four corners of the buildings as well as along the mid-sections of the building perimeters (see Figure 3.6). This layout is used for the buildings with 10, 20, 30, and 40 stories. The thickness of the shear walls is changed at every 10 floors while the dimensions of the columns are changed at every five floors. The columns are connected to each other through the beams. The story height is 3 meters, and the same for all the buildings. The dimensions of the slabs and beams are kept the same for all the floors as listed in Table 3.1. Similar to the other layouts, there is an opening at the center of each building extending from the ground floor to the top one, with an area equal to 144 m^2.

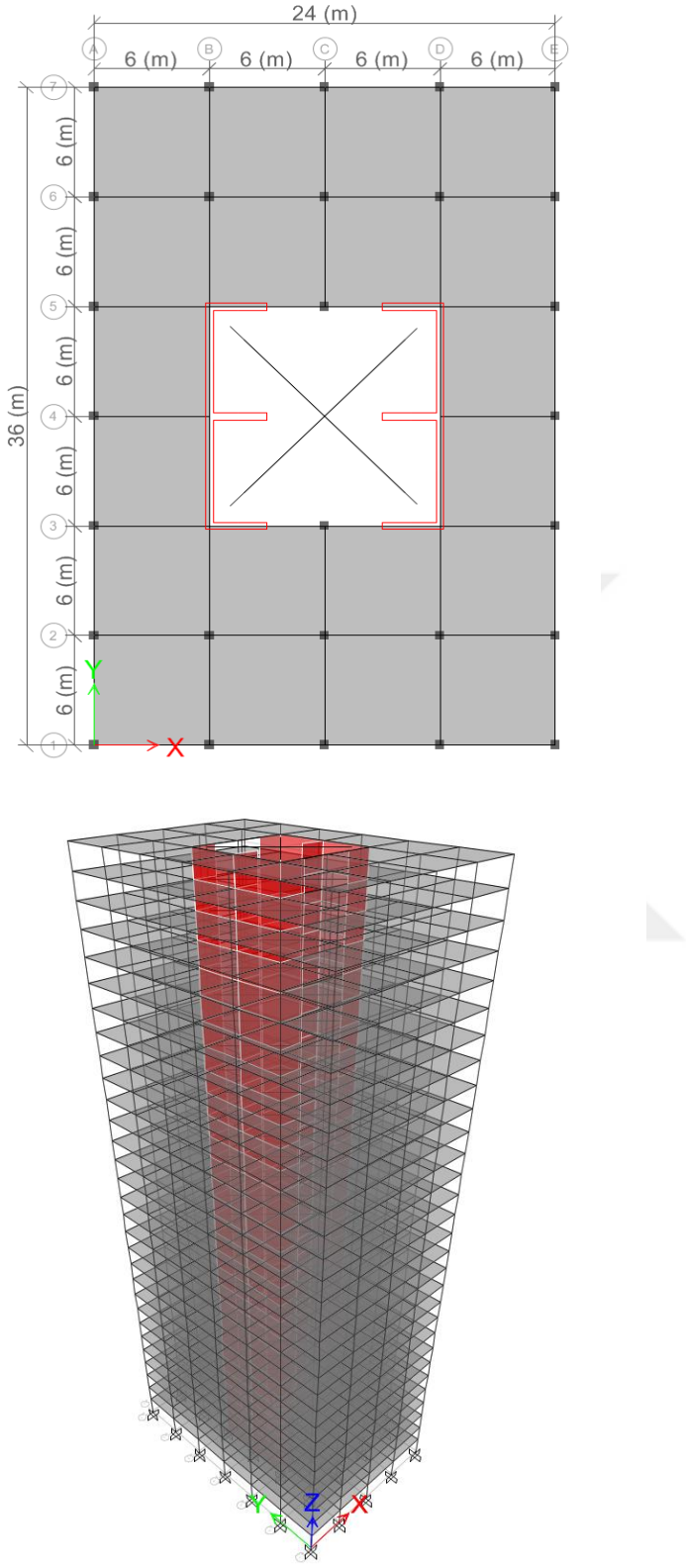

Figure 3.5 Layout No. 5

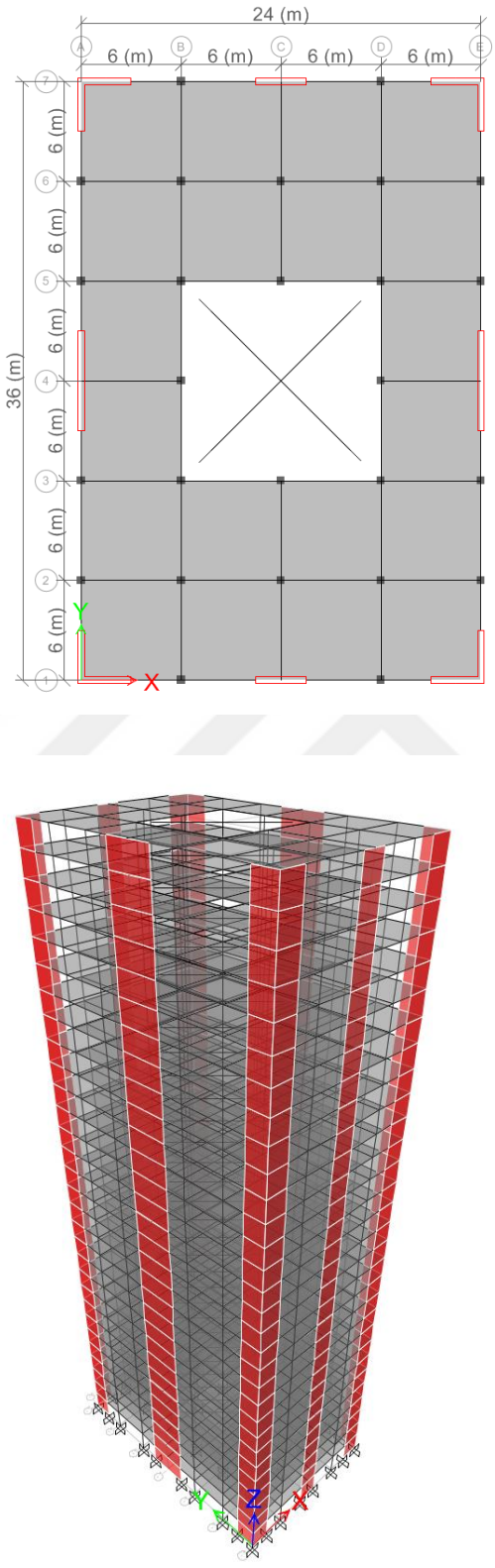

Figure 3.6 Layout No. 6

3.3. Material properties

For all structural elements, C35/C45 concrete is used. As stated in the Turkish Standards 500 (TS 500), the Poisson's Ratio of 0.2 is selected for C35. The modulus of elasticity for the C35 concrete is 33,000 MPa. In the self-weight calculations, the mass per unit weight for reinforced concrete is set equal to 2,500 kg/m^3. Since the study focuses on the analytical phase of the buildings, rebar specifications are not listed here.

3.4. Earthquake loads

The earthquake loads are calculated according to the details given in TEC 19. For this purpose, a total of 26 residential buildings are modeled. Their locations, as stated earlier, are determined to be in the city center of Sinop near the seashore. The details of the earthquake loads are provided in the next section.

3.4.1. TEC 19

The current Turkish earthquake code of TEC 19 is adopted to perform the dynamic analysis of the buildings under earthquake loads. As this stage depends on several earthquake parameters, they are discussed in detail in the next subsections.

a. Local Site Classes

Table 16.1 of TEC 19 specifies the site classes according to their composition from loose soil type to rock. The soil class ZB is assumed to be the soil class for all the building models in order not to encounter any problems with foundation types since weak soils with low bearing pressure might yield the use of piles.

b. Importance Factor (I):

Table 3.1 of TEC 19 describes the importance factor for various building types. Since the buildings in this study are all residential buildings, the importance factor is equal to 1. The building's occupancy class (BKS) is determined by using the same table as a value equal to 3 (BKS = 3).

c. Design stages

For tall buildings, there are three design stages in TEC 19. In constructing the models in ETABS; different coefficients are used for each stage. The details of these stages and the corresponding coefficients are explained below.

c.1. Design stage 1

The first design stage relies on DD2 type of earthquake with a return period of 475 years. The value of short second period, Ss, is 0.346, and the one second period, S1, is 0.135. These values are obtained for the building locations in Sinop using the earthquake hazard maps prepared by the Turkish Disaster and Emergency Management Authority (AFAD) [25]. The cracked concrete properties are selected at this design stage. The effective stiffness values of each structural element is obtained from Table 3.2 in TEC 19. In this design stage, the damping ratio for all buildings is assumed to be 5%, and the long-period (transition period) is set equal to 6 seconds. The structural system behavior factor is equal to 7 (R = 7), the system over strength is 2.5 (D = 2.5), and the occupancy class is 3 (BKS = 3), which yields to an importance factor of 1 (I=1) as shown in Table 3.1 of TEC 19.

Table 3.2 Effective Stiffness Values for DD2 in TEC 19

Component	Effective Stiffness Values	
Shear wall – slab (in plan)	Axial	Shear
Shear wall	0.50	0.50
Basement walls	0.80	0.50
Slabs	0.25	0.25
Shear wall- slab (out-of plan)	Flexural	Shear
Shear wall	0.25	1.00
Basement walls	0.50	1.00
Slabs	0.25	1.00
Structural members	Flexural	Shear
Coupling beams	0.15	1.00
Beams	0.35	1.00
Columns	0.70	1.00
Shear wall (equivalent column)	0.50	0.50

c.2 Design stage 2

The second design stage relies on DD4 types of earthquakes, which have a return period of 43 years. The values of the short second period, Ss is 0.076, and the one second period, S1 is 0.035, as per the earthquake hazard maps prepared by AFAD [25]. The cracked concrete properties are selected for this design stage. The stiffness values for the structural elements involved in the structure can be found in Table 3.3, which is directly taken from TEC 19. The damping ratio for all the buildings in this design stage is 2.5%, and the long-period (transition period) is set equal to 6 seconds. The structural system behavior factor is equal to 1 (R = 1), the system over strength (D = 1, and the importance factor is one (I = 1) as shown in Table 3.1 of TEC 19. This stage is used only for the tall buildings (the buildings with the following labels D4640, D4540, D4340 and D4240, see section 3.6 for the labels).

Table 3.3 Effective Stiffness Values for DD4 in TEC 19

Component	Effective Stiffness Values	
Shear wall – slab (in plan)	Axial	Shear
Shear wall	0.75	1.00
Basement walls	1.00	1.00
Slabs	0.50	0.80
Shear wall- slab (out-of plan)	Flexural	Shear
Shear wall	1.00	1.00
Basement walls	1.00	1.00
Slabs	0.50	1.00
Structural members	Flexural	Shear
Coupling beams	0.30	1.00
Beams	0.70	1.00
Columns	0.90	1.00
Shear wall (equivalent column)	0.80	1.00

Design stage 3

The design requirements for the third stage are not applied to the buildings since the higher lateral loads resulting from wind and earthquake loads are intended to be compared.

3.5 Wind loads

The effect of wind loads on buildings is similar to the effect of earthquake loads since they generate horizontal forces that need to be carefully evaluated in the case of tall buildings. This effect increases on taller and thinner buildings, especially those that are open or exposed.

Wind is strong in coastal areas due to the smooth surface of the water and the absence of obstacles. The land gains a higher thermal energy during the day than the sea as a result of solar radiation, which then leads to the formation of pressure differences resulting a wind movement from the sea towards the land. However, at night, the land cools faster than the sea, which causes winds to develop in the opposite direction from the land towards the sea. In order to include the effects of winds, the buildings in this study are assumed to be located near the shoreline of the city of Sinop.

The wind loads for each building model are be calculated twice, first according to the rules of TS 498, and then according to the rules and regulations of ASCE 7-16.

3.5.1 TS 498

The Turkish Standard, TS 498, defines the wind load related coefficients as a function of the following parameters:

a. Wind coefficients

In order to perform the wind loading in ETABS, it is necessary to determine the values of the wind coefficients specified in TS 498. These coefficients are the wind speeds denoted by "*V*" in m/sec, and it changes based on the building story height as shown in Table 5 of TS 498. The aerodynamic load coefficient, Cf, is set equal to 1.0 as per Section 11.2.2 of the standard. Therefore, the aerodynamics of the building shapes and façades are not included in the analysis stage.

b. Exposure Height

The building models are subjected to wind pressure with respect to each floor height from their base as listed in Table 5 of TS 498. Therefore, the varying wind pressures in line with the exposure height are applied to these buildings.

c. Wind Exposure Parameters

In this study, the wind loads are applied independently, first in the *x* direction at an angle of zero degrees, and then in the *y* axis at an angle of 90 degrees. External pressure coefficients for the windward and the leeward walls are set equal to 0.8 and 0.4, respectively (Cp coefficient is used for the windward direction and Cp coefficient is used for the leeward direction). However, for the buildings labeled D4640 and D4540 (for further information, please refer to Section 3.6) , the Cp in the windward direction is set equal to one while the one in the leeward direction is set equal to 0.6 since these buildings' definitions fit into tower type structures (or considered tall buildings).

d. Exposure and pressure coefficients

In this study, the option of exposure from the extent of each floor diaphragm as described in ETABS was selected to be the option in applying wind loads to the buildings.

3.5.2 ASCE 7–16

The rules and regulations specified in ASCE 7-16 are used to implement the wind loading in ETABS. According to ASCE 7-16, the wind loading depends on the exposure and pressure coefficients where the exposure is determined as the extent of each floor diaphragm. The wind pressure coefficients are automatically determined by the ETABS software as the wind exposure parameters.

a. Wind exposure parameters

1. Wind direction and exposure width

The wind is applied separately, once along the *x* axis at an angle of 0 degrees, and then along the *y* axis at an angle of 90 degrees.

2. Design wind load cases

All four loading cases are identified in 12 steps as shown in Figure 27.3-8 of ASCE 7-16. Tables 3.4 and 3.5 show the steps needed for the wind loading along with the associated wind angles, cases and eccentricities, which are denoted by e1 and e2 ratios.

Table 3.4 Wind Loading Parameters in *x* Direction According to ASCE 7-16

Step	Angle	ASCE Case	e1 Ratio	e2 Ratio
1	0	1	0	0
2	90	1	0	0
3	0	2	0.15	0
4	0	2	-0.15	0
5	90	2	0.15	0
6	90	2	-0.15	0
7	0	3	0	0
8	90	3	0	0
9	0	4	0.15	0.15
10	0	4	-0.15	-0.15
11	90	4	0.15	0.15
12	90	4	-0.15	-0.15

Table 3.5 Wind Loading Parameters in *y* Direction According to ASCE 7-16

Step	Angle	ASCE Case	e1 Ratio	e2 Ratio
1	90	1	0	0
2	180	1	0	0
3	90	2	0.15	0
4	90	2	-0.15	0
5	180	2	0.15	0
6	180	2	-0.15	0
7	90	3	0	0
8	180	3	0	0
9	90	4	0.15	0.15
10	90	4	-0.15	-0.15
11	180	4	0.15	0.15
12	180	4	-0.15	-0.15

3. Eccentricity Ratios for e1 and e2

The eccentricity ratios in the principal *x* and *y* axes (e1 and e2) are -0.15, 0 and 0.15 as listed in Tables 3.4 and 3.5, which are in line with the information given in Figure 27.3-8 of ASCE 7-16.

b. Wind coefficients

1. Wind speed (V)

The wind speed values are adopted from TS 498 by converting the values from m/sec to mph. It is important to note that the wind speed is a variable determined base the height of each floor, as shown in the Table 3.6.

Table 3.6 Wind speed according to ASCE 7-16

Story number	Height (m)	Wind speed (mph)
Base - 3	0 - 9	62.63
4 - 7	10 - 21	80.53
8- 33	22 - 100	93.95
34 - 40	> 100	102.90

2. Exposure type

The type of exposure in these buildings is assumed to be D (surface roughness) due to the fact that they are all located next to the sea as determined according to Section 26.7.3 of ASCE 7-16.

3. Ground height factor (Ke)

It is the factor that controls the density of air, and is set equal to one as described in Table 26.9-1 of ASCE 7-16.

4. Topographic factor (Kzt)

The Kzt in this study is set equal to one which is in line with the requirements of Section 26.8.2 of ASCE 7-16.

5. Gust-effects factor (Gf)

The value of this parameter changes from one building to another depending on the value of the frequency of the building under consideration. The gust-effect factors for each building are listed in Table 3.7.

6. Wind directionality factor (Kd)

The direction of wind has an effect on the wind loads, and it depends on the rational analysis of the different wind speeds. The value of the wind direction coefficient, Kd, in this study is set equal to 0.85 as defined in Table 26.6 -1 of ASCE 7-16.

Table 3.7 Gust-Effect Factor

Model name	Gust factor
D2640	1.03
D2540	1.03
D2340	1.03
D2240	1.02
D4640	0.97
D4540	0.97
D4340	1.00
D4240	0.97
D2630	0.98
D2530	0.98
D2430	1.04
D2330	1.02
D2230	1.02
D2130	1.10
D2620	0.93
D2520	0.93
D2420	0.96
D2320	0.93
D2220	0.93
D2120	0.96
D2610	0.85
D2510	0.89
D2410	0.99
D2310	0.85
D2210	0.89
D2110	0.91

3.6. Modeling in ETABS

ETABS is the acronym for extended 3D analysis of a building system. It is a program that specializes in the analysis and design of facilities under any type of loading, including earthquake and wind loads using either static or dynamic approach.

The 26 building models are constructed in ETABS. The Turkish Earthquake Code, TEC 19, is used to carry out the earthquake analyses of the buildings according to the response spectrum method, which is applied both in *x* and *y* directions. As for the wind load analysis, the TS 498 and ASCE 7-16 generated loads are applied separately again both in *x* and *y* directions. In ETABS, all the buildings are assumed to be fixed at the base, and that the diaphragm is a rigid one.

Each building model is labeled according to the following method. A total of 5 digits are used for each model. The first two digits, including a letter and a number, symbolizes the earthquake design stage. The third digit in the label is used to define the layout number. Finally, the last two digits are used to describe the total number of floors. For example, in the building labeled D2640, the symbol D2 indicates the first design stage DD2, the number 6 refers to the layout number 6, and the number 40 refers to a 40 story building. Table 3.8 has the list of all 26 building labels.

Table 3.8 Building Names

Building Name	Earthquake Type	Layout No.	Number of Floors	Building Height (m)
D4640	DD4	6	40	120
D4540	DD4	5	40	120
D4340	DD4	3	40	120
D4240	DD4	2	40	120
D2640	DD2	6	40	120
D2540	DD2	5	40	120
D2340	DD2	3	40	120
D2240	DD2	2	40	120
D2630	DD2	6	30	90
D2530	DD2	5	30	90
D2430	DD2	4	30	90
D2330	DD2	3	30	90
D2230	DD2	2	30	90
D2130	DD2	1	30	90
D2620	DD2	6	20	60
D2520	DD2	5	20	60
D2420	DD2	4	20	60
D2320	DD2	3	20	60
D2220	DD2	2	20	60
D2120	DD2	1	20	60
D2610	DD2	6	10	30
D2510	DD2	5	10	30
D2410	DD2	4	10	30
D2310	DD2	3	10	30
D2210	DD2	2	10	30
D2110	DD2	1	10	30

Table 3.9 shows the load combinations used in ETABS. All of the symbols used in Table 3.9 are explained in detail in Table 3.10.

Table 3.9 Load Combinations

No.	Load Combination Equation
1	$1.4\ D + 1.4\ SD + 1.6\ L$
2	$D + SD + 0.3\ L$
3	$D + SD + L \pm S_X$
4	$D + SD + L \pm S_Y$
5	$D + SD + L \pm S_X \pm 0.3\ S_Y$
6	$D + SD + L \pm 0.3\ S_X \pm S_Y$
7	$\pm S_X \pm 0.3\ S_Y$
8	$\pm 0.3\ S_X \pm S_Y$
9	$D + L + 0.2\ Sn \pm S_X \pm 0.3\ S_X^Z$
10	$D + L + 0.2\ Sn \pm S_Y \pm 0.3\ S_Y^Z$
11	$D + L + 0.2\ Sn \pm S_X \pm 0.3\ S_Y + 0.3\ S_X^Z$
12	$D + L + 0.2\ Sn \pm 0.3\ S_X \pm S_Y + 0.3\ S_Y^Z$
13	$D + 1.3\ L \pm 1.3\ W_X$
14	$D + 1.3\ L \pm 1.3\ W_Y$
15	$0.9\ D \pm 1.3\ W_X$
16	$0.9\ D \pm 1.3\ W_Y$

Table 3.10 Symbols Used in Load Combinations

Symbol No.	Symbol	Load Type
1	D	Dead load
2	L	Live load
3	SD	Superimposed dead load
4	Sn	Snow load
5	Sx	Seismic load in X direction
6	Sy	Seismic load in Y direction
7	Sx^z	Seismic load in Z direction for the X axis
8	Sy^z	Seismic load in Z direction for the Y axis
9	Wx	Wind load in X direction
10	Wy	Wind load in Y direction

CHAPTER 4

RESULTS OF PARAMETRIC STUDY

4.1 Results

In order to discuss the analytical results of the buildings that are subjected to code prescribed earthquake and wind loads (TEC 19 for the earthquake load, and TS 498 and ASCE 7-16 for the wind loads), the buildings are divided into different groups according to their number of floors and the six layouts whose details are explained in Section 3.2. In the case of the 40 story buildings since the buildings are considered tall, the results are discussed in two groups based on the expected earthquake levels; one for the DD4 type of earthquakes, and the other for the DD2 ones where both groups consist of four layouts. The analytical results are investigated by studying the following parameters: base shear force, maximum story displacement, fundamental periods, maximum story drift, and the weight of each building.

4.2 Building Details

In order to clarify the results of the analysis process for all the building models under the influence of lateral loads, and to simplify the comparison process between these results, the buildings are divided into five groups. Each group has the same number of floors and height, and is exposed to the same type of earthquakes keeping in mind that each building has a different layout from the others within the same group. The further details of these groups are explained in the next subsections.

4.2.1 Group No. 1

This group consists of four building models. Each model has its own layout that differs from each other. All of these 40-story models with a height of 120 meters are subjected to the DD4 earthquake type, and the wind loads of TS498 and ASCE 7-16.

4.2.2 Group No. 2

All the models in this group have 40 floors with a total height of 120 meters. The group consists of four buildings with different layouts which are all subjected to the DD2 earthquake types and the wind loads of TS498 and ASCE 7-16.

4.2.3 Group No. 3

This group consists of six building models. Each model has its own unique layout. All the models have 30 floors with a total height of 90 meters, and they are all subjected to the DD2 earthquake type and the wind loads of TS498 and ASCE 7-16.

4.2.4 Group No. 4

All the models in this group have 20 floors with a total height of 60 meters. This group consists of six buildings with different layouts, which are subjected to the DD2 earthquake type and the wind loads of TS498 and ASCE 7-16.

4.2.5 Group No. 5

In this group, the comparison is made among 6 different building models with each model has its own layout. All the models are 10 stories with a total height of 30 meters. The buildings in this group are all subjected to the same earthquake type load of DD2 type and to the wind loads of TS498 and ASCE 7-16.

4.3 Base Shear

In this section, the results of the base shear forces of all building models are discussed. The base shear force in each building is calculated for the following three cases; first for the earthquake load calculated according to TEC 19, second for the wind load extracted from TS 498, and finally for the wind load determined according to ASCE 7-16. The results of the five groups are investigated in the next subsections.

4.3.1 Group No. 1 (40 story buildings with DD4)

a. Building Model D4640

Table 4.1 lists the base shear forces for the model D4640. Based on the results, it can be observed that the base shear force resulting from the wind loads of ASCE 7-16 acting in the direction of *x* axis is higher than the one acting in the direction of *y* axis. The same conclusion is valid for the base shear forces of TS 498. As for the earthquake loads, the base shear force in the *y* direction is higher than the one in the *x* direction, which is opposite to the outcome of the wind load case. The wind loads in both directions from TS 498 and ASCE 7-16 are larger than their counterparts resulting from TEC 19. The results also indicate that the weight of the building used in the wind loads is higher than the one used in the earthquake loads.

Table 4.1 Base Shear Forces for the Building Model D4640

ASCE (1) STEP 1/CASE 1				TS 498 (1)				TEC 19 (1)			
W_x (kN)		W_y (kN)		W_x (kN) COMB 45 (2)		W_y (kN) COMB 46 (2)		S_x (kN)		S_y (kN)	
F_x	F_y	F_x	F_y	F_x	F_y	F_x	F_y	F_x	F_y	F_x	F_y
6337	0	0	3871	6766	0	0	4510	2686	0.5	0.5	2951

(1) The total seismic weight of the building is 385,855 kN. The total weight of the building for the wind loads is 386,611 kN.

(2) For the details of the load combination, see Appendix A.

b. Building Model D4540

The base shear forces of the model D4540 are given in Table 4.2. The force under the wind loads of TS 498 acting in the direction of *x* axis is higher than the one in the direction of *y* axis. The results from ASCE 7-16 confirm the same outcome. However, the earthquake generated base shear forces resulted higher value in the *y* direction. The highest value of the base shear is due to wind loads of TS 498 in the *x* direction while the lowest value is due to earthquake loads of TEC 19. According to the results, it can be observed that the weight of the building used in the wind loads is higher than the weight used in the earthquake loads.

Table 4.2 Base Shear for Building Model D4540

ASCE [1] STEP 1/CASE 1				TS 498 [1]				TEC 19 [1]			
W_x (kN)		W_y (kN)		W_x (kN) COMB 45 [2]		W_y (kN) COMB 46 [2]		S_x (kN)		S_y (kN)	
F_x	F_y	F_x	F_y	F_x	F_y	F_x	F_y	F_x	F_y	F_x	F_y
6344	0	0	3875	6766	0	0	4510	2725	1.2	1.2	4300

(1) The total seismic weight of the building is 393,033 kN. The total weight of the building for the wind loads is 393,789 kN.

(2) For the details of the load combination, see Appendix A.

c. Building Model D4340

In this building model, the base shear forces resulting from the wind loads acting in the *x* and *y* directions according to ASCE 7-16 are equal to each other (see Table 4.3). The same outcome is observed for the base shear forces of TS 498. In the earthquake load case, the base shear value is higher in the *y* direction. As listed in Table 4.3, it can be observed that the highest value of the base shear is due to the wind loads of ASCE 7-16, while the lowest value is due to earthquake load of TEC 19 acting in the *x* direction. The weight of the building according to the wind loads is higher than the weight according to the earthquake loads.

Table 4.3 Base Shear for Building Model D4340

ASCE [1] STEP 1/CASE 1				TS 498 [1]				TEC 19 [1]			
W_x (kN)		W_y (kN)		W_x (kN) COMB 45 [2]		W_y (kN) COMB 46 [2]		S_x (kN)		S_y (kN)	
F_x	F_y	F_x	F_y	F_x	F_y	F_x	F_y	F_x	F_y	F_x	F_y
6507	0	0	6507	5074	0	0	5074	3448	0	0	3910

(1) The total seismic weight of the building is 574,551 kN. The total weight of the building for the wind loads is 575,760 kN.

(2) For the details of the load combination, see Appendix A.

d. Building Model D4240

Table 4.4 has the base shear forces of the Model D4240. Based on the results, it can be observed that the value of the base shear in the *y* direction is higher than the value

in the *x* direction when the building is subjected to the earthquake loads of TEC 19. The base shear forces of the wind loading from ASCE 7-16 are equal to each other both in the *x* and *y* directions. The same observation is valid for the wind loading case of TS 498. In this building model, the highest value of the base shear is due to the wind loads of ASCE 7-16, while the lowest one is due to the earthquake loads of TEC 19 acting in the *x* direction. Based on the results, it can be concluded that the weight of the building according to the wind loads is higher than the weight according to the earthquake loads.

Table 4.4 Base Shear for Building Model D4240

ASCE (1) STEP 1/CASE 1				TS 498 (1)				TEC 19 (1)			
W_x (kN)		W_y (kN)		W_x (kN) COMB 45 (2)		W_y (kN) COMB 46 (2)		S_x (kN)		S_y (kN)	
F_x	F_y	F_x	F_y	F_x	F_y	F_x	F_y	F_x	F_y	F_x	F_y
6305	0	0	6305	5074	0	0	5074	4059	0.2	0.2	5818

(1) The total seismic weight of the building is 582,130 kN. The total weight of the building for the wind loads is 583,340 kN.

(2) For the details of the load combination, see Appendix A.

4.3.2 Group No. 2 (40 story buildings with DD2)

a. Building Model D2640

Table 4.5 lists the base shear forces for the model D2640. Based on the results, it can be observed that the base shear force resulting from the wind loads of ASCE 7-16 acting in the direction of *x* axis is higher than the one acting in the direction of *y* axis. The same conclusion is valid for the base shear forces of TS 498. As for the earthquake loads, the base shear force in the *y* direction is higher than the one in the *x* direction, which is opposite to the outcome of the wind load case. The base shear from earthquake loads generates larger base shear forces than those from the wind loads of both TS 498 and ASCE 7-16. The results also indicate that the weight of the building used in the wind loads is slightly higher than the one used in the earthquake loads.

Table 4.5 Base Shear for Building Model D2640

ASCE [1] STEP 1/CASE 1				TS 498 [1]				TEC 19 [1]			
W_x (kN)		W_y (kN)		W_x (kN) COMB 45 [2]		W_y (kN) COMB 46 [2]		S_x (kN)		S_y (kN)	
F_x	F_y	F_x	F_y	F_x	F_y	F_x	F_y	F_x	F_y	F_x	F_y
6729	0	0	4110	6766	0	0	4510	8445	0.3	0.3	9636

(1) The total seismic weight of the building is 384,734 kN. The total weight of the building for the wind loads is 385,490 kN.

(2) For the details of the load combination, see Appendix A.

b. Building Model D2540

The base shear forces of the model D2540 are given in Table 4.6. The force under the wind loads of TS 498 acting in the direction of *x* axis is higher than the one acting in the direction of *y* axis. The results from ASCE 7-16 confirm the same outcome. However, the earthquake generated base shear forces resulted higher value in the *y* direction. The highest value of the base shear is due to the earthquake loads of TEC 19 acting in the *y* direction while the lowest value is due to the wind loads of ASCE 7-16 acting again in the *y* direction. According to the results, it can be observed that the weight of the building used in the wind loads is higher than the weight used in the earthquake loads.

Table 4.6 Base Shear for Building Model D2540

ASCE [1] STEP 1/CASE 1				TS 498 [1]				TEC 19 [1]			
W_x (kN)		W_y (kN)		W_x (kN) COMB 45 [2]		W_y (kN) COMB 46 [2]		S_x (kN)		S_y (kN)	
F_x	F_y	F_x	F_y	F_x	F_y	F_x	F_y	F_x	F_y	F_x	F_y
6729	0	0	4110	6766	0	0	4510	8670	0.5	0.5	13989

(1) The total seismic weight of the building is 329,236 kN. The total weight of the building for the wind loads is 392,992 kN.

(2) For the details of the load combination, see Appendix A.

c. Building Model D2340

In this building model, the base shear forces resulting from the wind loads of ASCE 7-16 acting both in the *x* and *y* directions are equal to each other (see Table 4.7). The same outcome is also observed for the base shear forces of TS 498. In the earthquake load case, the base shear value is higher in the *y* direction. As listed in Table 4.7, it can be observed that the highest value of the base shear is due to the earthquake loads of TEC 19 acting in the *y* direction, while the lowest one is due to the wind load of TS 498 acting both in the *x* and *y* directions. The weight of the building according to the wind loads is slightly higher than the weight according to the earthquake loads.

Table 4.7 Base Shear for Building Model D2340

ASCE (1) STEP 1/CASE 1				TS 498 (1)				TEC 19 (1)			
W_x (kN)		W_y (kN)		W_x (kN) COMB 45 (2)		W_y (kN) COMB 46 (2)		S_x (kN)		S_y (kN)	
F_x	F_y	F_x	F_y	F_x	F_y	F_x	F_y	F_x	F_y	F_x	F_y
6729	0	0	6729	5074	0	0	5074	12240	0	0	13791

(1) The total seismic weight of the building is 574,551 kN. The total weight of the building for the wind loads is 575,760 kN.

(2) For the details of the load combination, see Appendix A.

d. Building Model D2240

Table 4.8 has the base shear forces of the model D2240. Based on the results, it can be observed that the value of the base shear in the *y* direction is higher than the value in the *x* direction when the building is subjected to the earthquake loads of TEC 19. The base shear forces of the wind loading from ASCE 7-16 is equal to each other in both *x* and *y* directions. The same observation is valid for the wind loading case of TS 498. In this building model, the highest value of the base shear is obtained from to the earthquake loads of ASCE 7-16, while the lowest one is obtained from the wind loading of TEC 19 acting both in the *x* and *y* directions. Based on the results, it can be concluded that the weight of the building according to the wind loads is slightly higher than the weight according to the earthquake loads.

Table 4.8 Base Shear for Building Model D2240

ASCE [1] STEP 1/CASE 1				TS 498 [1]				TEC 19 [1]			
W_x (kN)		W_y (kN)		W_x (kN) COMB 45 [2]		W_y (kN) COMB 46 [2]		S_x (kN)		S_y (kN)	
F_x	F_y	F_x	F_y	F_x	F_y	F_x	F_y	F_x	F_y	F_x	F_y
5161	0	0	6683	5074	0	0	5074	12708	0.6	0.6	19065

(1) The total seismic weight of the building is 583,130 kN. The total weight of the building for the wind loads is 583,340 kN.

(2) For the details of the load combination, see Appendix A.

4.3.3 Group No. 3 (30 story buildings with DD2)

a. Building Model D2630

Table 4.9 lists the base shear forces of the Model D2630. According to the table, the base shear forces of TS 498 acting in the direction of *x* axis is higher than the one acting in the direction of *y* axis. The same outcome is also valid for the wind loads of ASCE 7-16. However, in the earthquake load case, the base shear value is higher in the *y* direction. The highest value of the base shear is from the seismic loads acting in the *y* direction, while the lowest one is from the wind loads of TS 498 acting in the *y* direction. Based on the results, the earthquake generated base shear forces are higher than the ones generated by the wind loads of TS 498 and ASCE 7-16. The weight of the building used in the wind loads is higher than the one in the earthquake loads.

Table 4.9 Base Shear for Building Model D2630

ASCE [1] STEP 1/CASE 1				TS 498 [1]				TEC 19 [1]			
W_x (kN)		W_y (kN)		W_x (kN) COMB 45 [2]		W_y (kN) COMB 46 [2]		S_x (kN)		S_y (kN)	
F_x	F_y	F_x	F_y	F_x	F_y	F_x	F_y	F_x	F_y	F_x	F_y
4641	0	0	2835	3617	0	0	2411	7753	0.3	0.3	8807

(1) The total seismic weight of the building is 270,686 kN. The total weight of the building for the wind loads is 271,442 kN.

(2) For the details of the load combination, see Appendix A.

b. Building Model D2530

The base shear forces of the model D2530 are given in Table 4.10. The force under the wind loads of TS 498 acting in the direction of *x* axis is higher than the one acting in the direction of *y* axis. The results from ASCE 7-16 confirm the same outcome. However, the earthquake generated base shear forces result higher base shear value in the *y* direction. The highest value of the base shear is due to the earthquake loads of TEC 19 acting in the *y* direction while the lowest one is due to the wind loads of TS 498 acting again in the *y* direction. According to the results, it can be observed that the weight of the building used in the wind loads is slightly higher than the weight used in the earthquake loads.

Table 4.10 Base Shear for Building Model D2530

ASCE (1) STEP 1/CASE 1				TS 498 (1)				TEC 19 (1)			
W_x (kN)		W_y (kN)		W_x (kN) COMB 45 (2)		W_y (kN) COMB 46 (2)		S_x (kN)		S_y (kN)	
F_x	F_y	F_x	F_y	F_x	F_y	F_x	F_y	F_x	F_y	F_x	F_y
4627	0	0	2826	3617	0	0	2411	8038	0.5	0.5	13356

(1) The total seismic weight of the building is 276,128 kN. The total weight of the building for the wind loads is 276,884 kN.

(2) For the details of the load combination, see Appendix A.

c. Building Model D2430

Table 4.11 lists the base shear forces of the Model D2430. According to the table, the base shear forces of TS 498 acting in the direction of *x* axis is higher than the one acting in the direction of *y* axis. The same outcome is also valid for the wind loads of ASCE 7-16. However, in the earthquake load case, the base shear value is higher in the *y* direction. The highest value of the base shear is from the earthquake loads acting in the *y* direction, while the lowest one is from the wind loads of TS 498 acting in the *y* direction. Based on the results, the earthquake generated base shear forces are higher than the ones generated by the wind loads of TS 498 and ASCE 7-16. The weight of the building used in the earthquake loading is higher than the weight used in the wind loading.

Table 4.11 Base Shear for Building Model D2430

ASCE [1] STEP 1/CASE 1				TS 498 [1]				TEC 19 [1]			
W_x (kN)		W_y (kN)		W_x (kN) COMB 45 [2]		W_y (kN) COMB 46 [2]		S_x (kN)		S_y (kN)	
F_x	F_y	F_x	F_y	F_x	F_y	F_x	F_y	F_x	F_y	F_x	F_y
4925	0	0	3008	3617	0	0	2411	5173	0	0	5236

(1) The total seismic weight of the building is 267,128 kN. The total weight of the building for the wind loads is 246,284 kN.

(2) For the details of the load combination, see Appendix A.

d. Building Model D2330

In this building model, the base shear forces resulting from the wind loads of ASCE 7-16 acting both in the *x* and *y* directions are equal to each other (see Table 4.12). The same outcome is also observed for the base shear forces of TS 498. In the earthquake load case, the base shear value is higher in the *y* direction. As listed in Table 4.12, it can be observed that the highest value of the base shear is due to the earthquake loads of TEC 19 acting in the *y* direction, while the lowest one is due to the wind loading of TS 498 acting both in the *x* and *y* directions. The weight of the building according to the wind loads is slightly higher than the weight according to the earthquake loads.

Table 4.12 Base Shear for Building Model D2330

ASCE [1] STEP 1/CASE 1				TS 498 [1]				TEC 19 [1]			
W_x (kN)		W_y (kN)		W_x (kN) COMB 45 [2]		W_y (kN) COMB 46 [2]		S_x (kN)		S_y (kN)	
F_x	F_y	F_x	F_y	F_x	F_y	F_x	F_y	F_x	F_y	F_x	F_y
4797	0	0	4797	3617	0	0	3617	9932	0	0	11548

(1) The total seismic weight of the building is 398,663 kN. The total weight of the building for the wind loads is 399,873 kN.

(2) For the details of the load combination, see Appendix A.

e. Building Model D2230

Table 4.13 has the base shear forces of the Model D2230. Based on the results, it can be observed that the value of the base shear in the *y* direction is higher than the value in the *x* direction when the building is subjected to the earthquake loads of TEC 19. The base shear forces of the wind loading from ASCE 7-16 are equal to each other both in the *x* and *y* directions. The same observation is valid for the wind loading case of TS 498. In this building model, the highest value of the base shear is due to the earthquake loads of TEC 19 acting in the *y* direction, while the lowest one is due to the wind loads of TS 498 acting both in the *x* and *y* directions. Based on the results, it can be concluded that the weight of the building according to the wind loads is slightly higher than the weight according to the earthquake loads.

Table 4.13 Base Shear for Building Model D2230

ASCE (1) STEP 1/CASE 1				TS 498 (1)				TEC 19 (1)			
W_x (kN)		W_y (kN)		W_x (kN) COMB 45 (2)		W_y (kN) COMB 46 (2)		S_x (kN)		S_y (kN)	
F_x	F_y	F_x	F_y	F_x	F_y	F_x	F_y	F_x	F_y	F_x	F_y
4797	0	0	4797	3617	0	0	3617	9957	0.5	0.5	16420

(1) The total seismic weight of the building is 400,275 kN. The total weight of the building for the wind loads is 401,485 kN.

(2) For the details of the load combination, see Appendix A.

f. Building Model D2130

In this building model, the base shear forces resulting from the wind loads of ASCE 7-16 acting both in the *x* and *y* directions are equal to each other (see Table 4.14). The same outcome is also observed for the base shear forces of TS 498. In the earthquake load case, the base shear value is slightly higher in the *y* direction. As listed in Table 4.14, it can be observed that the highest value of the base shear is due to the earthquake loads of TEC 19 acting in the *y* direction, while the lowest one is due to the wind loading of TS 498 acting both in the *x* and *y* directions. The weight of the building according to the wind loads is slightly higher than the weight according to the earthquake loads.

Table 4.14 Base Shear for Building Model D2130

ASCE [1] STEP 1/CASE 1				TS 498 [1]				TEC 19 [1]			
W_x (kN)		W_y (kN)		W_x (kN) COMB 45 [2]		W_y (kN) COMB 46 [2]		S_x (kN)		S_y (kN)	
F_x	F_y	F_x	F_y	F_x	F_y	F_x	F_y	F_x	F_y	F_x	F_y
5213	0	0	5213	3617	0	0	3617	6409	0	0	6646

(1) The total seismic weight of the building is 368,201 kN. The total weight of the building for the wind loads is 369,411 kN.

(2) For the details of the load combination, see Appendix A.

4.3.4 Group No. 4 (20 story buildings with DD2)

a. Building Model D2620

Table 4.15 lists the base shear forces of the Model D2620. According to the table, the base shear forces of TS 498 acting in the direction of *x* axis is higher than the one acting in the direction of *y* axis. The same outcome is also valid for the wind loads of ASCE 7-16. However, in the earthquake load case, the base shear value is higher in the *y* direction. The highest value of the base shear is from the earthquake loads acting in the *y* direction, while the lowest one is from the wind loads of TS 498 acting in the *y* direction. Based on the results, the earthquake generated base shear forces are higher than the ones generated by the wind loads of TS 498 and ASCE 7-16. The weight of the building used in the wind loading is higher than the weight used in the earthquake loading.

Table 4.15 Base Shear for Building Model D2620

ASCE [1] STEP 1/CASE 1				TS 498 [1]				TEC 19 [1]			
W_x (kN)		W_y (kN)		W_x (kN) COMB 45 [2]		W_y (kN) COMB 46 [2]		S_x (kN)		S_y (kN)	
F_x	F_y	F_x	F_y	F_x	F_y	F_x	F_y	F_x	F_y	F_x	F_y
2383	0	0	1569	2188	0	0	1459	7726	0.2	0.2	9142

(1) The total seismic weight of the building is 174,775 kN. The total weight of the building for the wind loads is 175,531 kN.

(2) For the details of the load combination, see Appendix A.

b. Building Model D2520

The base shear forces of the model D2520 are given in Table 4.16. The force under the wind loads of TS 498 acting in the direction of *x* axis is higher than the one acting in the direction of *y* axis. The results from ASCE 7-16 confirm the same outcome. However, the earthquake generated base shear forces resulted higher base shear value in the *y* direction. The highest value of the base shear is due to the earthquake loads of TEC 19 acting in the *y* direction while the lowest one is due to the wind loads of ASCE 7-16 acting again in the *y* direction. According to the results, it can be observed that the weight of the building used in the wind loads is slightly higher than the weight used in the earthquake loads.

Table 4.16 Base Shear for Building Model D2520

ASCE (1) STEP 1/CASE 1				TS 498 (1)				TEC 19 (1)			
W_x (kN)		W_y (kN)		W_x (kN) COMB 45 (2)		W_y (kN) COMB 46 (2)		S_x (kN)		S_y (kN)	
F_x	F_y	F_x	F_y	F_x	F_y	F_x	F_y	F_x	F_y	F_x	F_y
2380	0	0	1455	2188	0	0	1459	7985	0.3	0.3	12577

(1) The total seismic weight of the building is 177,375 kN. The total weight of the building for the wind loads is 178,131 kN.

(2) For the details of the load combination, see Appendix A.

c. Building Model D2420

Table 4.17 lists the base shear forces of the Model D2420. According to the table, the base shear forces of TS 498 acting in the direction of *x* axis is higher than the one acting in the direction of *y* axis. The same outcome is also valid for the wind loads of ASCE 7-16. However, in the earthquake load case, the base shear value is higher in the *y* direction. The highest value of the base shear is from the earthquake loads acting in the *y* direction, while the lowest one is from the wind loads of TS 498 acting in the *y* direction. Based on the results, the earthquake generated base shear forces are higher than the ones generated by the wind loads of TS 498 and ASCE 7-16. The weight of the building used in the wind loading is higher than the weight used in the earthquake loading.

Table 4.17 Base Shear for Building Model D2420

ASCE [1] STEP 1/CASE 1				TS 498 [1]				TEC 19 [1]			
W_x (kN)		W_y (kN)		W_x (kN) COMB 45 [2]		W_y (kN) COMB 46 [2]		S_x (kN)		S_y (kN)	
F_x	F_y	F_x	F_y	F_x	F_y	F_x	F_y	F_x	F_y	F_x	F_y
2478	0	0	1514	2188	0	0	1459	5244	0	0	5515

(1) The total seismic weight of the building is 158,528 kN. The total weight of the building for the wind loads is 159,284 kN.

(2) For the details of the load combination, see Appendix A.

d. Building Model D2320

In this building model, the base shear forces resulting from the wind loads of ASCE 7-16 acting both in the *x* and *y* directions are equal to each other (see Table 4.18). The same outcome is also observed for the base shear forces of TS 498. In the earthquake load case, the base shear value is higher in the *y* direction. As listed in Table 4.18, the highest value of the base shear is due to the earthquake loads of TEC 19 acting in the *y* direction, while the lowest one is due to the wind loading of TS 498 acting both in the *x* and *y* directions. The weight of the building according to the wind loads is slightly higher than the weight according to the earthquake loads.

Table 4.18 Base Shear for Building Model D2320

ASCE [1] STEP 1/CASE 1				TS 498 [1]				TEC 19 [1]			
W_x (kN)		W_y (kN)		W_x (kN) COMB 45 [2]		W_y (kN) COMB 46 [2]		S_x (kN)		S_y (kN)	
F_x	F_y	F_x	F_y	F_x	F_y	F_x	F_y	F_x	F_y	F_x	F_y
2378	0	0	2378	2188	0	0	2188	13575	0.3	0.3	13789

(1) The total seismic weight of the building is 294,046 kN. The total weight of the building for the wind loads is 295,256 kN.

(2) For the details of the load combination, see Appendix A.

e. Building Model D2220

Table 4.19 has the base shear forces of the Model D2220. Based on the results, it can be observed that the value of the base shear in the *y* direction is higher than the value in the *x* direction when the building is subjected to the earthquake loads of TEC 19. The base shear forces of the wind loading from ASCE 7-16 are equal to each other both in the *x* and *y* directions. The same observation is valid for the wind loading case of TS 498. In this building model, the highest value of the base shear is due to the earthquake loads of TEC 19 acting in the *y* direction, while the lowest one is due to the wind loads of TS 498 acting both in the *x* and *y* directions. Based on the results, it can be concluded that the weight of the building according to the wind loads is slightly higher than the weight according to the earthquake loads.

Table 4.19 Base Shear for Building Model D2220

ASCE (1) STEP 1/CASE 1				TS 498 (1)				TEC 19 (1)			
W_x (kN)		W_y (kN)		W_x (kN) COMB 45 (2)		W_y (kN) COMB 46 (2)		S_x (kN)		S_y (kN)	
F_x	F_y	F_x	F_y	F_x	F_y	F_x	F_y	F_x	F_y	F_x	F_y
2398	0	0	2398	2188	0	0	2188	12715	0.5	0.5	19530

(1) The total seismic weight of the building is 301,182 kN. The total weight of the building for the wind loads is 302,391 kN.

(2) For the details of the load combination, see Appendix A.

f. Building Model D2120

In this building model, the base shear forces resulting from the wind loads of ASCE 7-16 acting both in the *x* and *y* directions are equal to each other (see Table 4.20). The same outcome is also observed for the base shear forces of TS 498. In the earthquake load case, the base shear value is higher in the *y* direction. As listed in Table 4.20, the highest value of the base shear is due to the earthquake loads of TEC 19 acting in the *y* direction, while the lowest one is due to the wind loading of TS 498 acting both in the *x* and *y* directions. The weight of the building according to the wind loads is slightly higher than the weight according to the earthquake loads.

Table 4.20 Base Shear for Building Model D2120

ASCE [1] STEP 1/CASE 1				TS 498 [1]				TEC 19 [1]			
W_x (kN)		W_y (kN)		W_x (kN) COMB 45 [2]		W_y (kN) COMB 46 [2]		S_x (kN)		S_y (kN)	
F_x	F_y	F_x	F_y	F_x	F_y	F_x	F_y	F_x	F_y	F_x	F_y
2460	0	0	2460	2188	0	0	2188	9856	0	0	10093

(1) The total seismic weight of the building is 282,839 kN. The total weight of the building for the wind loads is 284,049 kN.

(2) For the details of the load combination, see Appendix A.

4.3.5 Group No. 5 (10 story buildings with DD2)

a. Building Model D2610

The base shear forces of the model D2610 are given in Table 4.21. The force under the wind loads of TS 498 acting in the direction of *x* axis is higher than the one acting in the direction of *y* axis. The results from ASCE 7-16 confirm the same outcome. However, the earthquake generated base shear forces resulted higher base shear value in the *y* direction. The highest value of the base shear is due to the earthquake loads of TEC 19 acting in the *y* direction while the lowest one is due to the wind loads of ASCE 7-16 acting again in the *y* direction. According to the results, it can be observed that the weight of the building used in the wind loads is slightly higher than the weight used in the earthquake loads.

Table 4.21 Base Shear for Building Model D2610

ASCE [1] STEP 1/CASE 1				TS 498 [1]				TEC 19 [1]			
W_x (kN)		W_y (kN)		W_x (kN) COMB 45 [2]		W_y (kN) COMB 46 [2]		S_x (kN)		S_y (kN)	
F_x	F_y	F_x	F_y	F_x	F_y	F_x	F_y	F_x	F_y	F_x	F_y
474	0	0	291	760	0	0	506	6927	0.1	0.1	8146

(1) The total seismic weight of the building is 82,637 kN. The total weight of the building for the wind loads is 83,393 kN.

(2) For the details of the load combination, see Appendix A.

b. Building Model D2510

Table 4.22 lists the base shear forces of the Model D2510. According to the table, the base shear forces of TS 498 acting in the direction of *x* axis is higher than the one acting in the direction of *y* axis. The same outcome is also valid for the wind loads of ASCE 7-16. However, in the earthquake load case, the base shear value is higher in the *y* direction. The highest value of the base shear is from the earthquake loads acting in the *y* direction, while the lowest one is from the wind loads of ASCE 7-16 acting in the *y* direction. Based on the results, the earthquake generated base shear forces are higher than the ones generated by the wind loads of TS 498 and ASCE 7-16. The weight of the building used in the wind loading is slightly higher than the weight used in the earthquake loading.

Table 4.22 Base Shear for Building Model D2510

ASCE (1) STEP 1/CASE 1				TS 498 (1)				TEC 19 (1)			
W_x (kN)		W_y (kN)		W_x (kN) COMB 45 (2)		W_y (kN) COMB 46 (2)		S_x (kN)		S_y (kN)	
F_x	F_y	F_x	F_y	F_x	F_y	F_x	F_y	F_x	F_y	F_x	F_y
632	0	0	388	760	0	0	506	7164	0.2	0.2	12985

(1) The total seismic weight of the building is 83,667 kN. The total weight of the building for the wind loads is 84,423 kN.

(2) For the details of the load combination, see Appendix A.

c. Building Model D2410

The base shear forces of the model D2410 are given in Table 4.23. The base shear force of TS 498 acting in the direction of *x* axis is higher than the one acting in the direction of *y* axis. The results from ASCE 7-16 confirm the same outcome. However, the earthquake generated base shear forces resulted higher base shear value in the *y* direction. The highest value of the base shear is due to the earthquake loads of TEC 19 acting in the *y* direction while the lowest one is due to the wind loads of ASCE 7-16 acting again in the *y* direction. According to the results, it can be observed that the weight of the building used in the wind loads is slightly higher than the weight used in the earthquake loads.

Table 4.23 Base Shear for Building Model D2410

ASCE [1] STEP 1/CASE 1				TS 498 [1]				TEC 19 [1]			
W_x (kN)		W_y (kN)		W_x (kN) COMB 45 [2]		W_y (kN) COMB 46 [2]		S_x (kN)		S_y (kN)	
F_x	F_y	F_x	F_y	F_x	F_y	F_x	F_y	F_x	F_y	F_x	F_y
733	0	0	449	760	0	0	506	4544	0	0	4824

(1) The total seismic weight of the building is 75,378 kN. The total weight of the building for the wind loads is 76,134 kN.

(2) For the details of the load combination, see Appendix A.

d. Building Model D2310

In this building model, the base shear forces resulting from the wind loads of ASCE 7-16 acting both in the *x* and *y* directions are equal to each other (see Table 4.24). The same outcome is also observed for the base shear forces of TS 498. In the earthquake load case, the base shear value is higher in the *y* direction. As listed in Table 4.24, the highest value of the base shear is due to the earthquake loads of TEC 19 acting in the *y* direction, while the lowest one is due to the wind loading of ASCE 7-16 acting both in the *x* and *y* directions. The weight of the building according to the wind loads is slightly higher than the weight according to the earthquake loads.

Table 4.24 Base Shear for Building Model D2310

ASCE [1] STEP 1/CASE 1				TS 498 [1]				TEC 19 [1]			
W_x (kN)		W_y (kN)		W_x (kN) COMB 45 [2]		W_y (kN) COMB 46 [2]		S_x (kN)		S_y (kN)	
F_x	F_y	F_x	F_y	F_x	F_y	F_x	F_y	F_x	F_y	F_x	F_y
632	0	0	632	760	0	0	760	9394	0.1	0.1	11006

(1) The total seismic weight of the building is 123,417 kN. The total weight of the building for the wind loads is 124,627 kN.

(2) For the details of the load combination, see Appendix A.

e. Building Model D2210

Table 4.25 has the base shear forces of the Model D2210. Based on the results, it can be observed that the value of the base shear in the *y* direction is higher than the value in the *x* direction when the building is subjected to the earthquake loads of TEC 19. The base shear forces of the wind loading from ASCE 7-16 are equal to each other both in the *x* and *y* directions. The same observation is valid for the wind loading case of TS 498. In this building model, the highest value of the base shear is due to the earthquake loads of TEC 19 acting in the *y* direction, while the lowest one is due to the wind loads of ASCE 7-16 acting both in the *x* and *y* directions. Based on the results, it can be concluded that the weight of the building according to the wind loads is slightly higher than the weight according to the earthquake loads.

Table 4.25 Base Shear for Building Model D2210

ASCE (1) STEP 1/CASE 1				TS 498 (1)				TEC 19 (1)			
W_x (kN)		W_y (kN)		W_x (kN) COMB 45 (2)		W_y (kN) COMB 46 (2)		S_x (kN)		S_y (kN)	
F_x	F_y	F_x	F_y	F_x	F_y	F_x	F_y	F_x	F_y	F_x	F_y
632	0	0	632	760	0	0	760	9675	0.3	0.3	17019

(1) The total seismic weight of the building is 124,447 kN. The total weight of the building for the wind loads is 125,656 kN.

(2) For the details of the load combination, see Appendix A.

f. Building Model D2110

In this building model, the base shear forces resulting from the wind loads of ASCE 7-16 acting both in the *x* and *y* directions are equal to each other (see Table 4.26). The same outcome is also observed for the base shear forces of TS 498. In the earthquake load case, the base shear value is higher in the *y* direction. As listed in Table 4.26, the highest value of the base shear is due to the earthquake loads of TEC 19 acting in the *y* direction, while the lowest one is due to the wind loading of ASCE 7-16 acting both in the *x* and *y* directions. The weight of the building according to the wind loads is slightly higher than the weight according to the earthquake loads.

Table 4.26 Base Shear for Building Model D2110

ASCE [1] STEP 1/CASE 1				TS 498 [1]				TEC 19 [1]			
W_x (kN)		W_y (kN)		W_x (kN) COMB 45 [2]		W_y (kN) COMB 46 [2]		S_x (kN)		S_y (kN)	
F_x	F_y	F_x	F_y	F_x	F_y	F_x	F_y	F_x	F_y	F_x	F_y
679	0	0	679	760	0	0	760	6929	0	0	7187

(1) The total seismic weight of the building is 115,886 kN. The total weight of the building for the wind loads is 117,095 kN.

(2) For the details of the load combination, see Appendix A.

4.4 Maximum lateral rooftop displacements

In this part, maximum lateral displacements of the upper floors (rooftop displacements) of each building model are discussed. The building models are divided into five groups as described in Section 4.1. The comparison between the displacements of each floor is made according to the effects of the wind and earthquake loads resulting from ASCE 7-16, TS 498 and TEC 19. These five groups are listed in each table along with the name of the building, the type of loading and the amount of lateral displacement at the top floor as shown in Tables 4.27 through 4.31.

Table 4.27 Maximum Rooftop Displacements of 40 Story building with DD4 type earthquake

Model Name	Story	Code	Direction	Load Combo and Pattern (1)	Max. Displacement (mm)
D4640	40	ASCE 7-16	X	Wx 8-33	39.3
			Y	Wy 8-33	22.0
		TS 498	X	Wx 8-33	37.8
			Y	Wy 8-33	23.0
		TEC 19	X	Sx	23.7
			Y	Sy	22.8
D4540	40	ASCE 7-16	X	Wx 8-33	39.3
			Y	Wx 8-33	15.0
		TS 498	X	Wx 8-33	37.8
			Y	Wy 8-33	14.7
		TEC 19	X	Sx	24.2
			Y	Sy	19.0
D4340	40	ASCE 7-16	X	Wx 8-33	36.0
			Y	Wx 8-33	29.2
		TS 498	X	X 8-33	25.3
			Y	Y 8-33	20.5
		TEC 19	X	Sx	27.2
			Y	Sy	24.8
D4240	40	ASCE 7-16	X	Wx 34-40	24.3
			Y	Wx 34-40	16.9
		TS 498	X	X 8-33	17.7
			Y	Y 8-33	11.3
		TEC 19	X	Sx	22.9
			Y	Sy	19.2

(1) For the details of the load combinations, see Appendix A.

Table 4.28 Maximum Rooftop Displacements of 40 Story Buildings with DD2 type earthquake

Model	Story	Code	Direction	Load Combo and Pattern (1)	Max. Displacement (mm)
D2640	40	ASCE 7-16	X	Wx 8-33	75.6
			Y	Wx 8-33	39.2
		TS 498	X	X 34-40	42.1
			Y	Y 8-33	38.7
		TEC 19	X	Sx	117.2
			Y	Sy	109.2
D2540	40	ASCE 7-16	X	Wx 8-33	74.3
			Y	Wx 8-33	27.9
		TS 498	X	X 8-33	67.4
			Y	Y 8-33	25.8
		TEC 19	X	Sx	116.8
			Y	Sy	93.5
D2340	40	ASCE 7-16	X	Wx 8-33	51.1
			Y	Wx 8-33	41.0
		TS 498	X	X 8-33	34.8
			Y	Y 8-33	27.9
		TEC 19	X	Sx	118.2
			Y	Sy	106.9
D2240	40	ASCE 7-16	X	Wy 8-33	46.3
			Y	Wy 8-33	31.4
		TS 498	X	X 8-33	31.7
			Y	Y 8-33	19.7
		TEC 19	X	Sx	112.2
			Y	Sy	94.0

(1) For the details of the load combinations, see Appendix A.

Table 4.29 Maximum Rooftop Displacements of 30 Story Buildings with DD2 type earthquake

Model	Story	Code	Direction	Load Combo and Pattern (1)	Max. Displacement (mm)
D2630	30	ASCE 7-16	X	Wx 8-30	60.9
			Y	Wx 8-30	33.0
		TS 498	X	X 8-30	44.4
			Y	Y 8-33	26.2
		TEC 19	X	Sx	85.8
			Y	Sy	82.3
D2530	30	ASCE 7-16	X	Wx 8-30	58.0
			Y	Wx 8-30	22.6
		TS 498	X	X 8-30	42.4
			Y	Y 8-30	16.3
		TEC 19	X	Sx	84.6
			Y	Sy	66.2
D2430	30	ASCE 7-16	X	Wx 8-30	121.4
			Y	Wx 8-30	73.7
		TS 498	X	X 8-30	83.6
			Y	Y 8-30	55.3
		TEC 19	X	Sx	109.1
			Y	Sy	108.3
D2330	30	ASCE 7-16	X	Wx 8-30	60.6
			Y	Wx 8-30	47.1
		TS 498	X	X 8-30	42.8
			Y	Y 8-30	33.2
		TEC 19	X	Sx	102.0
			Y	Sy	90.9
D2230	30	ASCE 7-16	X	Wx 8-30	59.3
			Y	Wx 8-30	38.7
		TS 498	X	X 8-30	41.9
			Y	Y 8-30	23.7
		TEC 19	X	Sx	100.1
			Y	Sy	78.6
D2130	30	ASCE 7-16	X	Wy 8-30	134.5
			Y	Wy 8-30	129.1
		TS 498	X	X 8-30	87.6
			Y	Y 8-30	84.0
		TEC 19	X	Sx	134.5
			Y	Sy	131.8

(1) For the details of the load combinations, see to Appendix A.

Table 4.30 Maximum Rooftop Displacements of 20 Story Buildings with DD2 type earthquake

Model	Story	Code	Direction	Load Combo and Pattern (1)	Max. Displacement (mm)
D2620	20	ASCE 7-16	X	Wx 8-20	16.9
			Y	Wx 8-20	7.7
		TS 498	X	X 8-20	14.6
			Y	Y 8-20	7.2
		TEC 19	X	Sx	50.7
			Y	Sy	44.0
D2520	20	ASCE 7-16	X	Wx 8-20	16.3
			Y	Wx 8-20	5.7
		TS 498	X	X 8-20	14.0
			Y	Y 8-20	4.0
		TEC 19	X	Sx	49.9
			Y	Sy	33.5
D2420	20	ASCE 7-16	X	Wx 8-20	33.7
			Y	Wx 8-20	17.6
		TS 498	X	X 8-20	27.3
			Y	Y 8-20	15.9
		TEC 19	X	Sx	65.6
			Y	Sy	60.4
D2320	20	ASCE 7-16	X	Wx 8-20	9.5
			Y	Wx 8-20	9.1
		TS 498	X	X 8-20	8.2
			Y	Y 8-20	7.8
		TEC 19	X	Sx	50.2
			Y	Sy	49.0
D2220	20	ASCE 7-16	X	Wx 8-20	10.5
			Y	Wy 8-20	6.7
		TS 498	X	X 8-20	9.0
			Y	Y 8-20	4.7
		TEC 19	X	Sx	53.0
			Y	Sy	39.0
D2120	20	ASCE 7-16	X	Wx 8-20	16.2
			Y	Wx 8-20	15.2
		TS 498	X	X 8-20	13.6
			Y	Y 8-20	12.7
		TEC 19	X	Sx	62.6
			Y	Sy	60.1

(1) For the details of the load combinations, see Appendix A.

Table 4.31 Maximum Rooftop Displacements of 10 Story Buildings with DD2 type earthquake

Model	Story No.	Code	Direction	Load Combo and Pattern (1)	Max. Displacement (mm)
D2610	10	ASCE 7-16	X	Wy 8-10	1.2
			Y	Wy 8-10	0.5
		TS 498	X	X 8-10	1.5
			Y	Y 8-10	0.7
		TEC 19	X	Sx	24.1
			Y	Sy	19.6
D2510	10	ASCE 7-16	X	Wx 8-10	1.2
			Y	Wx 8-10	0.3
		TS 498	X	X 8-10	1.5
			Y	Y 8-10	0.3
		TEC 19	X	Sx	23.6
			Y	Sy	12.9
D2410	10	ASCE 7-16	X	Wx 8-10	3.3
			Y	Wx 8-10	1.7
		TS 498	X	X 8-10	3.4
			Y	Y 8-10	1.9
		TEC 19	X	Sx	33.4
			Y	Sy	30.7
D2310	10	ASCE 7-16	X	Wx 8-10	1.0
			Y	Wx 8-10	0.7
		TS 498	X	X 8-10	1.3
			Y	Y 8-10	0.9
		TEC 19	X	Sx	26.3
			Y	Sy	22.4
D2210	10	ASCE 7-16	X	Wx 8-10	1.0
			Y	Wx 8-10	0.5
		TS 498	X	X 8-10	1.2
			Y	Y 8-10	0.4
		TEC 19	X	Sx	25.4
			Y	Sy	15.8
D2110	10	ASCE 7-16	X	Wx 8-10	1.9
			Y	Wy 8-10	1.8
		TS 498	X	X 8-10	2.2
			Y	Y 8-10	2.0
		TEC 19	X	Sx	33.5
			Y	Sy	31.9

(1) For the details of the load combinations, see Appendix A.

Based on the values in Table 4.27, for almost all cases, the maximum lateral top floor deflections are obtained from the wind loading in ASCE 7-16 (except for the model D4640, where the wind of TS 498 generated slightly higher deflections in the *y* direction). The DD4 type earthquake generated less deflections both in the *x* and *y* directions. The earthquake generated deflections in the *x* direction at an average are 0.29% and 0.31% less than their counterparts from TS 498 and ASCE 7-16, respectively. The results of the 40 story building models are also studied for the DD2 type earthquake case (see Table 4.28). Unlike the results of DD4 type earthquake, the maximum lateral deflections both in the *x* and *y* directions are all observed in the earthquake case. On an average, the earthquake deflections are 1.65 times in the *x* direction and 2.75 times in the *y* direction are higher than their counterparts from TS 498 and ASCE 7-16, respectively. When the wind load generated deflections are compared, it is observed that the deflections from ASCE 7-16 are all higher than the ones of TS 498.

Similar to the 40 story case, the results of the 30 story buildings from the wind and earthquake loadings are also compared to each other (see Table 4.29). Based on the results, the maximum lateral deflections in both *x* and *y* directions are obtained from the earthquake loading. The average ratio of the maximum deflections from the earthquake load to the wind load are 154% and 157% in the *x* and *y* directions, respectively. In the wind loading case, regardless of the wind load direction, the deflections of ASCE 7-16 are always higher than the ones of TS 498.

The deflections of the 20 story buildings are also evaluated for both earthquake and wind loading cases (see Table 4.30). The deflections resulting from the earthquake loading are always larger than the deflections of the wind loading from TS 498 and ASCE 7-16 both in the *x* and *y* directions. When the wind load generated deflections of TS 498 and ASCE 7-16 are compared to each other, it is seen that the ASCE 7-16 has created larger deflections than the TS 498 both in the *x* and *y* directions.

Finally, the results of the 10 story buildings are studied (see Table 4.31). The earthquake generated deflections in both *x* and *y* directions are always much larger than their counterparts from the wind loading of TS 498 and ASCE 7-16. As for the deflections of the wind loading, unlike the trend it is observed for the 20, 30 and 40 story buildings, the TS 498 created larger deflections in almost all cases than the

ASCE 7-16 (except for the model D2210, where the ASCE 7-16 created slightly larger deflections in the *y* direction), again both in the *x* and *y* directions.

Based on the results given in Tables 4.27 through 4.31, it is seen that the minimum deflections are observed in the building models with D2510 and D2210 layouts while the maximum ones are observed in the models with D2130 and D2430 layouts. The maximum lateral floor deflection is recorded in the 30 story building model with layout D2130 for the DD2 type earthquake load which resulted a total deflection of 134.5 mm in the *x* direction. According to the results, the 40 story building models create less deflections than the 30 story ones implying the fact that the lateral strength of the structural members in the 40 story are more effective than the ones in the 30 story.

4.5 Fundamental periods

A building's periods are affected by several factors, such as building's total height, material properties, total number of floors, layout dimensions, framing system, and damping. In this section, the first three periods of the building models are presented. According to their layouts, the models are divided into five groups. The first group consists of four models with different layouts, with each of them consisting of 40 floors that are subjected to DD4 type of earthquake. The second groups consists of the same layouts of the first group, but are subjected to DD2 type of earthquake. The third, fourth and fifth groups include six models each with varying layouts with 30, 20 and 10 floors, respectively.

4.5.1 Group No. 1 (40 story buildings with DD4)

Tables 4.32 through 4.35 show the first three building periods and their directions for each building model. The fundamental period of each model is a combination of lateral displacement either in the *x* or *y* direction and rotation around *y* axis, where the lateral displacement is a dominant component. The largest fundamental period of 3.19 seconds is obtained for the model D4340 while the lowest one is obtained as 2.68 seconds for the model D4240.

Table 4.32 Fundamental Periods for Building Model D4640

Mode Number	Periods (sec/cycle)	Direction
1	2.77	$U_x + R_y$
2	2.62	$U_y + R_x$
3	1.82	R_z

Table 4.33 Fundamental Periods for Building Model D4540

Mode Number	Periods (sec/cycle)	Direction
1	2.78	$U_x + R_y$
2	2.06	$U_y + R_z$
3	2.05	$U_y + R_x$

Table 4.34 Fundamental Periods for Building Model D4340

Mode Number	Periods (sec/cycle)	Direction
1	3.19	$U_x + R_y$
2	2.85	$U_y + R_x$
3	2.17	R_z

Table 4.35 Fundamental Periods for Building Model D4240

Mode Number	Periods (sec/cycle)	Direction
1	2.68	$U_x + R_y$
2	2.26	R_z
3	2.08	$U_y + R_x$

4.5.2 Group No. 2 (40 story buildings with DD2)

The first three building periods and their directions are given for each building model as shown in Tables 4.36 through 4.39. The fundamental period of each model is a combination of lateral displacement in the *x* direction and rotation around *y* axis, where the lateral displacement is a dominant component. The largest fundamental period of 3.74 seconds is obtained for the model D2340 while the lowest one is obtained as 3.61 seconds for the model D2240. When the results of DD2 and DD4 earthquake types are considered, an increase is observed in the period values of DD2 since the stiffness of each building increased due to their relative effective stiffness values.

Table 4.36 Fundamental Periods for Building Model D2640

Mode Number	Periods (sec/cycle)	Direction
1	3.71	$U_x + R_y$
2	3.38	$U_y + R_x$
3	2.38	R_z

Table 4.37 Fundamental Periods for Building Model D2540

Mode Number	Periods (sec/cycle)	Direction
1	3.72	$U_x + R_y$
2	2.74	$U_y + R_z$
3	2.73	$U_y + R_x$

Table 4.38 Fundamental Periods for Building Model D2340

Mode Number	Periods (sec/cycle)	Direction
1	3.74	$U_x + R_y$
2	3.33	$U_y + R_x$
3	2.52	R_z

Table 4.39 Fundamental Periods for Building Model D2240

Mode Number	Periods (sec/cycle)	Direction
1	3.61	$U_x + R_y$
2	3.03	R_z
3	2.76	$U_y + R_x$

4.5.3 Group No. 3 (30 story buildings with DD2)

Tables 4.40 through 4.45 show the first three building periods and their directions for each building model. The fundamental period of each model is a combination of lateral displacement in the *x* direction and rotation around *y* axis, where the lateral displacement is a dominant component. The largest fundamental period of 4.50 seconds is obtained for the model D2130 while the lowest one is obtained as 2.66 seconds for the model D2530.

Table 4.40 Fundamental Periods for Building Model D2630

Mode Number	Periods (sec/cycle)	Direction
1	2.70	$U_x + R_y$
2	2.46	$U_y + R_x$
3	1.73	R_z

Table 4.41 Fundamental Periods for Building Model D2530

Mode Number	Periods (sec/cycle)	Direction
1	2.66	$U_x + R_y$
2	2.01	R_z
3	1.90	$U_y + R_x$

Table 4.42 Fundamental Periods for Building Model D2430

Mode Number	Periods (sec/cycle)	Direction
1	3.59	$U_x + R_y$
2	3.57	$U_y + R_x$
3	2.95	R_z

Table 4.43 Fundamental Periods for Building Model D2330

Mode Number	Periods (sec/cycle)	Direction
1	3.19	$U_x + R_y$
2	2.68	R_z
3	2.25	$U_y + R_x$

Table 4.44 Fundamental Periods for Building Model D2230

Mode Number	Periods (sec/cycle)	Direction
1	3.18	$U_x + R_y$
2	2.68	R_z
3	2.25	$U_y + R_x$

Table 4.45 Fundamental Periods for Building Model D2130

Mode Number	Periods (sec/cycle)	Direction
1	4.50	$U_x + R_y$
2	4.40	$U_y + R_x$
3	3.86	R_z

4.5.4 Group No. 4 (20 story buildings with DD2)

The first three building periods and their directions are given for each building model as shown in Tables 4.46 through 4.51. The fundamental period of each model is a combination of lateral displacement in the *x* direction and rotation around *y* axis, where the lateral displacement is a dominant component. The largest fundamental period of 2.14 seconds is obtained for the model D2420 while the lowest one is obtained as 1.57 seconds for the model D2320.

Table 4.46 Fundamental Periods for Building Model D2620

Mode Number	Periods (sec/cycle)	Direction
1	1.61	$U_x + R_y$
2	1.36	$U_y + R_x$
3	1.06	R_z

Table 4.47 Fundamental Periods for Building Model D2520

Mode Number	Periods (sec/cycle)	Direction
1	1.58	$U_x + R_y$
2	1.24	R_z
3	0.99	$U_y + R_x$

Table 4.48 Fundamental Periods for Building Model D2420

Mode Number	Periods (sec/cycle)	Direction
1	2.14	$U_x + R_y$
2	2.01	$U_y + R_x$
3	1.85	R_z

Table 4.49 Fundamental Periods for Building Model D2320

Mode Number	Periods (sec/cycle)	Direction
1	1.57	$U_x + R_y$
2	1.54	$U_y + R_x$
3	1.13	R_z

Table 4.50 Fundamental Periods for Building Model D2220

Mode Number	Periods (sec/cycle)	Direction
1	1.71	$U_x + R_y$
2	1.47	R_z
3	1.17	$U_y + R_x$

Table 4.51 Fundamental Periods for Building Model D2120

Mode Number	Periods (sec/cycle)	Direction
1	2.05	$U_x + R_y$
2	1.99	$U_y + R_x$
3	1.80	R_z

4.5.5 Group No. 5 (10 story buildings with DD2)

Tables 4.52 through 4.57 show the first three building periods and their directions for each building model. The fundamental period of each model is a combination of lateral displacement in the *x* direction and rotation around *y* axis, where the lateral displacement is a dominant component. The largest fundamental period of 2.06 seconds is obtained for the model D2410 while the lowest one is obtained as 0.73 second for the model D2510.

Table 4.52 Fundamental Periods for Building Model D2610

Mode Number	Periods (sec/cycle)	Direction
1	0.75	$U_x + R_y$
2	0.61	$U_y + R_x$
3	0.48	R_z

Table 4.53 Fundamental Periods for Building Model D2510

Mode Number	Periods (sec/cycle)	Direction
1	0.73	$U_x + R_y$
2	0.58	R_z
3	0.40	$U_y + R_x$

Table 4.54 Fundamental Periods for Building Model D2410

Mode Number	Periods (sec/cycle)	Direction
1	2.06	$U_x + R_y$
2	1.72	$U_y + R_x$
3	1.11	$U_x + R_y$

Table 4.55 Fundamental Periods for Building Model D2310

Mode Number	Periods (sec/cycle)	Direction
1	0.83	$U_x + R_y$
2	0.69	$U_y + R_x$
3	0.52	$U_x + R_y$

Table 4.56 Fundamental Periods for Building Model D2210

Mode Number	Periods (sec/cycle)	Direction
1	0.80	$U_x + R_y$
2	0.70	R_z
3	0.45	$U_y + R_x$

Table 4.57 Fundamental Periods for Building Model D2110

Mode Number	Periods (sec/cycle)	Direction
1	1.12	$U_x + R_y$
2	1.07	$U_y + R_x$
3	0.99	R_z

4.6 Maximum Story Drift

It is the side-sway that happens between two consecutive floors of a building. It is, therefore, calculated as the difference between the lateral deflections of the successive floors. The maximum stıry drifts gives us an idea about the structural behavior of a building under the effects of earthquake or wind loads.

4.6.1 Group No. 1 (40 story buildings with DD4)

Figures 4.1 through 4.4 display the drift values for both *x* and *y* directions. As expected the drift values in the *y* direction are less than the ones in the *x* direction – except for the top ten floors of the model D4240. This observation confirms the fact that the lateral strength in the *y* direction is a lot more pronounced than the one in the *x* direction. In this group, it is noticed that the drifts reach their highest value between the 10th and the 15th floors, which then begins to decrease gradually until they reach to nearly 0.5 mm at the top floor.

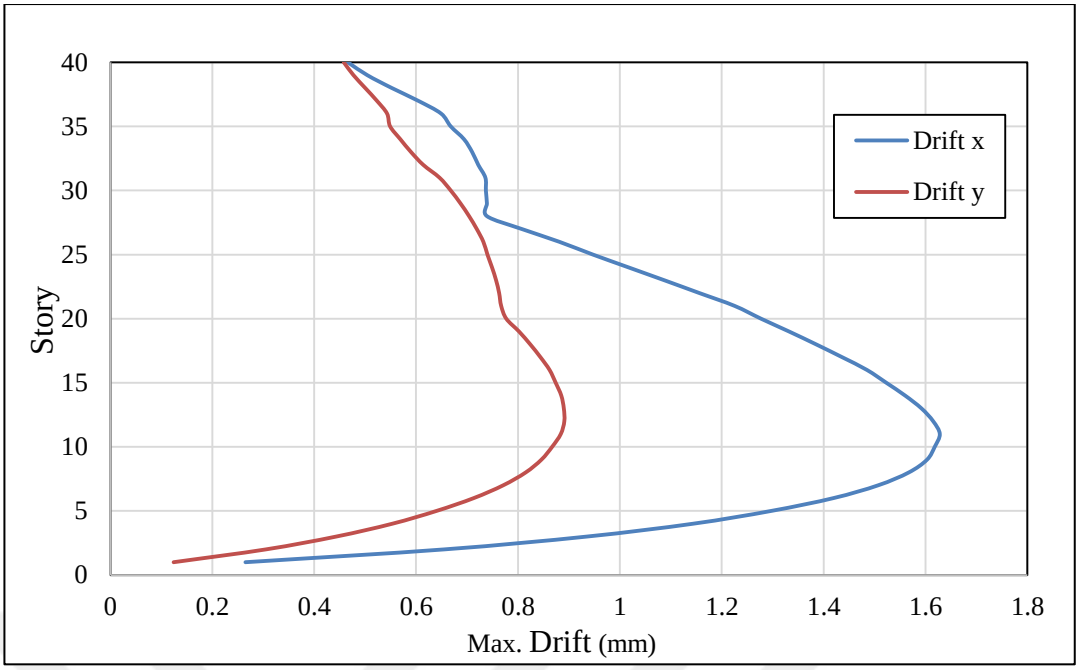

Figure 4.1 Maximum Drift for Building D4640

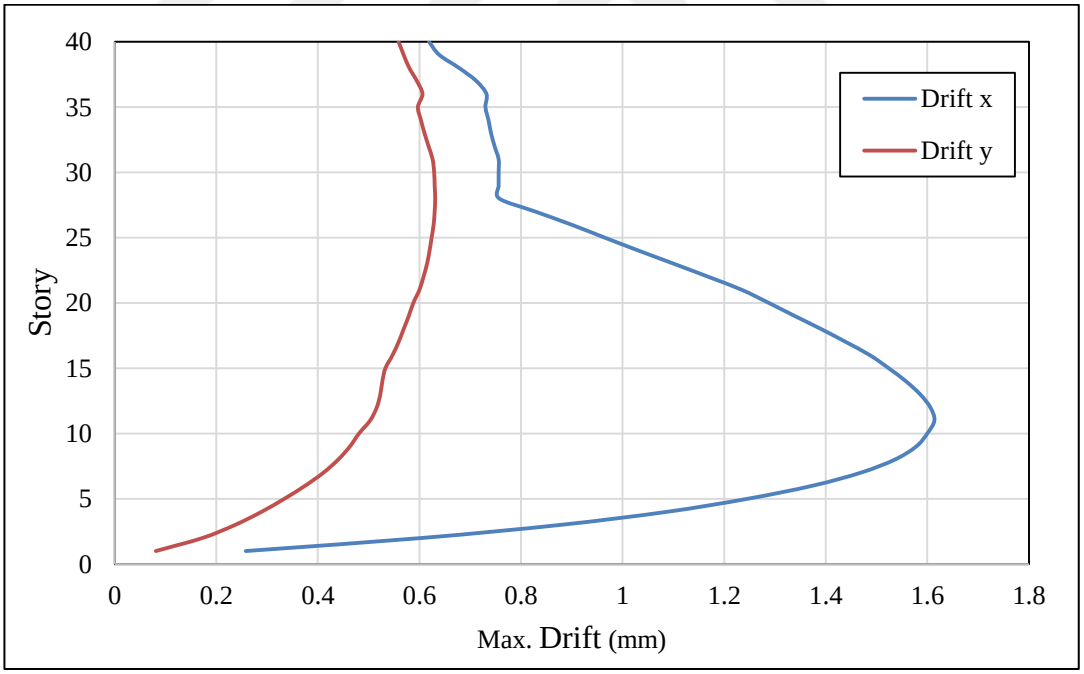

Figure 4.2 Maximum Drift for Building D4540

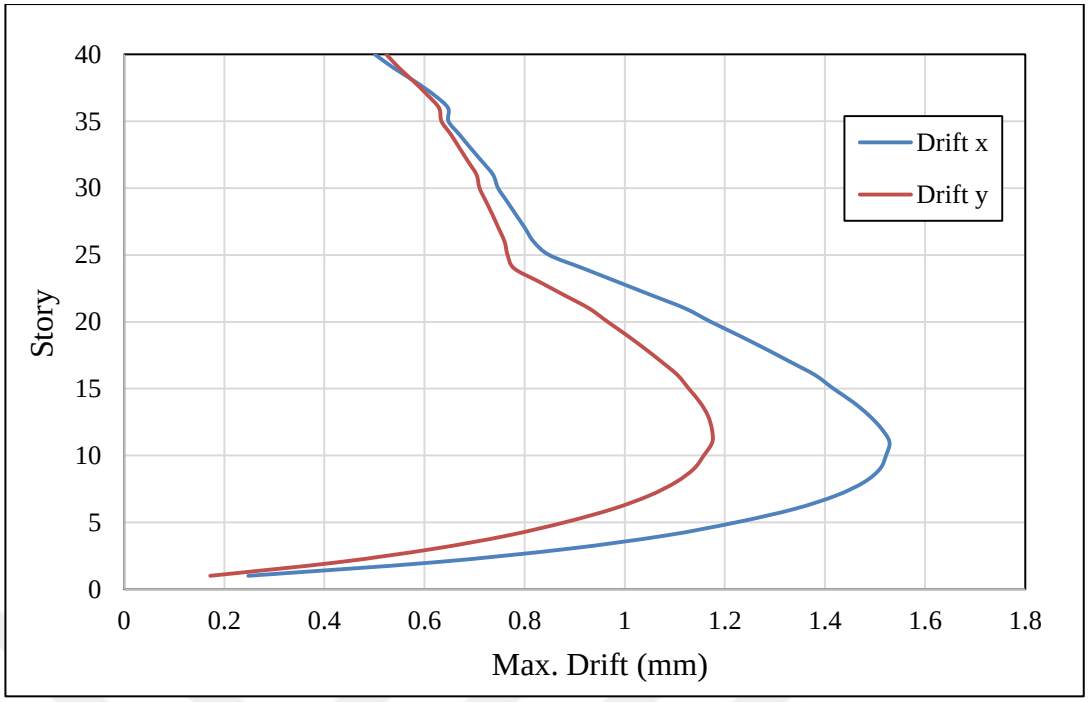

Figure 4.3 Maximum Drift for Building D4340

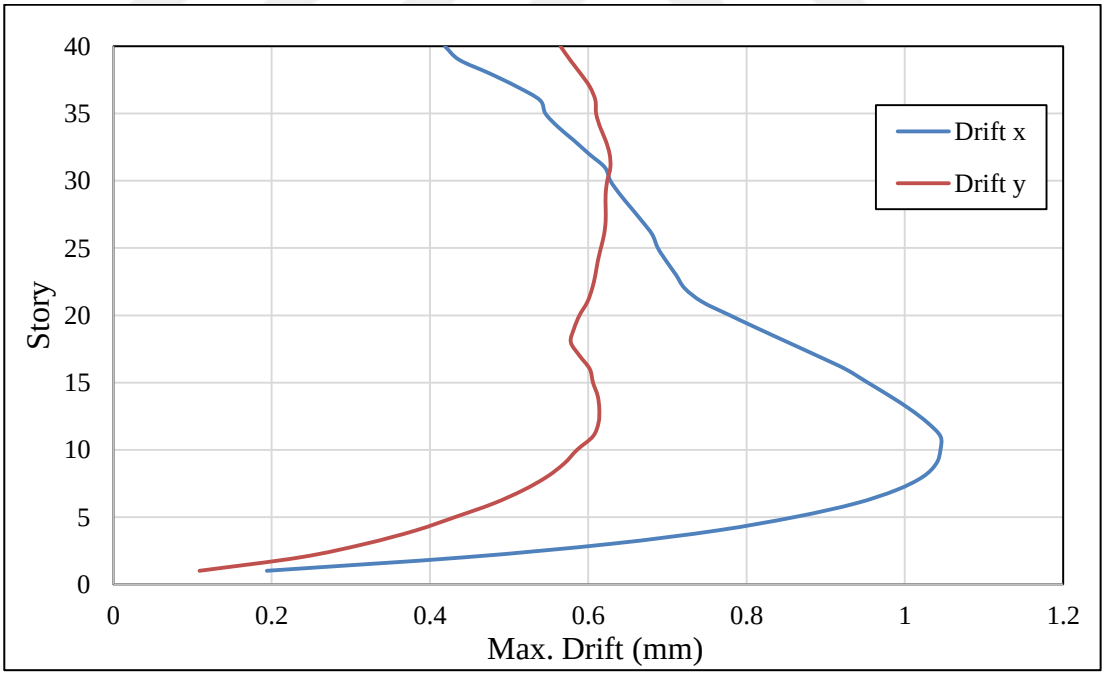

Figure 4.4 Maximum Drift for Building D4240

4.6.2 Group No. 2 (40 story buildings with DD2)

The drift values of the 40 story building are plotted in Figures 4.5 through 4.8 both in the *x* and *y* directions. The drift values are a lot more pronounced than the ones in Group 1, where DD4 earthquake type is used. Similar to the trend in Group 1, generally speaking, the drifts in the *y* direction are less than the ones in the *x* direction. This observation confirms the fact that the lateral strength in the *y* direction is a lot more pronounced than the one in the *x* direction. The drift in this group is less than 1 mm for the first few floors, but then begins to increase until it reaches its highest value between the 10th and 15th floors. After that, the drift begins to decrease gradually as the building rises.

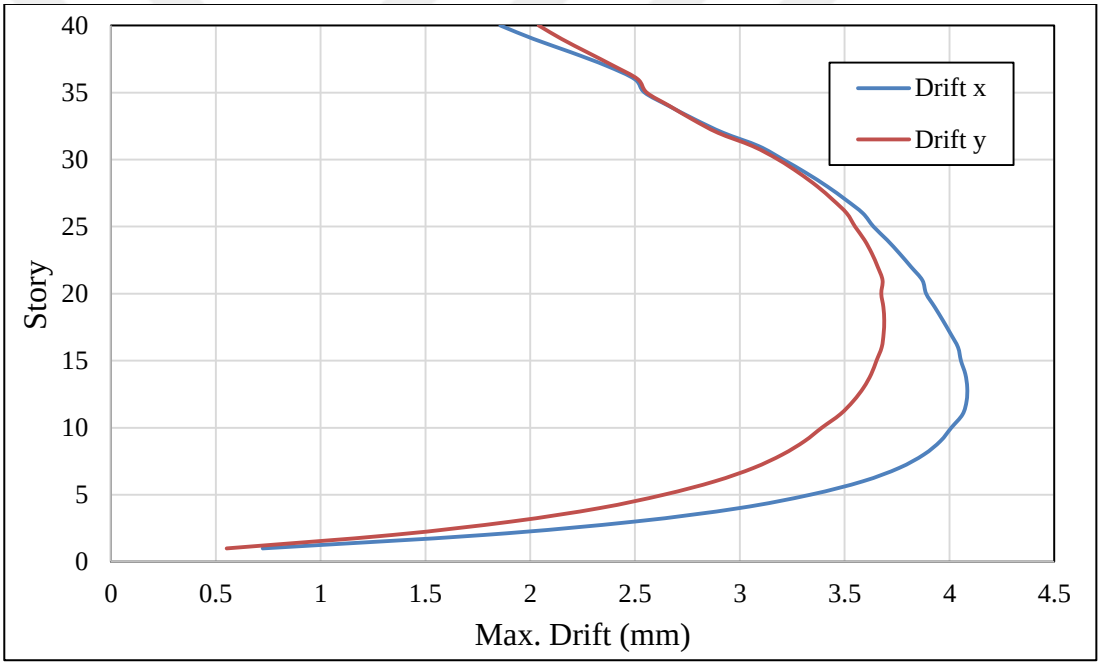

Figure 4.5 Maximum Drift for Building D2640

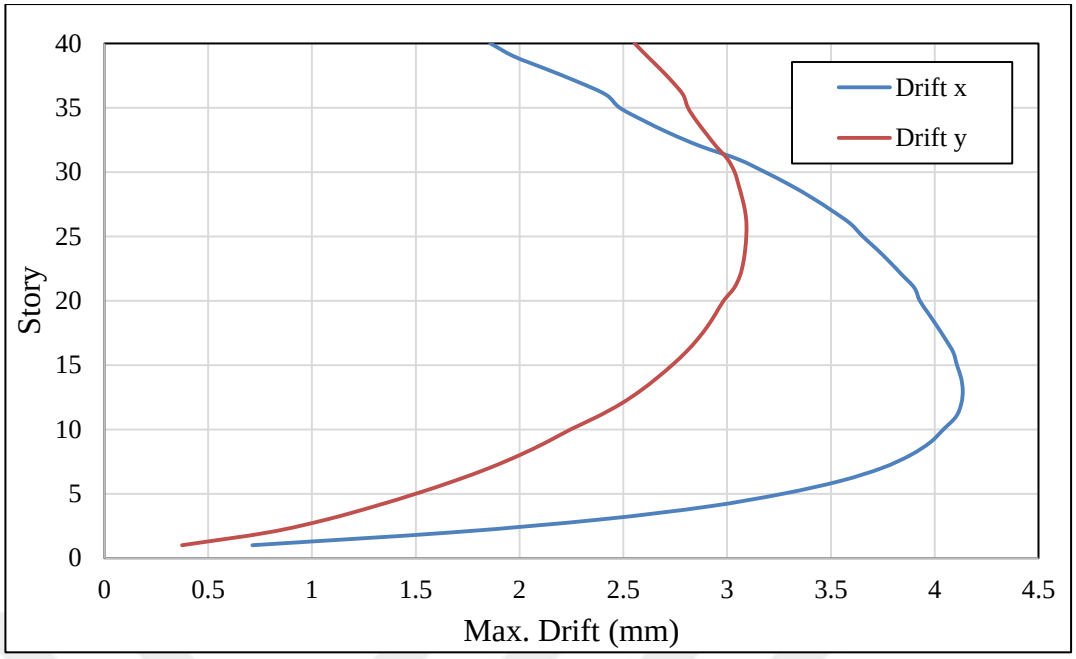

Figure 4.6 Maximum Drift for Building D2540

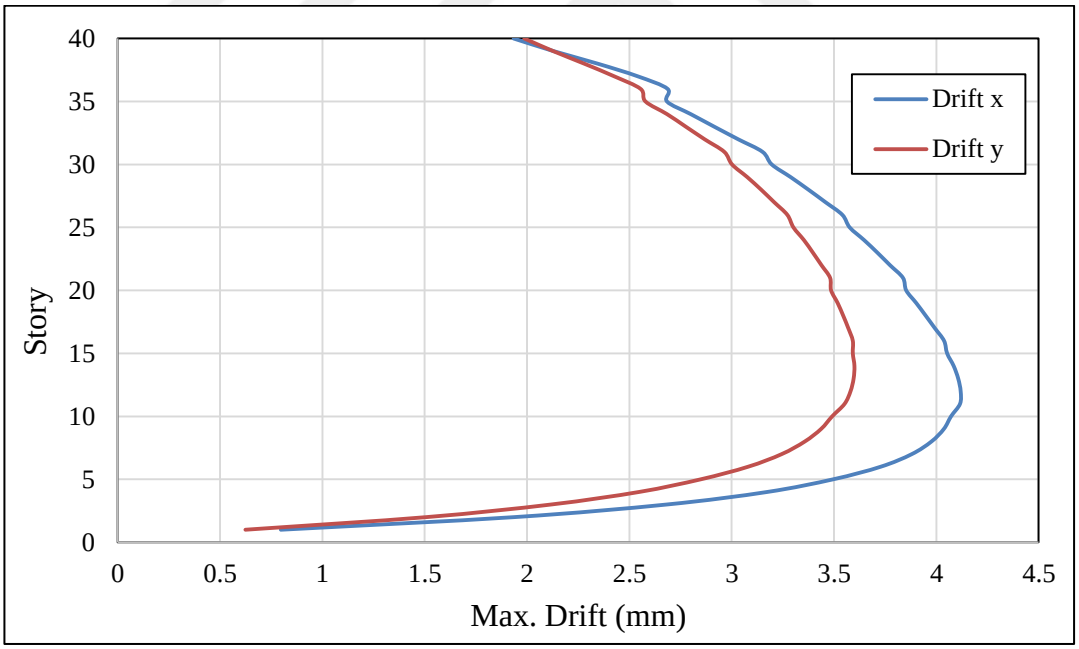

Figure 4.7 Maximum Drift for Building D2340

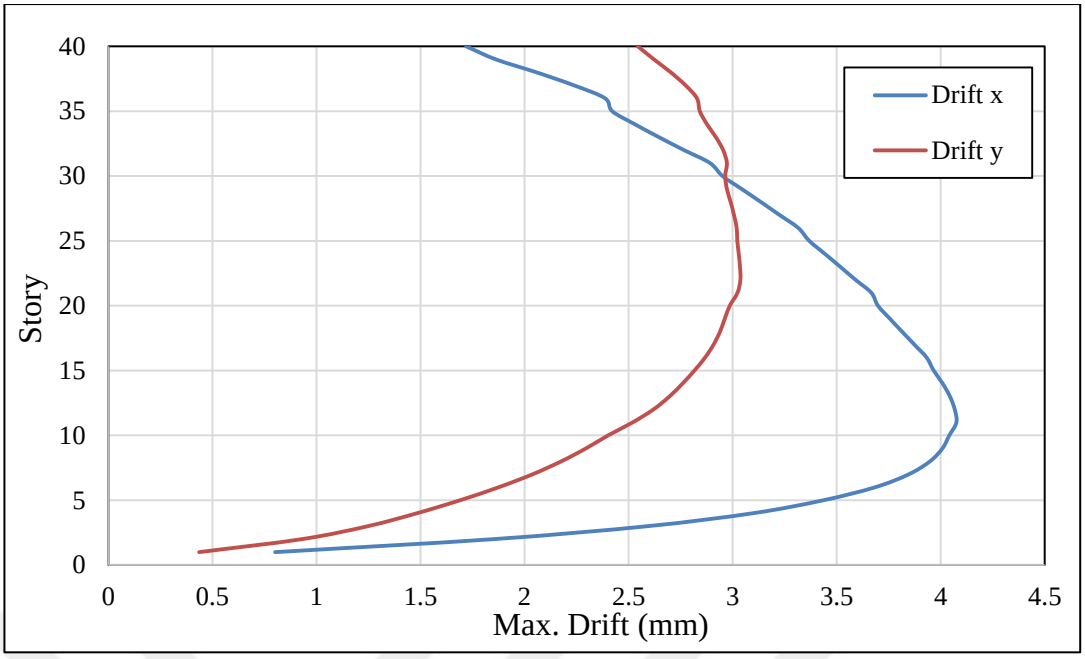

Figure 4.8 Maximum Drift for Building D2240

4.6.3 Group No. 3 (30 story buildings with DD2)

Figures 4.9 through 4.14 display the drift values for both *x* and *y* directions. As expected -except for the top 7 to 10 floors of the models D2230, D2530, and D2630- the drift values in the *y* direction are less than the ones in the *x* direction. This observation again confirms the fact that the lateral strength in the *y* direction is a lot more pronounced than the one in the *x* direction. The drift in this group reaches the highest value between the 10th and 15th floors, except for the D2430 and D2130 models, where the highest value of the drift is between the 5th and the 10th floors. This difference is attributed to the fact that these buildings do not have shear walls, unlike the other buildings of this group.

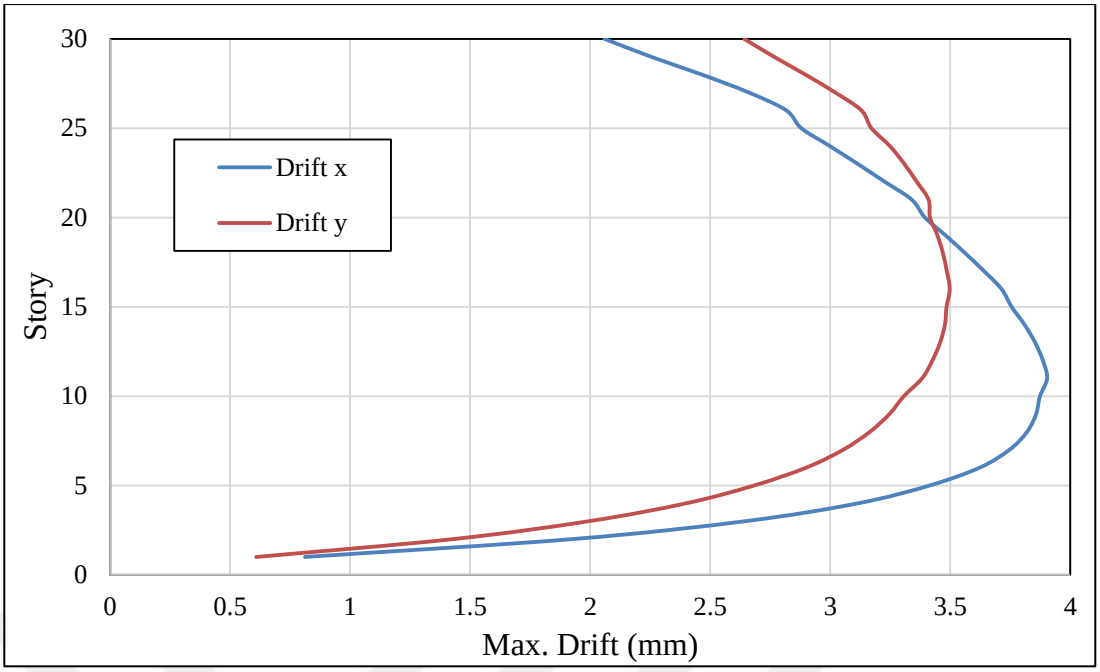

Figure 4.9 Maximum Drift for Building D2630

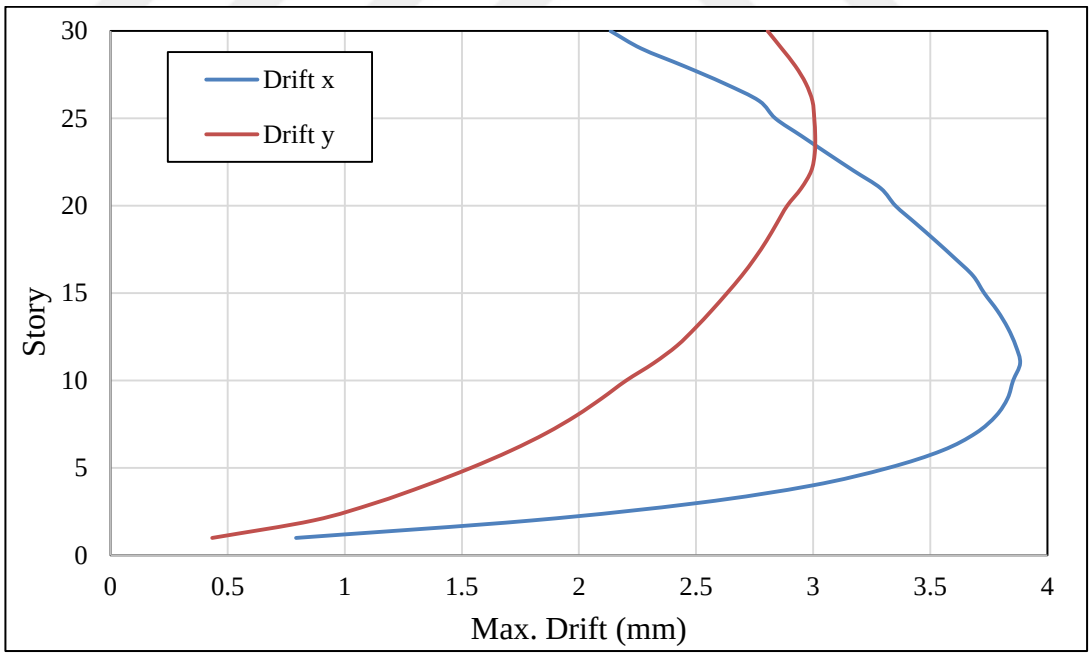

Figure 4.10 Maximum Drift for Building D2530

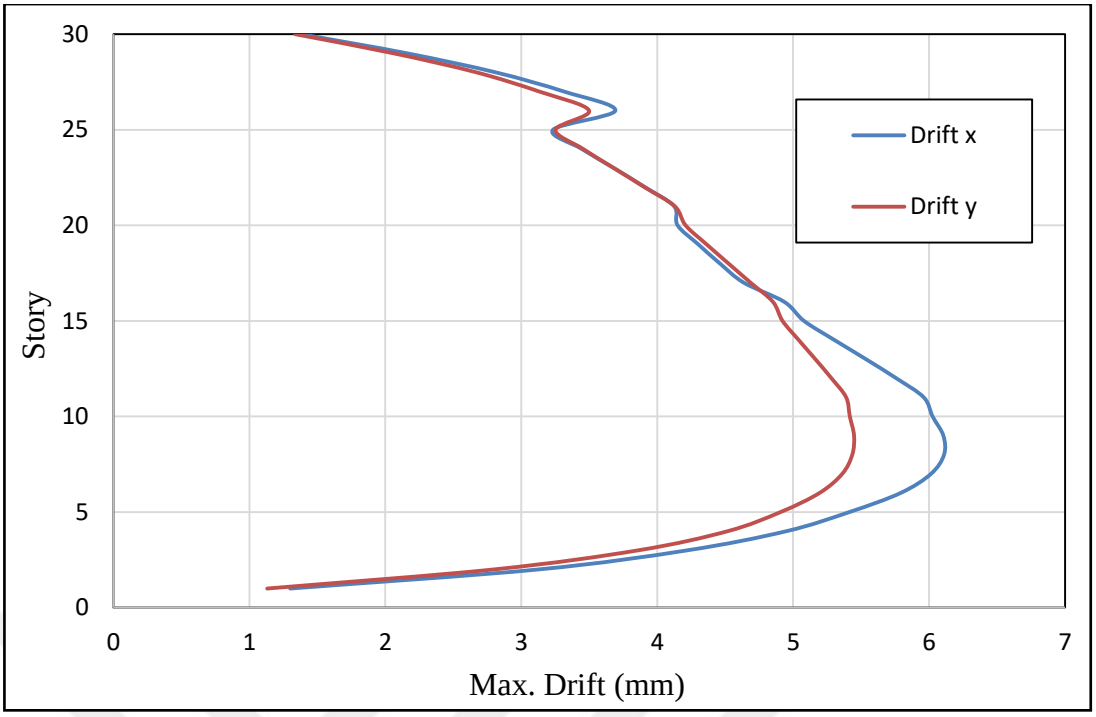

Figure 4.11 Maximum Drift for Building D2430

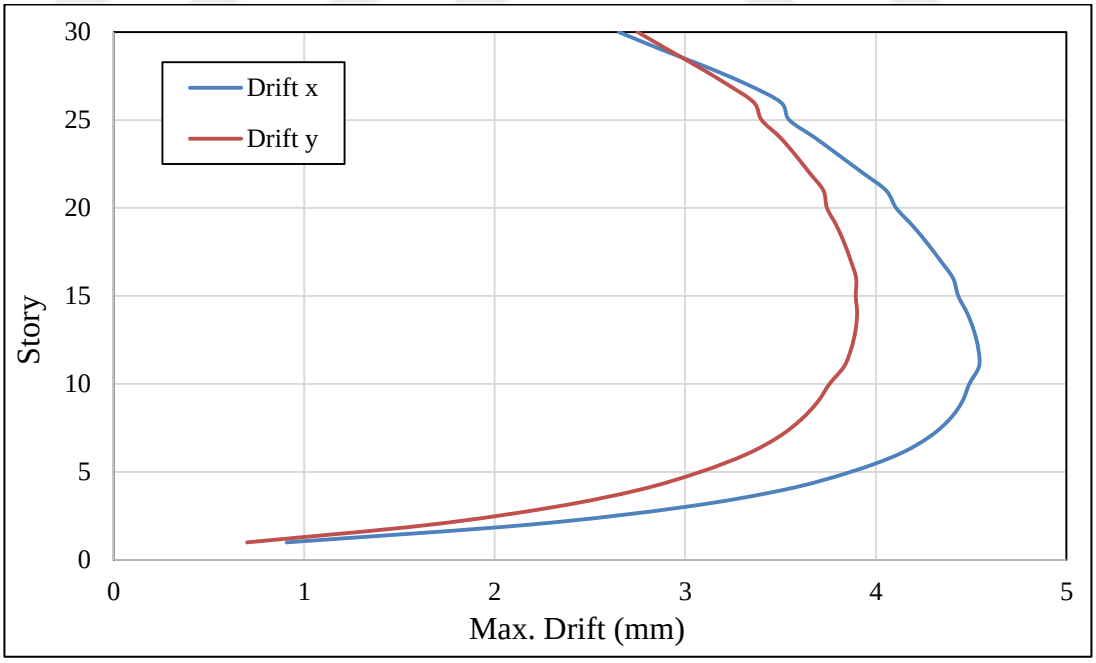

Figure 4.12 Maximum Drift for Building D2330

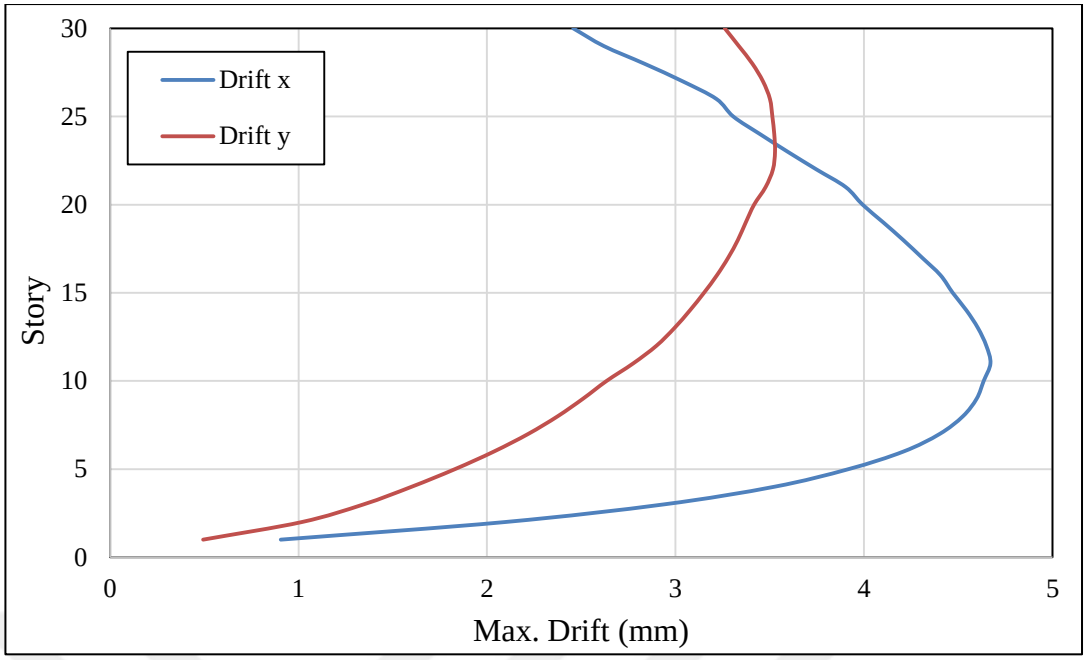

Figure 4.13 Maximum Drift for Building D2230

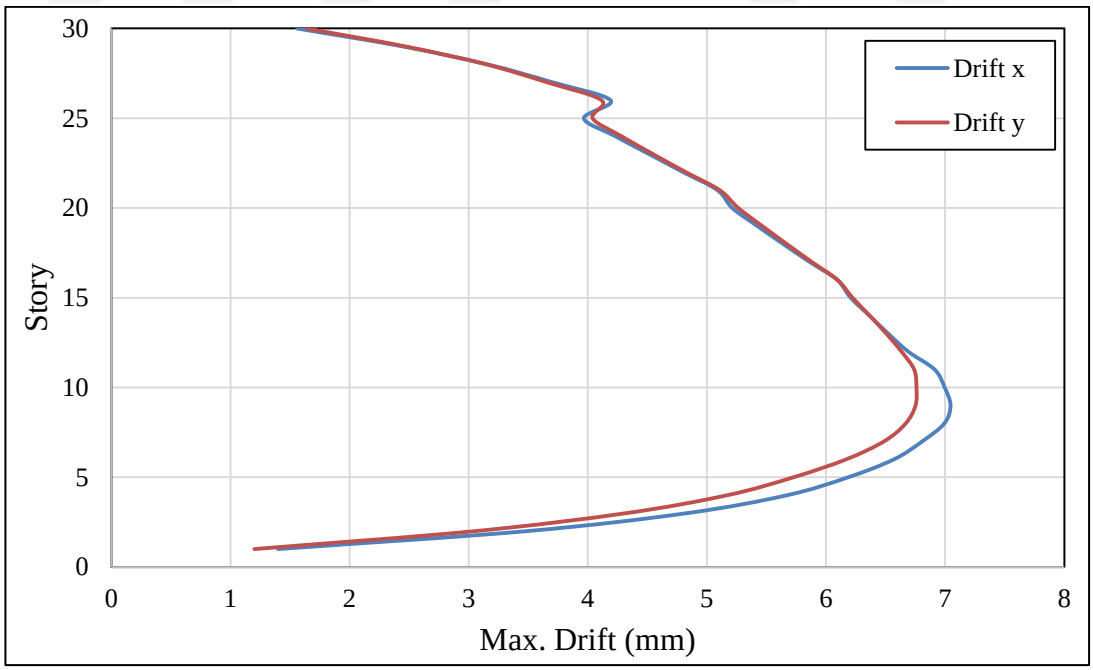

Figure 4.14 Maximum Drift for Building D2130

4.6.4 Group No. 4 (20 story buildings with DD2)

The drift values of the 20 story building are plotted in Figures 4.15 through 4.20 both in the *x* and *y* directions. The drift values in the *y* direction are less than the ones in the *x* direction. This observation confirms the fact that the building's lateral strength in the *y* direction is a lot more prominent than the one in the *x* direction. The drift values for this group of buildings begin to increase from the first floor to reach its highest value between the 4th and 6th floors. After that, the drift begins to decrease down to 2 to 2.5 mm at the top floor. For the D2420 and D2120 building models, the drift at the top floor is 1 to 2 mm, where the drift curves of these models differ from the curves of the rest of the group's models since the building in these two models do not contain any shear walls. For D2320 it can be noticed that the drifts curves in *x* and *y* directions are close to each other starting from 0.8 mm at the first four floors and ending in 2.25mm at the top floor as shown in Figure 4.18.

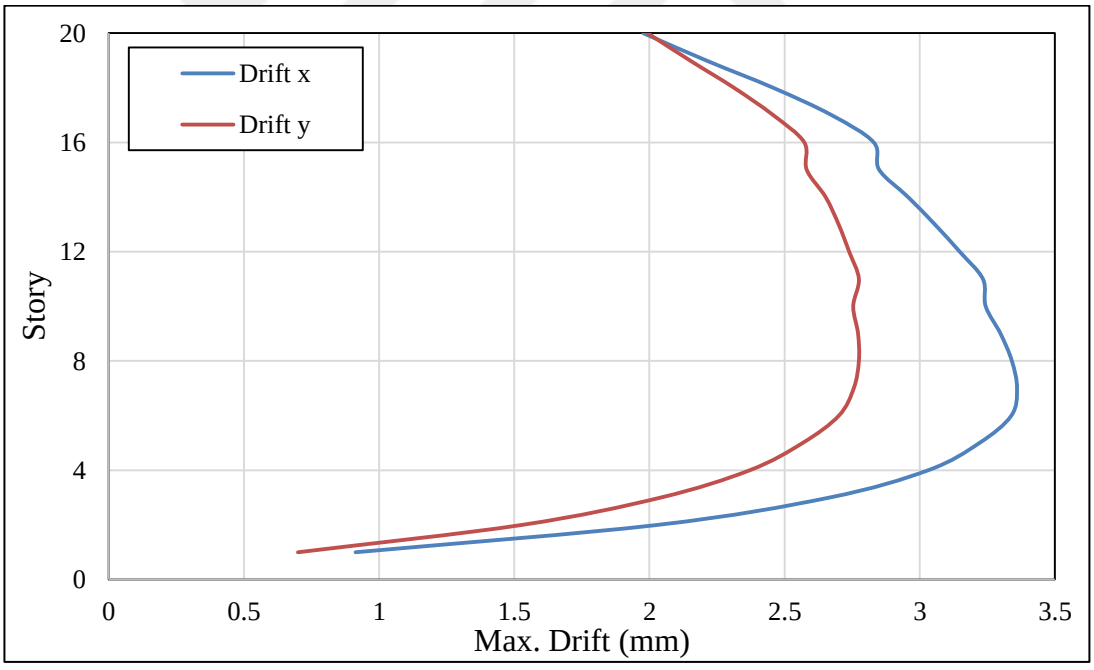

Figure 4.15 Maximum Drift for Building D2620

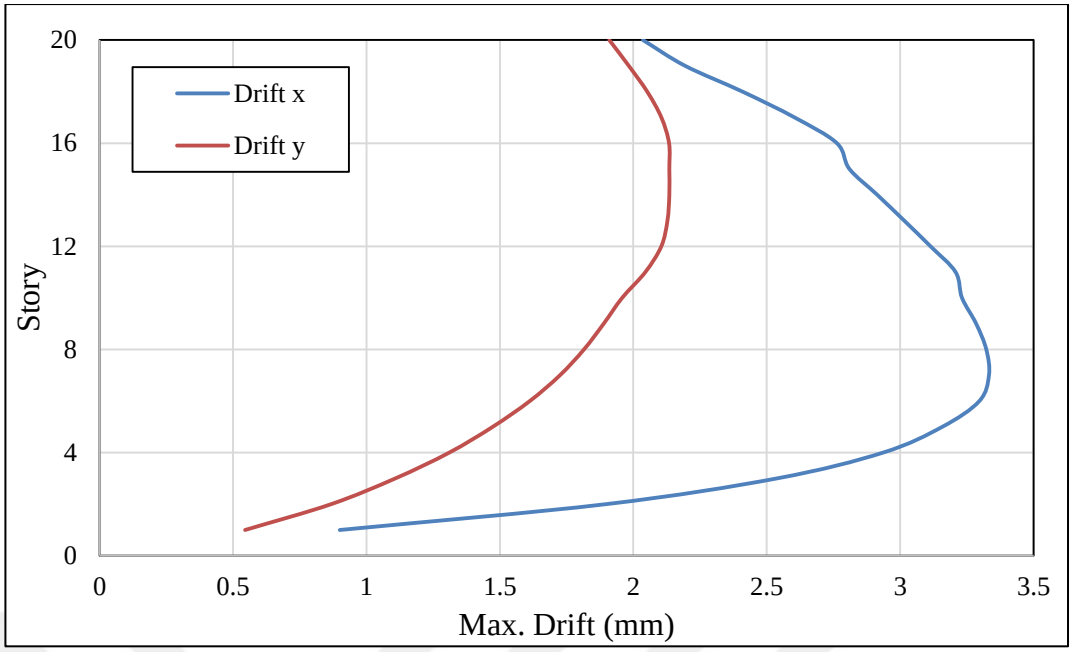

Figure 4.16 Maximum Drift for Building D2520

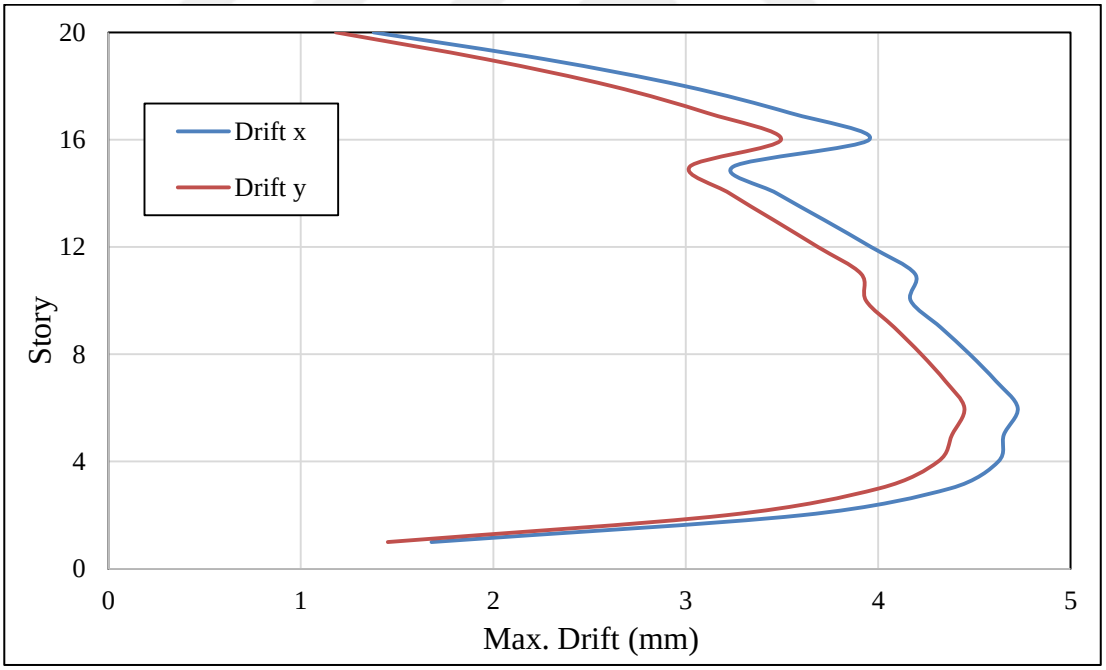

Figure 4.17 Maximum Drift for Building D2420

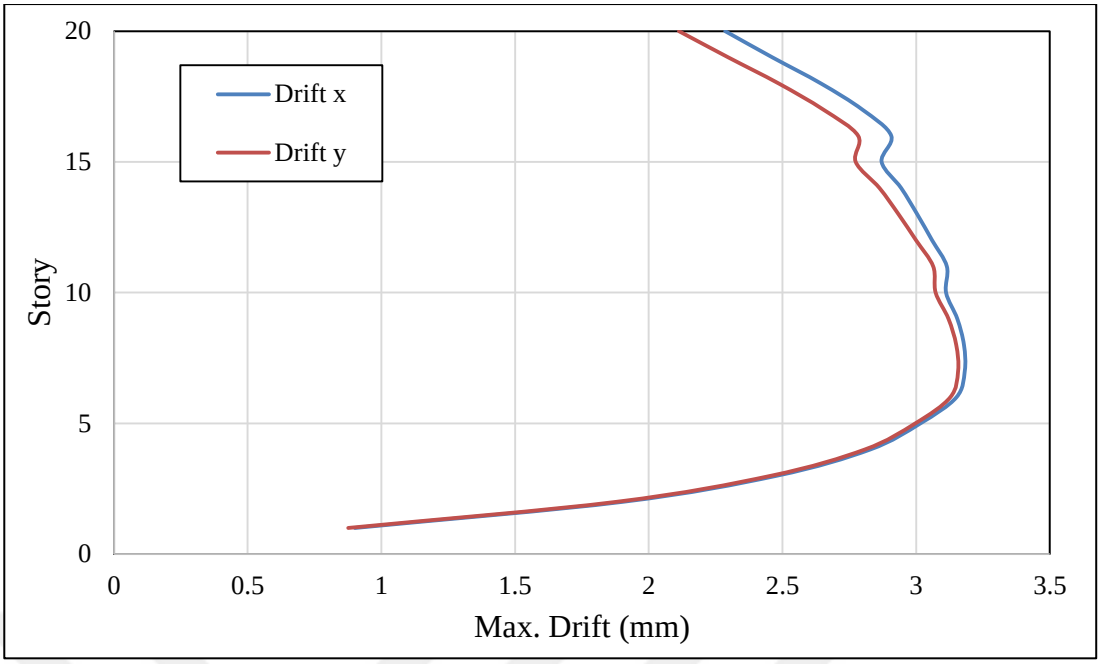

Figure 4.18 Maximum Drift for Building D2320

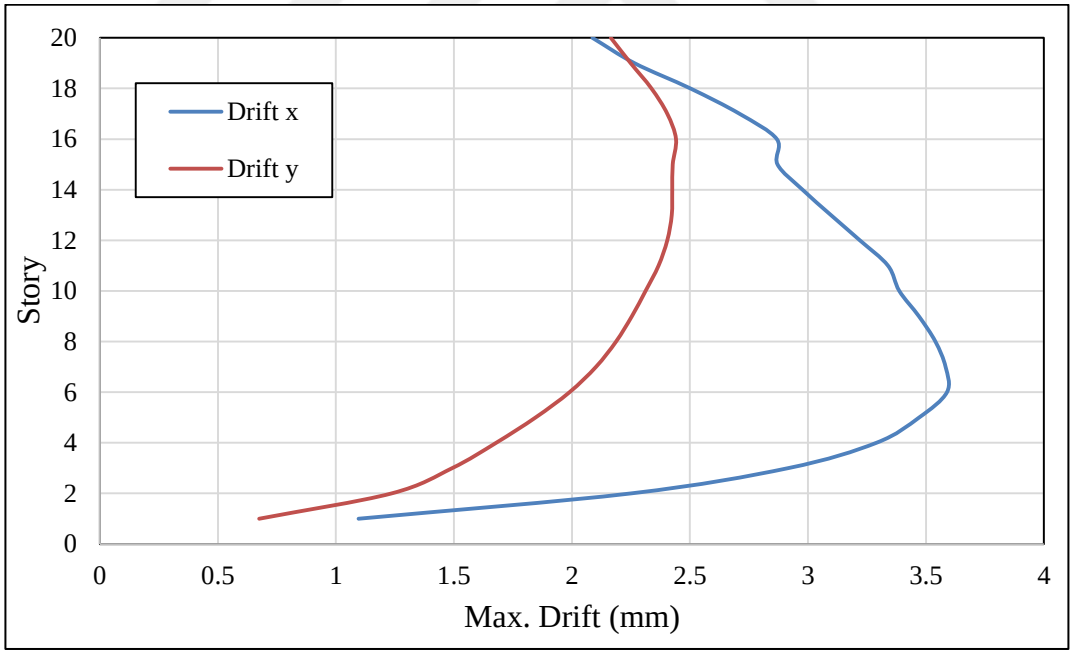

Figure 4.19 Maximum Drift for Building D2220

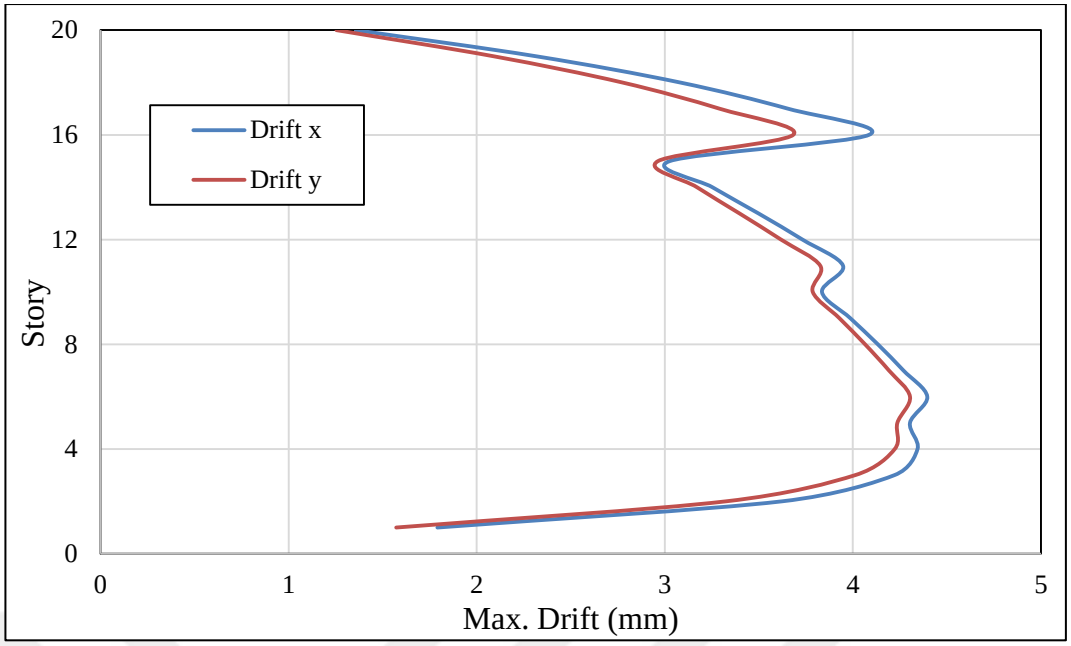

Figure 4.20 Maximum Drift for Building D2120

4.6.5 Group No. 5 (10 story buildings with DD2)

Figures 4.21 through 4.26 display the drift values for both *x* and *y* directions. The drift values in the *y* direction are less than the ones in the *x* direction. In some models (D2510 and D2210) the difference between the drifts of *x* and *y* is a lot more noticeable confirming the fact that the lateral strength in the *y* direction is significantly larger than the one in the *x* direction. The highest value of drift in the 5th group occurs at the sixth floor in the x direction. The building model D2410 has the highest value of drift at the 10th floor where it reaches its peak around 14.9 mm due to the fact that the building model D2410 is treated as a not rigid building due to the fact that its frequency value is less than 1. For model D2110 the drift curves of this model differ from the curves of the rest of the group's models since the building in this model does not contain any shear walls.

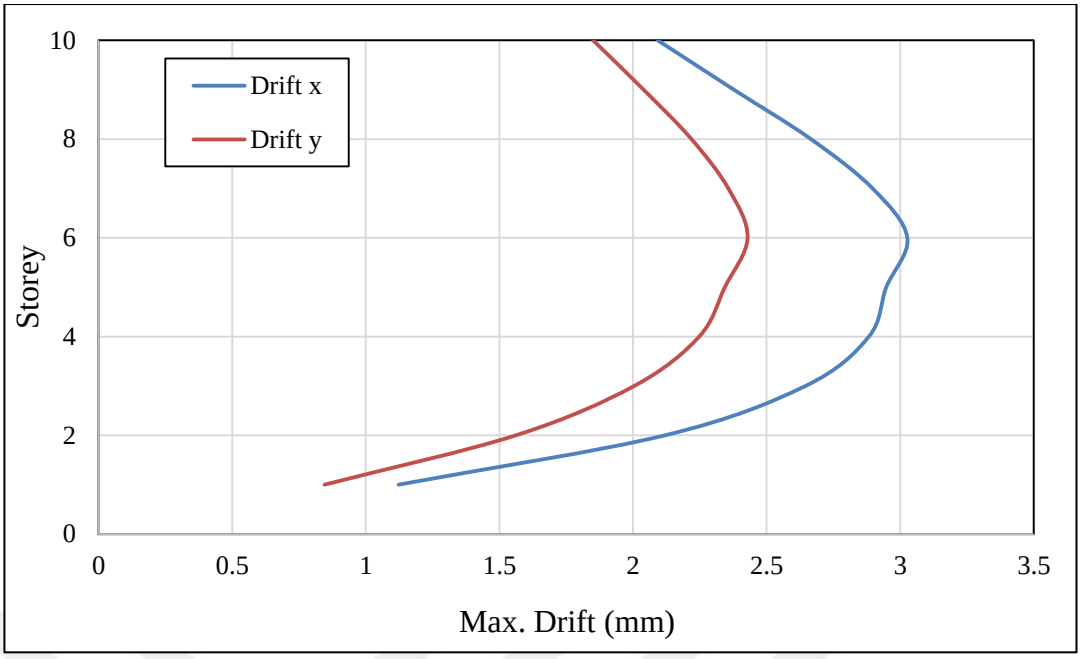

Figure 4.21 Maximum Drift for Building D2610

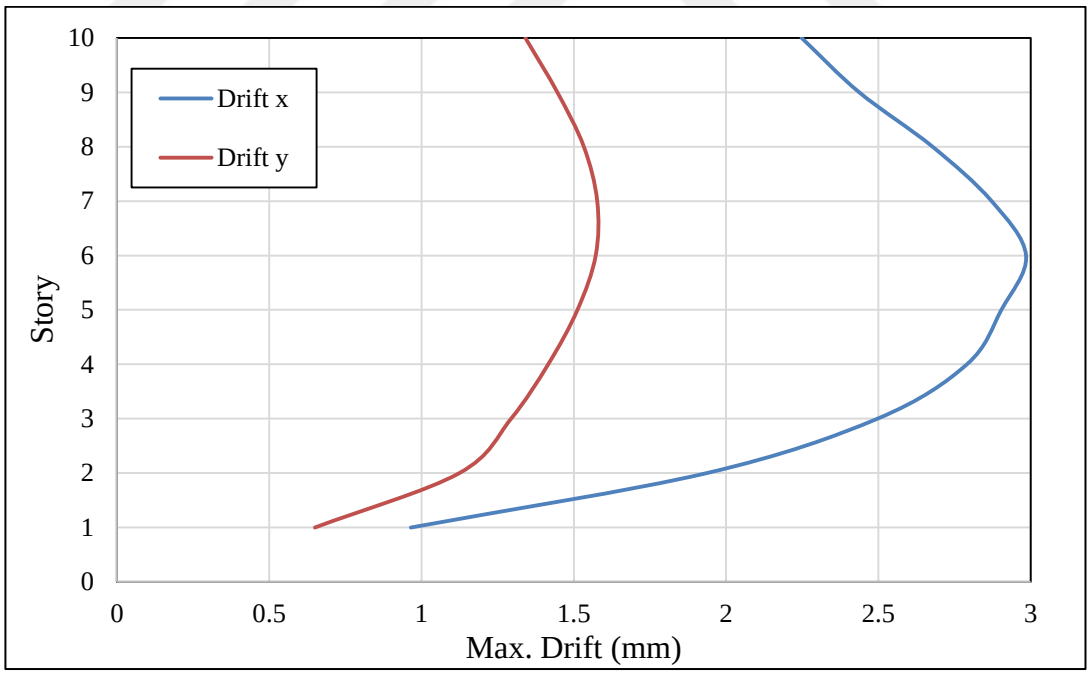

Figure 4.22 Maximum Drift for Building D2510

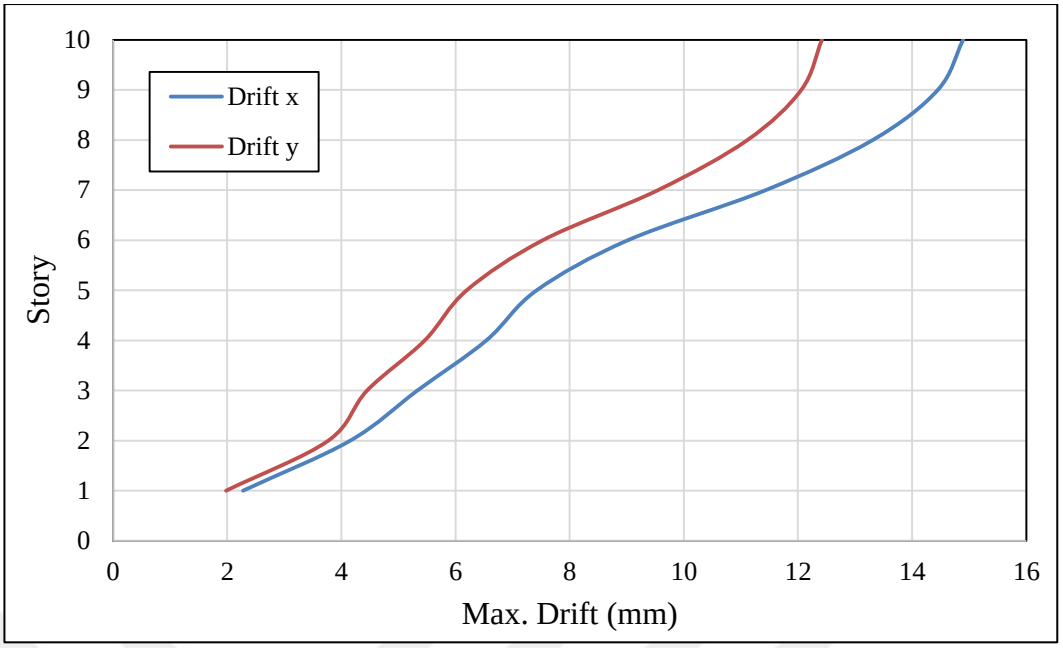

Figure 4.23 Maximum Drift for Building D2410

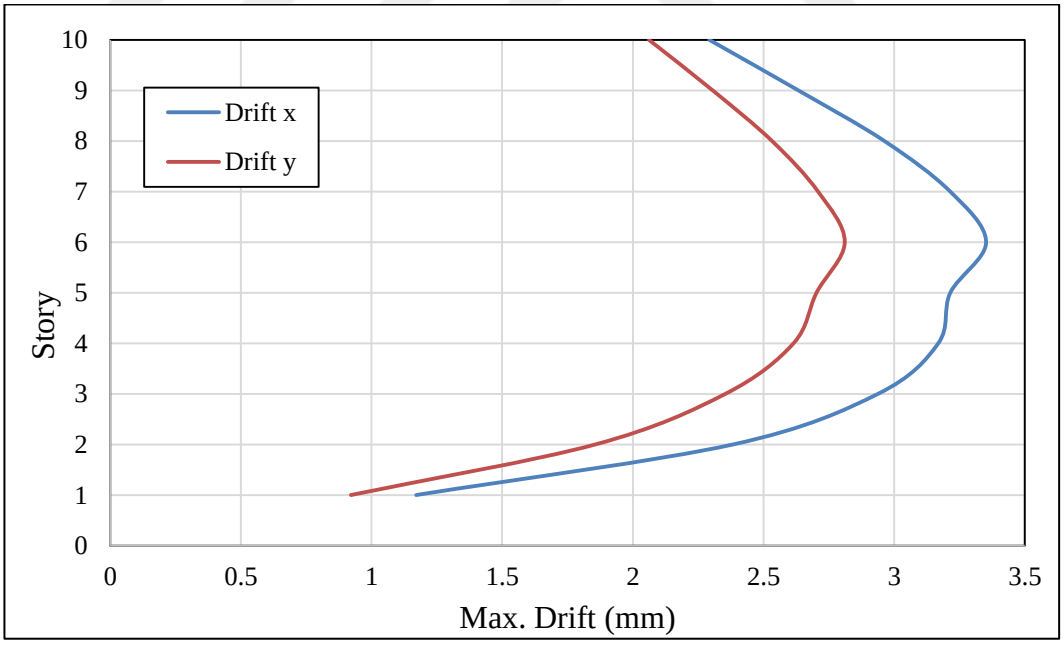

Figure 4.24 Maximum Drift for Building D2310

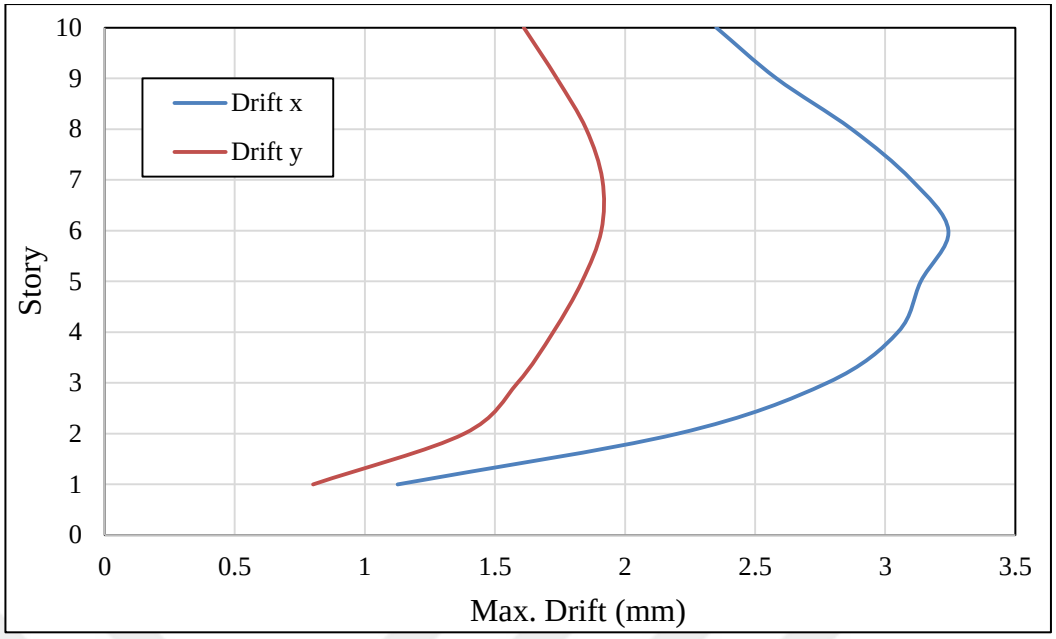

Figure 4.25 Maximum Drift for Building D2210

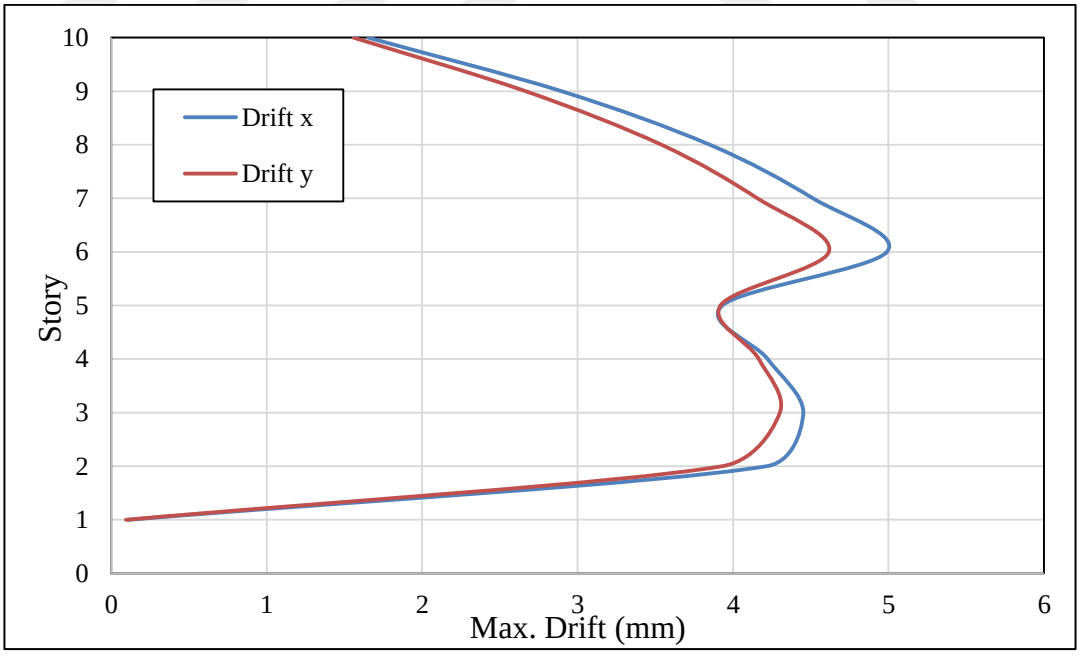

Figure 4.26 Maximum Drift for Building D2110

CHAPTER 5

CONCLUSIONS AND RECOMMENDATIONS

5.1 Introduction

The purpose of this research is to make a comparison between the effect of wind and earthquakes loads on buildings. For this purpose, a total of 26 building models with different layouts are analyzed using ETABS. These buildings are residential buildings located on the shore of Sinop, and divided into 5 groups with each group has the same number of floors but differs in its design in terms of the following parameters: (a) building shape, (b) the presence of shear walls, (c) the layout of shear walls. The buildings are selected as 10, 20, 30, and 40 story buildings. Two types of lateral loads are applied, wind and earthquake loads. For the wind loads, the Turkish code of TS 498, and the American code of ASCE 7-16 are used. For the earthquake loads, the Turkish earthquake code of TEC 19 is used. The results are compared by investigating the following parameters: (a) base shear forces, (b) maximum rooftop displacements, (b) building's first three periods, and (d) maximum drifts.

The thesis contains five chapters. In the first chapter, the purpose of the study and an introduction are presented. The second chapter includes a literature review of the previous studies. The third chapter provides information on the material properties used in the modeling phase, the dimensions of the structural elements, building layouts, type of loading, and the building code rules and regulations. The chapter four explains the analytical results of the building models by comparing the change in the base shear forces, maximum rooftop displacements, fundamental periods and maximum drifts. The conclusions, recommendations, and future studies are all suggested in Chapter 5.

5.2 Conclusions

This study discusses the effects of wind and earthquake loads on multi-story buildings by investigating the results of 26 reinforced concrete buildings modelled in ETABS. These 26 building models are created with different number of floors and different layouts with varying shear wall shape and location. Some of the building models are created with no shear wall effect. The following conclusions are withdrawn from the analytical studies of these buildings with 10, 20, 30, and 40 floors. The conclusions are listed in five groups, which is similar to the number of groups used in Chapter 4 where the results of buildings are evaluated.

5.2.1 Group No. 1 (40 story buildings with DD4)

- In this group, the maximum base shear force value of 6507 kN is observed both in the *x* and *y* directions of the building model of D4340 due to the wind loading of ASCE 7-16. The minimum one of 2686 kN is recorded in the *x* direction of the building model of D4640 due to the earthquake load of TEC 19.
- The maximum lateral rooftop displacements of 39.3 mm generated in the building models of D4540 and D4640 under the effects of the wind loads of ASCE 7-16. The minimum lateral rooftop displacement of 11.3 mm is observed in the building model of D4240 due to the wind loads of TS 498.
- The largest fundamental period of 3.19 seconds is obtained for the model D4340 while the lowest one of 2.68 seconds is obtained for the model D4240.
- The drifts reach their maximum values between the 10th and the 15th floors, which then begins to decrease gradually until they reach their minimum value at the top floor. In general, the drifts in the *y* direction are less than the ones in the *x* direction.

5.2.2 Group No. 2 (40 story buildings with DD2)

- The maximum value of the base shear of 19065 kN in this group is obtained in the *y* direction of the model D2240 due to the earthquake load of TEC 19.

The minimum base shear value of 4110 kN are recorded in the *y* direction of the models of D2540 and D2640 due to the wind loading of ASCE 7-16.

- The building model D2340 has the maximum rooftop displacement of 118.2 mm in the *x* direction which is generated by the earthquake loads of TEC 19. The building model D2240 has the minimum rooftop displacement of 19.7 mm in the y direction due to the wind loads of TS 498.
- The largest fundamental period of 3.74 seconds is obtained for the model D2340 while the lowest one of 3.61 seconds is obtained for the model D2240.
- The drift in this group begins to increase from the first five floors until it reaches its highest value between the 10th and 15th floors. After that, the drift begins to decrease gradually as the building rises. The drifts in the *y* direction are less than the ones in the *x* direction.

5.2.3 Group No. 3 (30 story buildings with DD2)

- The base shear reaches its highest value of 16420 kN in the *y* direction of the building model D2230 due to the earthquake load of TEC 19. The lowest base shear value of 2411 kN is observed in the *y* direction of the models D2430, D2530, and D2630 due to the wind loading of TS 498.
- Roof top displacement reaches its maximum value of about 134.5 mm in the *x* direction in the model D2130 due to the wind and earthquake loadings of ASCE 7-16 and TEC 19, respectively. The minimum displacement value of 16.3 mm is obtained in the *y* direction of the model D2530 due to the wind loading of TS 498.
- The largest fundamental period value of 4.50 seconds is obtained for the model D2130 while the lowest one of 2.66 seconds is obtained for the model D2530.
- In this group, the drifts in the *x* direction are higher than the ones in the *y* direction. The drift reaches its highest value between the 10th and 15th floors, except for the D2130 and D2430 models, where the highest value of the drift is between the 5th and the 10th floors. The difference is attributed the absence of the shear walls for the building models of D2130 and D2430.

5.2.4 Group No. 4 (20 story buildings with DD2)

- The building model D2220 has the highest base shear value of 19530 kN in the *y* direction due to the earthquake loads of TEC 19. The building model D2520 has the lowest base shear value of 1455 kN in the *y* direction due to the wind loading of ASCE 7-16.
- The building model D2420 has the maximum rooftop displacement of 65.6 mm in the x direction, which is generated by the earthquake loads of TEC 19. The building model of D2520 has the minimum rooftop displacement of 4.0 mm in the *y* direction, which is generated by the wind loads of TS 498.
- The largest fundamental period of 2.15 seconds is obtained for the model D2420 while the lowest one of 1.57 seconds is obtained for the model D2320.
- The drift values for this group of buildings reach their maximum values between the 4th and 6th floors. Then, the drift begins to decrease until it reaches its minimum value at the top floor. For the building models D2220 and D2420, the drift curves are different than the ones of the rest of the group's models. This difference is attributed to the shear walls since these two building models have no shear walls. Based on the results, it is also seen that the drifts in the *y* direction are less than the ones in the *x* direction.

5.2.5 Group No. 5 (10 story buildings with DD2)

- The maximum base shear force value of 17019 kN is generated in the *y* direction of the model D2210 due to the earthquake loads of TEC 19. The minimum base shear force value of 291 kN is generated in the *y* direction of the model D2610 due to the wind loads of ASCE 7-16.
- The maximum rooftop displacement of 33.5 mm is observed in the *x* direction of the model D2110, which is generated by the earthquake loads of TEC 19. The minimum rooftop displacement of 0.3 mm is observed in the *y* direction of the building model D2510 due to the wind loads of ASCE 7-16 and TS 498.

- The largest fundamental period value of 2.06 seconds is obtained for the model D2410 while the lowest value of 0.73 second is obtained for the model D2510.
- The highest value of drift occurs on the sixth floor in the *x* direction. The building model D2410 has the highest drift value at the 10th floor since this building is treated as a non-rigid building. For all the buildings in this group, the drift values in the *y* direction are less than their counterparts in the *x* direction.

5.2.6 Others

- When the results of the base shear forces of all buildings resulting from wind and earthquake loads are compared to each other, it is concluded that the earthquake loads of DD2 generate the largest base shear forces for all types of buildings.
- When the results of the base shear forces resulting from earthquake loads of DD4 are compared against the maximum base shear forces of wind loads from TS 498 and ASCE 7-16, it is observed that only in the *x* direction, the DD4 earthquakes generate less.
- The base shear forces of DD2 are compared to the maximum base shear forces resulting from the wind loads of TS 498 and ASCE 7-16. Based on the results, it is apparent that the DD2 generate much larger forces both in the *x* and *y* directions. The difference between the results of DD2 and wind loads are a lot more pronounced when the number of floors are less.
- When the results of the base shear generated by the wind loads of TS 498 and ASCE 7-16 are compared to each other, it is seen that the maximum base shear forces are obtained from TS 498 for the buildings of the first, second, and fifth groups. For the buildings in the third and fourth groups, the highest base shear value is produced by the wind loads of ASCE 7-16.
- If the base shear forces and rooftop displacements of DD2 are compared to the maximum values of TS 498 and ASCE 7-16, it is concluded that the earthquake comes first in generating the largest amount of rooftop displacement and base shear forces.

- Finally, based on the results, there is no obvious favourite between the square-shaped layout with core shear walls and the rectangular-shaped layout with core shear walls, although both of these layouts are better than the rest investigated in this study.

5.3 Recommendations

Based on this study and its results, some recommendations are listed below to obtain the best layout for buildings with different heights under the effect of wind and earthquake loads.

- In the 40 story building case, which the building is subjected to a DD4 earthquake type and the wind loads, the square shaped layout with the shear walls located at the center (core walls) exhibits good structural performance, therefore can be recommended.
- In the 40 story building case, which the building is subjected to a DD2 earthquake type and the wind loads, the best structural performance is obtained for the building with a square shaped layout having shear walls located at its center. Therefore, a square shaped layout with core walls is recommended for both wind and earthquake loads.
- In the 30 story building case with DD2 earthquake type, the rectangular layout with the shear walls located at center of the building gives good structural performance under both wind and earthquake loads. Therefore, a rectangular shaped layout with core walls is also recommended for the 30 story buildings when they are subjected to both wind and earthquake loads. The advantage of having rectangular shape over square shape is related to the lateral strength of the building which has a lot more in the rectangular case since the number of walls are decided to be kept the same for both layouts.
- In the 20 story building case with DD2 earthquake type, the rectangular layout with shear walls located at its center gives good structural performance under both wind and earthquake loads. However, in terms of fundamental period the minimum value is obtained for a square shaped layout with shear walls located around the perimeter of the buildings. As stated before, the advantage of having rectangular shape over square shape is

related to the lateral strength of the building which has a lot more in the rectangular case since the number of walls are decided to be kept the same for both layouts.

- In the 10 story building with DD2 earthquake type, in order to get the best structural performance under lateral loads, its recommended to design the building with rectangular shape and to locate the shear walls in its center. However, in terms of base shear forces, the minimum value is obtained for the rectangular shaped layout with shear walls located around the perimeter of the buildings. Again, the advantage of having rectangular shape over square shape is related to the lateral strength of the building which has a lot more in the rectangular case since the number of walls are decided to be kept the same for both layouts.

5.4 Future Research Suggestions

The impact of wind and earthquake loads on buildings is conducted on 26 reinforced concrete buildings of four different heights 30, 60, 90 and 120 meters with square and rectangular shapes. Thus, the study investigated the structural behaviors of the 10, 20, 30 and 40 story buildings. For future works, it is recommended to study buildings with different layouts such as circular, oval shape or rectangular and square shape layouts with corners trimmed. Floor layouts with number of openings should also be studied in order to determine the impact of wind and earthquake loads. It is also possible to change the location and area of the shear walls used in these buildings with varying heights from the base to a certain floor level. Buildings' structural behaviors should also be studied when dampers are added to the framing system for both earthquake and wind loads. The building location can be another parameter in comparing the results of wind loading to earthquake loading. In order to further understand the effect of code generated wind loading on lateral resisting members either small wind tunnel tests or computational fluid dynamics models should also be used to verify the results of the code generated loadings.

REFERENCES

[1] S. K. Mitra 1993 “Mixed-Use High Rise Building in Response to Natural Forces” Master’s Thesis, University of Southern California, August 1993.

[2] Xin Qiu 1997, “Control of Response of Tall Multi-story Building Under Wind Excitation” Doctor’s Thesis, Florida Atlantic University Boca Raton, Florida, April 1997.

[3] O. AlShamrani 2007, “Selection of Structural System and Materials: Minimizing Lateral Drift and Cost of Tall Building in Saudi Arabia” Master’s Thesis, University of Southern California, May 2007.

[4] P. Mendis, T. Ngo, N. Haritos, A. Hira, B. Samali and J. Cheung “Wind Loading on Tall Buildings”, EJSE Special Issue: Loading on Structures (2007).

[5] H. Mingfeng 2008, “Performance-based Serviceability Design Optimization of Wind Sensitive Tall Buildings” Doctor’s Thesis, The Hong Kong University of Science and Technology, August 2008.

[6] Adrian Pozos Estrada 2009, “Reliability of Wind- Sensitive Building: A Serviceability Design Consideration” Doctor’s Thesis, The University of Western Ontario, 2009.

[7] M. Montgomery 2011, “Fork Configuration Dampers (FCDS) for or Enhanced Dynamic Performance of High-Rise Building” Doctor’s Thesis, University of Toronto, 2011.

[8] Baldev D. Prajapati1 & D. R. Panchal "Study of Seismic and Wind Effect on Multi Storey R.C.C., Steel and Composite Building" International Journal of Advances in Engineering & Technology. ISSN: 22311963, 2013.

[9] G. Cheng "A Framework for Life-Cycle Cost Optimization of Building Under Seismic and Wind Hazards" Master's Thesis, Colorado State University, Summer 2014.

[10] Vikram.M.B1, Chandradhara G. P, Keerthi Gowda B.S " A study on effect of Wind on The Static and Dynamic Analysis" International Journal of Emerging Trends in Engineering and Development Issue 4, Vol.3, 2014.

[11] Md. Mahmud Sazzad, Md. Samdani Azad "Effect of building shape on the response to wind and earthquake" International Journal of Advanced Structures and Geotechnical Engineering ISSN 2319-5347, Vol. 04, No. 04, 2015.

[12] Aneeket T. Patil and Sachin B. Kadam "Behaviour of Multistorey Building under the Effect of Wind and Earthquake for Different Configuration of Shear Wall" Journal of Civil Engineering and Environmental Technology, Volume 3, Issue 6, pp. 558-563, 2016.

[13] Shaikh Muffassir, L.G. Kalurkar "Comparative Study on Wind Analysis of Multi-story RCC and Composite Structure for Different Plan Configuration" IOSR Journal of Mechanical and Civil Engineering (IOSR-JMCE) Volume 13, Issue 4 Ver. VII 2016.

[14] A. Mohammadi, 2016, "Wınd Performance Based Design for High-Rise Buildings" PhD dissertation, Florida International University, November, 2016.

[15] Gourav P. Bajaj, G. B. Bhaskar, "Wind Behavior of Building with and without Shear wall (in Different Location) for Structural Stability and

Economy" International Journal for Technological Research in Engineering Volume 4, Issue 3, November-2016.

[16] F. Steffen 2016, "Wind-Induced Vibrations in High-Rise Building" Master's Thesis, Lund University, June 2016.

[17] S. Ebrahimi 2016, "Effect of Vertical Component of Ground Motion on Dual System Tall Buildings" Master's Thesis, University of California Irvine, 2016.

[18] MD. Rokanuzzaman , F. Khanam, A. Das and S. R. Chowdhury, "Effective Location of Shear Wall on Performance of Building Frame Subjected to Lateral Loading" International Journal of Advances in Mechanical and Civil Engineering, ISSN: 2394-2827 Volume-4, Issue-6, 2017.

[19] E. Azimi 2017, "The Effects of High winds on Existing buildings in New York City" Doctor's Thesis, New York University, May2017.

[20] N. Longarini, L. Cabras, M. Zucca, S. Chapain, and A. Mousaad" Structural Improvements for Tall Buildings under Wind Loads: Comparative Study" Hindawi Shock and Vibration, Article ID 2031248, Volume 2017.

[21] S. Thilakarathna, N. Anwar, P. Norachan F. Naja "The Effect of Wind Loads on the Seismic Performance of Tall Buildings" Athens Journal of Technology and Engineering - Volume 5, Issue 3, 2018.

[22] A. Naga Sai, G. Radha Devi, "Seismic and Wind Effects on High Rise Structure Using ETABS" International Journal for Research in Applied Science & Engineering Technology (IJRASET) ,Volume 6 Issue II, February 2018.

[23] M. V. Kulkarni, "Effect of Seismic Forces and Wind on Base Shear of High-Rise Building by IS 1893: PART- I & IS 875: PART 3", International

Journal of Civil Engineering and Technology (IJCIET) Volume 9, Issue 10, pp. 1444–1453, Article ID: IJCIET_09_10_144, October 2018.

[24] M. D. Kumbhar, N.S. Vaidkar and U. Kalwane, “Literature Review on Seismic and Wind Analysis of Multi storied RC Building with Different Plan Shapes” Resincap Journal of Science and Engineering Volume 2, ISSN: 2456-9976, Issue 4 April 2018.

[25] TEC 19. “Turkish Earthquake Code,”, Ankara, Turkey, 2019.

[26] American Society of Civil Engineers, “Minimum Design Loads for Buildings and Other Structures,” ASCE 7-16, 2016.

[27] TS 498, “Turkish standards Design loads for buildings,”, November 1997.

[28] Simiu, E. "Wind Spectra and Dynamic Along wind Response," J. Struct. Dir., ASCE, Vol. 100, No. ST9, Proc. Paper 10815, 1974, pp. 1897-1910.

[29] Davenport, A. G., "The Spectrum of Horizontal Gustiness Near the Ground in High winds," Quart. Journal Royal Meteorological Society, Vol.87, 1961, pp.

[30] ETABS Version 17.0.1, Computers and Structures Inc.

[31] STAAD Pro 2005.

APPENDIX A

Table below has the list of all load combinations and load patterns used in this study.

Table A.1 Load Combinations and load patterns

No.	Load Combination Equations
1	S_X
2	S_Y
3	1.4 D + 1.4 SD + 1.6 L
4	D + SD+ 0.3 L
5	D + SD+ L + S_X
6	D + SD+ L - S_X
7	D + SD + L + S_Y
8	D + SD + L - S_Y
9	D + SD + L + S_X + 0.3 S_Y
10	D + SD + L + S_X - 0.3 S_Y
11	D + SD + L - S_X + 0.3 S_Y
12	D + SD + L - S_X - 0.3 S_Y
13	D + SD + L + 0.3 S_X + S_Y
14	D + SD + L + 0.3 S_X - S_Y
15	D + SD + L - 0.3 S_X + S_Y
16	D + SD + L - 0.3 S_X - S_Y
17	S_X + 0.3 S_Y
18	S_X - 0.3 S_Y
19	- S_X + 0.3 S_Y
20	- S_X - 0.3 S_Y
21	0.3 S_X + S_Y
22	0.3 S_X - S_Y
23	- 0.3 S_X + S_Y
24	- 0.3 S_X - S_Y
25	D + L + 0.2 Sn + S_X + 0.3 S_X^Z
26	D + L + 0.2 Sn - S_X + 0.3 S_X^Z
27	D + L + 0.2 Sn + S_Y + 0.3 S_Y^Z
28	D + L + 0.2 Sn - S_Y + 0.3 S_Y^Z

29	$D + L + 0.2\ Sn + S_X + 0.3\ S_Y + 0.3\ S_X^Z$
30	$D + L + 0.2\ Sn - S_X - 0.3\ S_Y + 0.3\ S_X^Z$
31	$D + L + 0.2\ Sn + S_X - 0.3\ S_Y + 0.3\ S_X^Z$
32	$D + L + 0.2\ Sn - S_X + 0.3\ S_Y + 0.3\ S_X^Z$
33	$D + L + 0.2\ Sn + 0.3\ S_X + S_Y + 0.3\ S_Y^Z$
34	$D + L + 0.2\ Sn - 0.3\ S_X - S_Y + 0.3\ S_Y^Z$
35	$D + L + 0.2\ Sn + 0.3\ S_X - S_Y + 0.3\ S_Y^Z$
36	$D + L + 0.2\ Sn - 0.3\ S_X + S_Y + 0.3\ S_Y^Z$
37	$D + 1.3\ L + 1.3\ W_X$
38	$D + 1.3\ L - 1.3\ W_X$
39	$D + 1.3\ L + 1.3\ W_Y$
40	$D + 1.3\ L - 1.3\ W_Y$
41	$0.9\ D + 1.3\ W_X$
42	$0.9\ D - 1.3\ W_X$
43	$0.9\ D + 1.3\ W_Y$
44	$0.9\ D - 1.3\ W_Y$
45	$W_X = W_{X1} + W_{X2} + W_{X3} + W_{X4}$ (see note 1)
46	$W_Y = W_{Y1} + W_{Y2} + W_{Y3} + W_{Y4}$ (see note 1)
47	$Ww = Sn + D + 0.3\ L + SD$
48	$W_S = D + SD + n\ (L + Sn)$
Load Patterns	
49	Dead Load
50	Live Load
51	Snow Load
52	Super Dead Load
53	Seismic (X,Y)

Note 1 The wind loads were applied to each building model separately and according to their number of floors, which were in line with the height requirements of TS 498 (see Section 3.5.1b). For example, in the 40 story-building case, the wind loads were applied to the floors as four seperate loads but acting concurrently: (a) from the base to the 3rd floor, (b) from the 4th to 7th floor, (c) from the 8th to to the 33rd floor, and (d) from the 34th to the 40th floor. These loads were applied in a similar fashion both in the *x* and *y* directions. After this stage of loading, these separate load patterns, which were denoted by subscripts 1, 2, 3 and 4 in load combinations 45 and 46, were combined into a single load combination to be used as a wind load.